UNIVERSITY OF ROME

"TOR VERGATA"

FACULTY OF ENGINEERING

Ph.D. PROGRAM in

ENERGY AND ENVIRONMENT ENGINEERING

XX CYCLE

SPATIAL DISTRIBUTION OF TRAFFIC-RELATED POLLUTANTS FROM TAILPIPE-TO-ROAD-TO-AMBIENT. THE CASE OF ULTRAFINE-PARTICLES

Tutor: Prof. Vittorio Rocco

Coordinator:Prof. Fabio Gori

Co-Tutor:Prof. Stefano Cordiner

Candidate: Francesca Costabile

Keywords: traffic air pollution, spatial variation, ultrafine particles, frequency distributions, motor engine emissions.

CONTENTS

SUMMARY

INTRODUCTION

During the last decades a growing body of research has investigated worldwide the extremely vast subject of urban air quality [e.g., Fenger, 1999]. Measuring any potential effect of any urban air pollutant requires the understanding of its variation and distribution in both space and time. Traffic-related pollution and its spatial variations are particular concerns; a comprehensive understanding is crucial [e.g., Morawska et al. 2002; Briggs, 2000; Ito et al., 2004; Kim et al., 2005; Pinto et al., 2004; Wilson et al., 2005; Zhu et al., 2002]. However, current actions are particularly hampered by a lack of knowledge when characterising the spatial variability within urban areas [e.g., Lebret et al., 2000].

The understanding of emissions' spatial variation can indicate to what extent ambient concentrations measured at a single fixed site (e.g., the emission point) reflect the outdoor concentrations at other sites in the area. For particles, the spatial variability depends on the size fraction. Particles smaller than 100 nm (the so-called ultrafine particles, UFPs) are more variable in space and time than fine particles as they have a higher dependence on particle sources, and a faster removal from the atmosphere [e.g., WHO, 2006; Pekkanen and Kulmala, 2004; Monn, 2001]. Consequently, their spatial variability is believed to be an important issue to assess air pollution fate and exposure.

Internal combustion engines are known to be a major emission source of UFPs [e.g., Weijers et al., 2004; Charron and Harrison, 2003; Alam et al., 2003; Kittelson et al., 2004; Morawska et al., 2003]. However, in spite of extensive laboratory studies on engine emissions, there are few investigations of how particle mobile emissions evolve and affect air quality establishing a link between sources and receptors [e.g., Abdul-Khalek et al., 1999; Scheer et al., 2005; Giechaskiel et al., 2005]. Moreover, there is little information on particles smaller than 10 nm, which have been regarded as evidence of particles either truly emitted (Figure 1) [e.g., Scheer et al., 2005; Giechaskiel et al., 2005] or newly formed in the atmosphere (Figure 2) [e.g., Kulmala, 2003; Charron and Harrison, 2003; Shi et al., 2001; Alam et al., 2003].

Recent field data have shown that the size distribution of emitted particles evolves substantially within a few hundred meters of emission [e.g., Shi et al., 2001; Zhu et al., 2002]. With this respect, it has been shown that not only is total particle

concentration important, but also the particle size distribution [e.g., Kittelson et al., 2004; Whitby and Cantrell, 1976; ICEP, 1994]. After release into the atmosphere, UFPs are subjected to complex dilution and transformation processes. Neither current models nor those that will be available in the near future are tough to be able to cover all the spatial and temporal scales that are involved from the emission (centimetres, milliseconds) to the urban/regional scale (kilometres, hours) [Ketzel and Berkowicz, 2004].

CONCEPTION OF THE WORK

In this work, the major objective was to analyse the spatial variation of traffic related air pollution, especially focussing on UFPs. The process has been analysed using a two stage structure, namely, 'tailpipe-to-road' and 'road-to-ambient' [e.g., Zhang and Wexler, 2004a,b]. Considering an exhaust parcel emitted from the tailpipe, and dispersing to the background; this parcel experiences two very distinct processes. First it is diluted and diffused by the strong turbulence generated by the moving traffic, moving it from tailpipe to roadside (stage 1: tailpipe-to-road). Then, by the atmospheric turbulence induced mainly by wind and atmospheric instability, it is moved from roadside to ambient air (stage 2: road-to-ambient). These stages are extremely different in both of their temporal and spatial scales. The understanding of how this parcel and its concentration in air distributes in regard to the major factors influencing it was conducted here. The methodology was firstly based on the analysis of its frequency distribution (FD). In principle, air pollutant FD tends to be log-normal since extreme high concentrations are possible but negative values are not, as explained by the theory of successive random dilution (Ott, 1990). However, air pollutant concentrations were expressed in this work as space series at different time periods rather than time series at different locations. Therefore, the study of their FDs in space could be used to understand how diffusion mechanisms in atmosphere (revealed by Normal-FD) can couple with mixing and diluting of source emissions to produce air pollutant spatial variations [Costabile et al., 2006a]. This level of analysis has enhanced the comprehension of air pollution variation in both space and time, in both stage 1 and stage 2, revealing governing factors (i.e., emission levels, meteorological conditions, chemistry, geography and local morphology) [Costabile et

al., 2007a] and principal components (i.e., major emission sources and "aging processes") [Costabile et al., 2008].

RESULTS

The methodological approach before described was developed at both the stages, and applied firstly for major traffic-related air pollutants, and then to UFPs. Initially, a new methodology for assessing the spatial distributions of traffic air pollutants at urban (road-to-ambient) scale was developed [Costabile et al., 2006a]. Concurrently, a new approach to link air quality and traffic air pollution at urban scale (stage road-to-ambient) was studied [Costabile et al., 2008a]. Therefore, the two above mentioned approaches were applied to analyse a real case of UFP variation in an urban area (stage road-to-ambient) [Costabile et al., 2007b]. Then, the spatial distribution of reactive traffic-related air pollutants into a street-canyon (namely including chemistry and fluid-dynamics effects) was analyzed (stage tailpipe-to-road) [Costabile et al., 2007a]. Finally, the major findings of this work guided the assessment of ultrafine particles near-road, at stage tailpipe-to-road [Costabile et al., 2008b].

DISCUSSION

The methodology to analyse the spatial variation of traffic air pollution was developed by considering air pollutants' concentration in terms of frequency distributions (FD) of its space series. The dilution processes (indicated by a LogNormal FD, as explained by the theory of successive random dilution) was shown to be not the dominant process to fit the spatial variations. Conversely, space-FDs of traffic air pollutants were found to be fitted by the Gaussian FD, that is the data matched the pattern expected if the data was drawn from a population with a Normal distribution. When traffic emissions in urban areas can be considered as sources spatially diffused (no highways, etc.), pollutants mainly emitted by vehicle emissions show a Normal space-FD being other factors less relevant. This result is very important in understanding the characteristic of the spatial trend of these pollutants. Every process where the pollutant particles show a Normal distribution of the spatial trend density, satisfies the diffusion equation and thus represent such a mechanism. The predominant factors influencing the spatial FD type of air pollutant concentrations may, therefore, be associated to the diffusion mechanisms in

atmosphere, rather than mixing and diluting of source emissions. These factors are meteorology, presence of relevant emission sources, emission seasonality, changes in photochemistry, and topography. Moreover, being the spatial data distribution Normal, mean and median values (quite same) can correctly be used to represent the concentration values of these pollutants all over the city for air quality management purposes and calculation of air pollution indexes.

The methodology to allow the communication at road-to-ambient scale between transport emissions and air quality in real-time was developed by considering integrated systems. The successful approach, currently under way as case-study in Beijing, considered the integration of the modeling to interpret the data measured with the measurements to validate the data modeled. The work was intended to better understand how the improvement of transport technology, both private and public, the reduction of vehicles pollution proportion by technological, political and scientific measures and the improvement of emission performances, could be integrated with "intelligent" transport management system. However, there remains a need to continue research to improve our understanding of the mechanisms leading to air pollution impacts from transport emissions, to reduce the uncertainty in our ability to quantify the relationships between all emissions and all impacts. For urban air pollutants from road traffic there remain some doubts concerning both the existence and the mechanisms of cause and effect, particularly for particles, which are currently one of the air pollutants causing most concern.

To this meaning, the number concentration of UFPs were analysed at stage 1, from road-to-ambient both near emission sources and at a background location. They were found to be a clear indication of vehicle exhaust sources in ambient air. At urban scale UFPs resulted from three prevailing contributions. Firstly, a very low urban background UFP concentration (lower than 1000 #/cm^3) particularly visible in summer. Secondly, a significant contribution due to local traffic sources, up to 100.000 #/cm^3 (traffic site in winter time). Finally, a significant contribution due to secondary transformation processes closely linked to meteorology, particularly solar radiation. Transport from sources nearby were also found to be significant, indicating significant UFP lifetime in atmosphere. The conditions near mobile emission sources were found to differ from typical background conditions in that particle number concentrations were much higher, and dilution processes were much faster and stronger. The stronger variability induced more rapid concentration fluctuations,

probably due to faster and more intense dilution processes, which can reduce the number concentration more rapidly, as well as trigger physical processes other than dilution, such as nucleation, coagulation, and condensation.

The analysis of the stage 2, from tailpipe-to road, revealed traffic pollutants emitted at road level to vary relevantly on the vertical coordinate even to less than 15 m. The analysis of the frequency distribution (FD) of the (spatial) differences between the two measured (time) concentrations (for each pollutant) gave insights into the pollutant diffusion mechanisms in atmosphere from tailpipe to road (Costabile et al., 2006b). The spatial distribution of a pollutant governed largely by local vehicle emissions (e.g. NO into a street-canyon) was largely determined by the vertical diffusion of emissions: difference of concentrations distributed statistically according to the Gaussian curve. The higher the chemical reactivity of the pollutant (e.g., O3), the lower the spatial distribution with a variability strongly influenced by local fluid-dynamics effects, and a FD influenced by systematic factors deviating it from the Normal FD.

Finally, the number distribution of aerosol particles spanning from 6 nm to more than 20 μm was analysed on the road (stage 2, from tailpipe-to-road). It was found to be governed by the interaction of four Principal Components at 92.28% of total variance explained. This indicated major sources (traffic emissions and long-range transport) and “aging” processes of particles after the emission (dilution, coagulation, nucleation and condensation, and gravitational settling), grouped over the four orders of magnitude of diameters. The analysis of variables governing the occurrence of these processes revealed the number concentration of particles in the 6-26 nm size range (N_{6-26}, including nucleation mode particles) to be largely influenced by the surface area of particles smaller than 800 nm ($S_{300-800}$, including accumulation mode particles) and ambient T. The highest values of N_{6-26} occurred for threshold values of both $S_{300-800}$ and T. In absence of additional data, it was argued that the balance between two prevailing processes probably triggered the increase of N_{6-26}: the availability of $S_{300-800}$ for condensation of the vapours emitted, and the T-controlled availability of stable clusters for nucleation of the same emitted gases. This finding was a further evidence that nucleation particles can be both directly emitted from the engine and formed in atmosphere soon after the emission according to some governing factors.

OUTLOOK

There appear at least two directions to proceed from the present study. First, the pursuing towards a stage 0 for UFPs number size distribution from engine to tailpipe. In order to control level of atmospheric pollution caused by vehicle engine emissions, the international legislation has indeed established over the years a series of tests designed with the purpose of simulating real engine operating conditions by the performance of both steady and transient test cycles. For several sources the non-steady-state emissions are suspected to be a significant portion of the total air pollution emitted, and hence, their quantification may be important towards determining average emission factors, pollutant exposure and mode-specific pollutant minimization. The Engine Exhaust Particle Sizer (EEPS™, mod.3090, TSI Inc., MN, USA) spectrometer acquired by the Department of Mechanical Engineering of Tor Vergata university during this Ph.D. work is an instrument designed specifically for measuring ultrafine particles emitted from internal combustion engines and vehicles with the fastest time resolution available—10 times per second—. Therefore, it's possible to investigate particle size distribution not only in steady-state engine operation but also in transient engine operation, representing real-world driving behaviour. The main findings of this further study could, then, drive a further direction of research closing the circle indicated by this work, that is the assessment of the spatial distribution of UFP number size distribution from engine-to-tailpipe-to-road-to-ambient. This has the potential to finally indicate to what extent number size concentrations of UFPs measured at the exhausts of a single engine could reflect the outdoor concentrations in ambient air in a whole urban area.

LIST OF FIGURES

LIST OF TABLES

CHAPTER 1. INTRODUCTION

1.1. CONCEPTUAL OF THE WORK AND MAJOR OBJECTIVE

During the last decades a growing body of research has investigated worldwide the extremely vast subject of urban air quality [e.g., Fenger, 1999]. Measuring any potential effect of any urban air pollutant requires the understanding of its variation and distribution in both space and time. Traffic-related pollution and its spatial variations are particular concerns; a comprehensive understanding is crucial [e.g., Morawska et al. 2002; Briggs, 2000; Ito et al., 2004; Kim et al., 2005; Pinto et al., 2004; Wilson et al., 2005; Zhu et al., 2002]. However, current actions are particularly hampered by a lack of knowledge when characterising the spatial variability within urban areas [e.g., Lebret et al., 2000].

The understanding of emissions' spatial variation can indicate to what extent ambient concentrations measured at a single fixed site (e.g., the emission point) reflect the outdoor concentrations at other sites in the area. For particles, the spatial variability depends on the size fraction. Particles smaller than 100 nm (the so-called ultrafine particles, UFPs) are more variable in space and time than fine particles as they have a higher dependence on particle sources, and a faster removal from the atmosphere [e.g., WHO, 2006; Pekkanen and Kulmala, 2004; Monn, 2001]. Consequently, their spatial variability is believed to be an important issue to assess air pollution fate and exposure.

Internal combustion engines are known to be a major emission source of UFPs [e.g., Weijers et al., 2004; Charron and Harrison, 2003; Alam et al., 2003; Kittelson et al., 2004; Morawska et al., 2003]. However, in spite of extensive laboratory studies on engine emissions, there are few investigations of how particle mobile emissions evolve and affect air quality establishing a link between sources and receptors [e.g., Abdul-Khalek et al., 1999; Scheer et al., 2005; Giechaskiel et al., 2005]. Moreover, there is little information on particles smaller than 10 nm, which have been regarded as evidence of particles either truly emitted (Figure 1) [e.g., Scheer et al., 2005; Giechaskiel et al., 2005] or newly formed in the atmosphere (Figure 2) [e.g., Kulmala, 2003; Charron and Harrison, 2003; Shi et al., 2001; Alam et al., 2003].

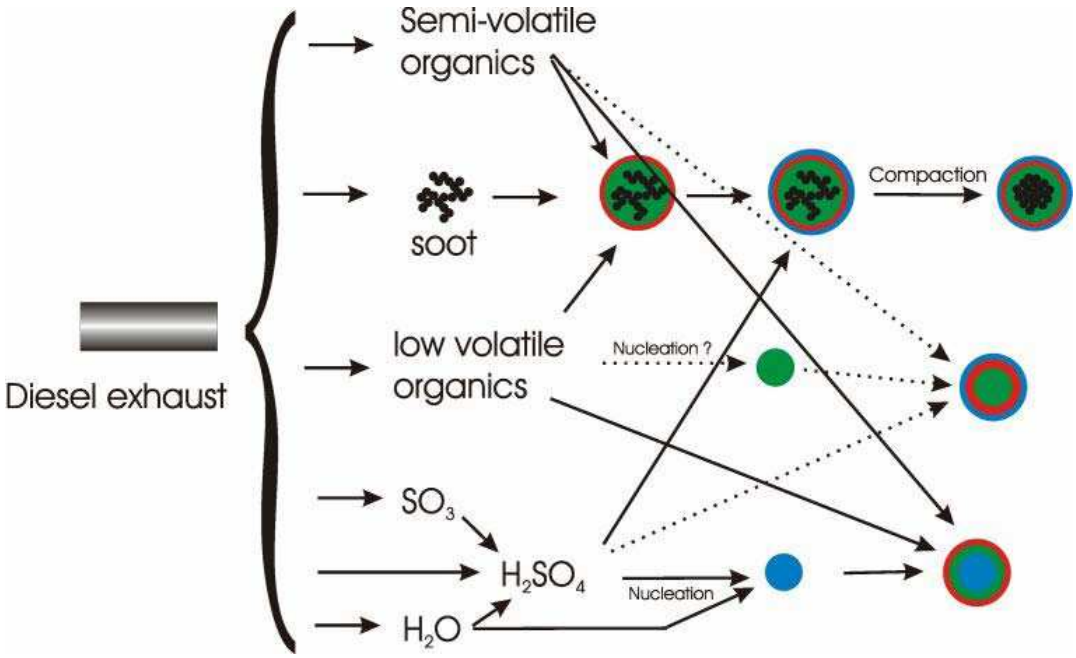

Figure 1. Simplified schematic mechanism of the condensation and nucleation process during diesel exhaust dilution and cooling. Blue: volatile (H_2SO_4); red: semi-volatile organics (unburned fuel); green: low-volatile organics (lube oil) [Reproduced from Scheer et al., 2005].

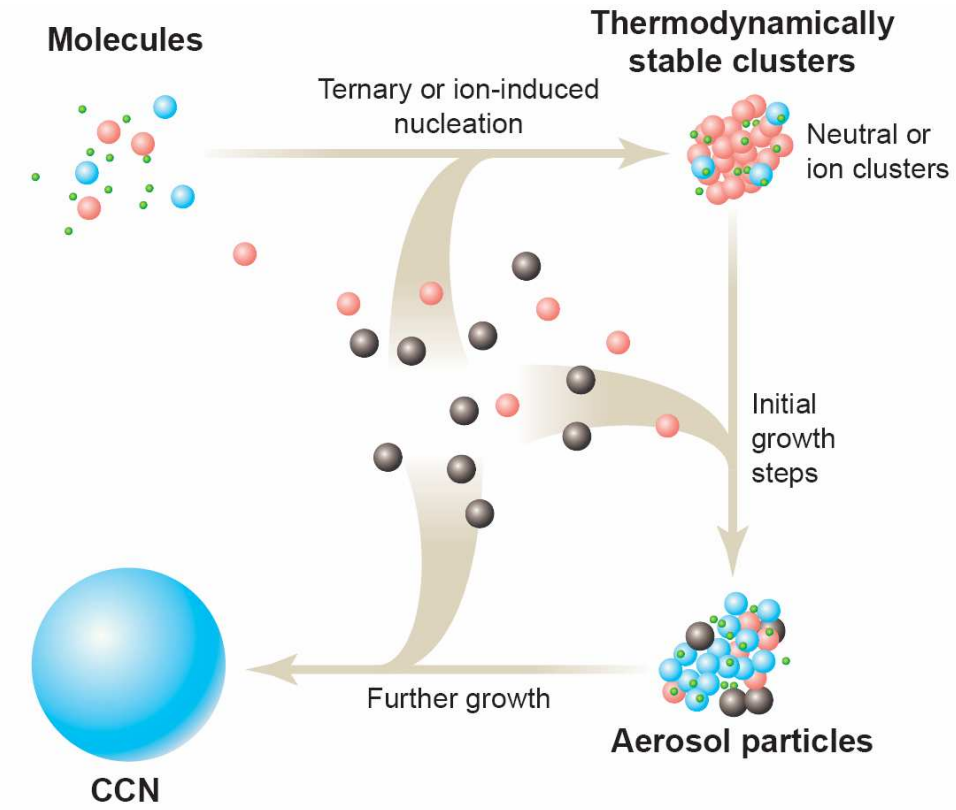

Figure 2. How particle form and grow. Nucleation may involve homogeneous ternary water–sulfuric acid–ammonia mixtures or may be ion-induced. The initial steps of growth include activation of inorganic clusters by soluble organic molecules, heterogeneous nucleation of insoluble organic vapors on inorganic clusters, and chemical reactions of organic molecules at surfaces of inorganic clusters. Finally, cloud condensation nuclei (CCN) form through addition of organic and sulfuric acid molecules. [Reproduced from Kulmala, 2003]

Recent field data have shown that the size distribution of emitted particles evolves substantially within a few hundred meters of emission [e.g., Shi et al., 2001; Zhu et al., 2002]. With this respect, it has been shown that not only is total particle concentration important, but also the particle size distribution (Figure 3).

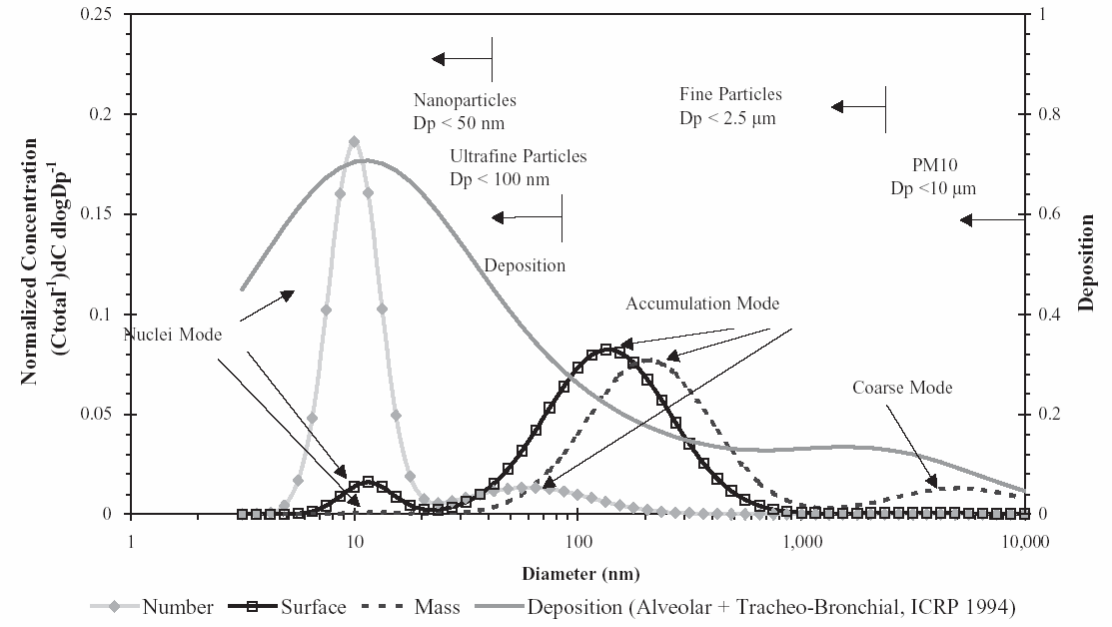

Figure 3. Typical Diesel surface and number weighted [Kittelson et al., 2004] shown with mass weighted size [Whitby and Cantrell, 1976], and alveolar deposition [ICRP, 1994].

After release into the atmosphere, UFPs are subjected to complex dilution and transformation processes. Neither current models nor those that will be available in the near future are tough to be able to cover all the spatial and temporal scales that are involved from the emission (centimetres, milliseconds) to the urban/regional scale (kilometres, hours) [Ketzel and Berkowicz, 2004].

In this work, the major objective was to analyse the spatial variation of traffic related air pollution, especially focussing on UFPs. The process has been analysed using a two stage structure, namely, ‘tailpipe-to-road’ and ‘road-to-ambient’ [e.g., Zhang and Wexler, 2004]. Considering an exhaust parcel emitted from the tailpipe, and dispersing to the background; this parcel experiences two very distinct processes. First it is diluted and diffused by the strong turbulence generated by the moving traffic, moving it from tailpipe to roadside (stage 1: tailpipe-to-road). Then, by the atmospheric turbulence induced mainly by wind and atmospheric instability, it is moved from roadside to ambient air (stage 2: road-to-ambient). These stages are extremely different in both of their temporal and spatial scales (e.g., dilution scales, table 1).

	Stage 1	Stage 2
Mixing force	**Moving traffic**	**Atmospheric shear and stability**
Characteristic speed, u (m/s)	**20-30**	**1-10**
Characteristic length scale, l (m)	**2-3**	**50-100**
Dissipation rate, $\varepsilon \sim u^3/l$ (m^2/s^3)	**2500-14000**	**0.01-20**
Dilution ratio (1/f)	**~1000 in 1 sec**	**<10 in 10 min**
Temperature gradient	**Steep**	**Flat**

Table 1. Comparison between the two stages of dilution processes [Zhang and Wexler, 2004]

The understanding of how this parcel and its concentration in air distributes in regard to the major factors influencing it was conducted here. The methodology was firstly based on the analysis of its frequency distribution (FD). In principle, air pollutant FD tends to be log-normal since extreme high concentrations are possible but negative values are not, as explained by the theory of successive random dilution [Ott, 1990]. However, air pollutant concentrations were expressed in this work as space series at different time periods rather than time series at different locations. Therefore, the study of their FDs in space could be used to understand how diffusion mechanisms in atmosphere (revealed by Normal-FD) can couple with mixing and diluting of source emissions to produce air pollutant spatial variations (Figure 4) [Costabile et al., 2006a].

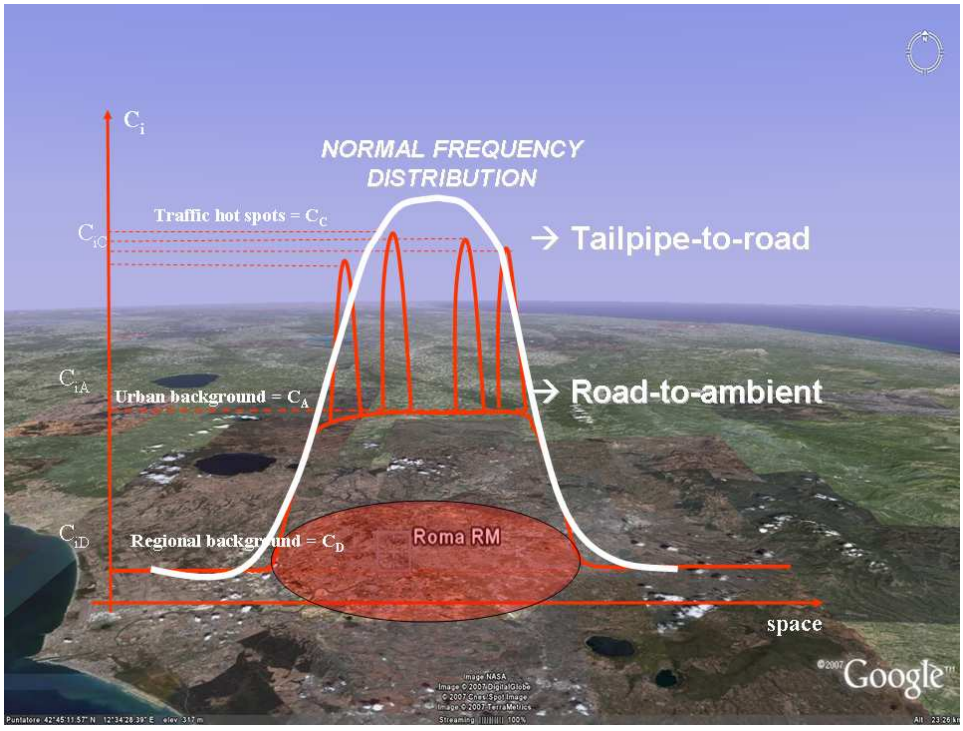

Figure 4. Schematic of the concentration in space for the pollutant i at urban scale. The two-stage variation is indicated, including the traffic hot spots (tailpipe-to-road processes) and urban background (road-to-ambient processes).

This level of analysis has enhanced the comprehension of air pollution variation in both space and time, in both stage 1 and stage 2, revealing governing factors (i.e., emission levels, meteorological conditions, chemistry, geography and local morphology) [Costabile et al., 2007a] and principal components (i.e., major emission sources and “aging processes”) [Costabile et al., 2008].

1.2. ORGANISATION OF DISSERTATION

The current thesis has been divided into 7 Chapters:

Chapter 1: The introduction (this one).

Chapter 2: in this chapter the basic definitions and theory for the air pollutants generated by vehicle exhaust are summarised. Particularly, it is pointed out on particle emissions, to introduce to the concept of ultrafine particles described in chapter 3.

Chapter 3: in this chapter the main concepts for ultrafine particles are introduced, with particular reference to Legislation, toxicity, dynamics and lifetime in ambient air.

Chapter 4: This section presents a new methodology for assessing the spatial distributions of the main urban air pollutants at urban scale (stage road-to-ambient)

Chapter 5: This section presents a new approach to link air quality and traffic air pollution at urban scale (stage road-to-ambient).

Chapter 6: This section presents the application of the two above mentioned approaches to the case of ultrafine particles in an urban area (stage road-to-ambient).

Chapter 7: This section presents the analysis of the spatial distribution of reactive air pollutants into a street-canyon (stage tailpipe-to-road).

Chapter 8: This section presents an assessment of ultrafine particles measured near-road (stage tailpipe-to-road).

Chapter 9: Conclusions and future plans are presented in this chapter.

Appendix: This section describes the principal features of the instrument acquired by this Department during this Ph.D. work

CHAPTER 2.
VEHICLE EXHAUST EMISSIONS

2.1. GASES

Diesel and Otto engines (fuelled mainly by gasoline, diesel oil, compressed natural gas, and LPG-liquefied petroleum gas) are actually one of the major source of urban air pollution in developed Countries. Exhausts principally contain: (i) NOx, CO, and HC from Otto engines; (ii) HC, particulate matter, and NOx, from Diesel engines. Sulfur contained into both gasoline (less) and diesel oil (more) is emitted as SO_2 and/or SO_3. If complete combustion takes place, all Carbon in fuel reacts with the Oxygen to form CO_2, and all Hydrogen is transformed into water, according to equation (Eq.1):

$$C_nH_m + \left(n + \frac{m}{4}\right)O_2 \rightarrow nCO_2 + \frac{m}{2}H_2O \qquad \text{(Eq.1).}$$

However, several reasons can modify the completeness of the combustion in relation to the combustion and fuels types. They are: (i) insufficient oxygen and/or air excess available for complete combustion; (ii) inadequate mixing between fuel and combustion air (local air shortages); (iii) insufficient solid fuel pulverisation and/or liquid fuel atomisation; (iv) gas flame cooling due to contact with the combustion chamber walls; (v) too short residence time at high temperatures; (vi) flames burning under difficult geometric conditions (moved up), which let the intermediate products to pass under the flame (and avoid the complete combustion). When hydrocarbons are not completely oxidised by the combustion, exhaust gases contain several intermediate products, such as alcohols, aldehydes, and organic acids, by e.g. equation (Eq.2):

$$\underset{\text{hydrocarbon}}{CH_4} \rightarrow \underset{\text{alcohol}}{CH_3OH} \rightarrow \underset{\text{aldehyde}}{HCOH} \rightarrow \underset{\text{acid}}{HCOOH} \rightarrow CO \rightarrow CO_2, H_2O \qquad \text{(Eq2)}$$

methane *methanol* *formaldehyde* *formic·acid* *carbon·monoxide*

During either an incomplete combustion or an insufficient mixing of fuel and air in flame, part of the fuel can go out unburned with the exhausts. On the other hand, air shortages can cause thermal decomposition processes (pyrolysis). Such decomposition processes can either follow the partial oxidation reaction (Eq2) or bring to the formation of new hydrocarbons via separation of hydrogen atoms. That's the case of the processes forming both the aromatics benzene, toluene and xilene (BTX), and the

polycyclic aromatic hydrocarbons (PAH). According to this polycyclic formation, the reaction process can be summarised as it follows: (1) addiction of smaller aliphatic compounds and cycling into hydroaromatic hydrocarbons with medium size molecules; (2) transformation of hydroaromatic hydrocarbons into totally aromatic hydrocarbons; (3); formation of bigger polycyclic aromatic hydrocarbons starting from the smaller ones. If the hydrocarbon-containing fuel is heated with no oxygen, thermal decomposition processes can take place (as said), with hydrogen progressively separating and soot becoming the final product, namely agglomerates of elemental carbon and hydrocarbons (Figure 5).

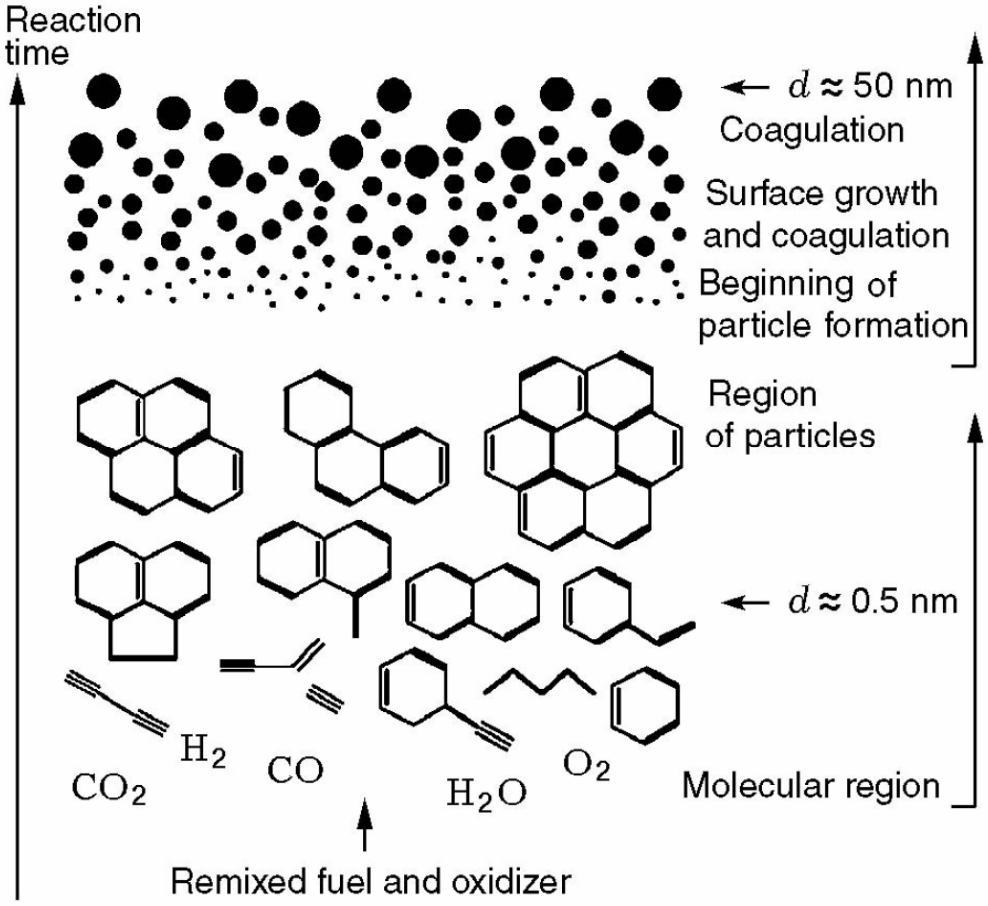

Figure 5. Schematic diagram of soot formation in homogeneous systems or in premixed flames [Reproduced from Mansurov, 2005].

2.2. PARTICULATES

Ambient particulate matter PM is composed of a heterogeneous mixture of particles varying in size and chemical composition. Particles differ in sources, size ranges, formation mechanisms, and chemical composition and are characterized by various physical and chemical properties. While physical properties affect the transport and

deposition of particles in the human respiratory system, chemical composition strongly influence their impact on health [e.g., El-Fadel, 2000]. Particles can be emitted directly from such sources and are commonly referred to as primary particulates, or formed in the atmosphere from gaseous precursors and are called secondary particulates. The chemical complexity of PM requires that sources of a large number of primary and secondary components be considered. Although a number of national inventories have been developed for primary anthropogenic fine particulates [e.g., UK APEG 1999], a detailed particulates emission inventory for Europe that has been developed is that by TNO [Berdowski et al, 1997]. Figure 6 shows the source contributions in the original, as published, TNO inventory.

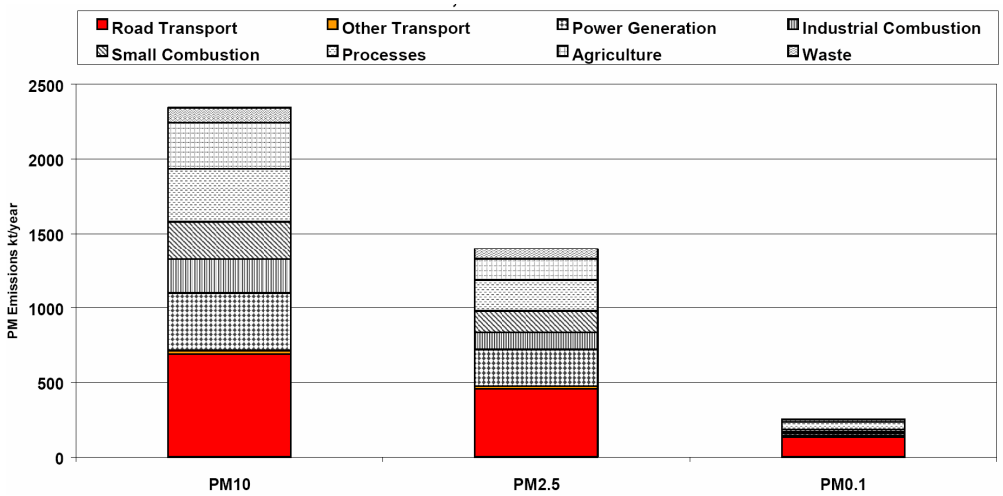

Figure 6. EU-15 Primary Anthropogenic Particulate Emission Inventory [Reproduced from TNO (Berdowski et al, 1997)].

A more recent estimate of ambient PM concentrations in European cities is shown in Figure 7.

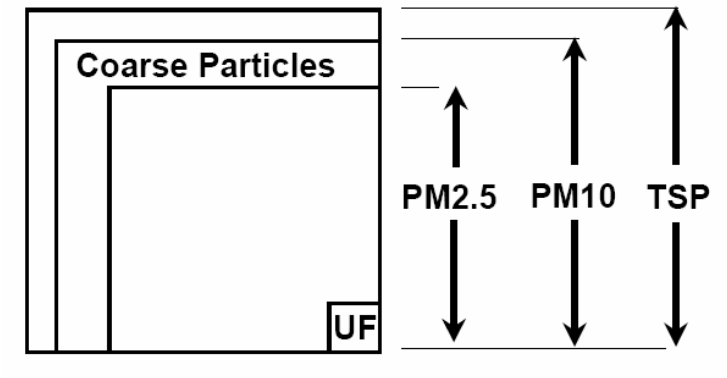

Figure 7. The areas of the respective squares roughly show the relative contribution of the respective fractions to current ambient PM concentrations in European cities [Reproduced from: *Englert (2004)]*

Diesel particulates are defined by the US Environmental Protection Agency (EPA) as "all compounds collected on a pre-conditioned filter in diluted diesel exhaust gases at a maximum temperature of 325 K (125°F)". These particulates consist of soot nuclei (carbon) including inorganic material, adsorbed hydrocarbons (often referred to as SOF: soluble organic fraction), SO, (or sulphuric acid) and some water [Neeft et al., 1996]. A schematic representation of the composition is given in Figure 1 and Figure 8. The size of the individual soot spheres is 5÷25 nm and the size of the total particulates is ≈200 nm.

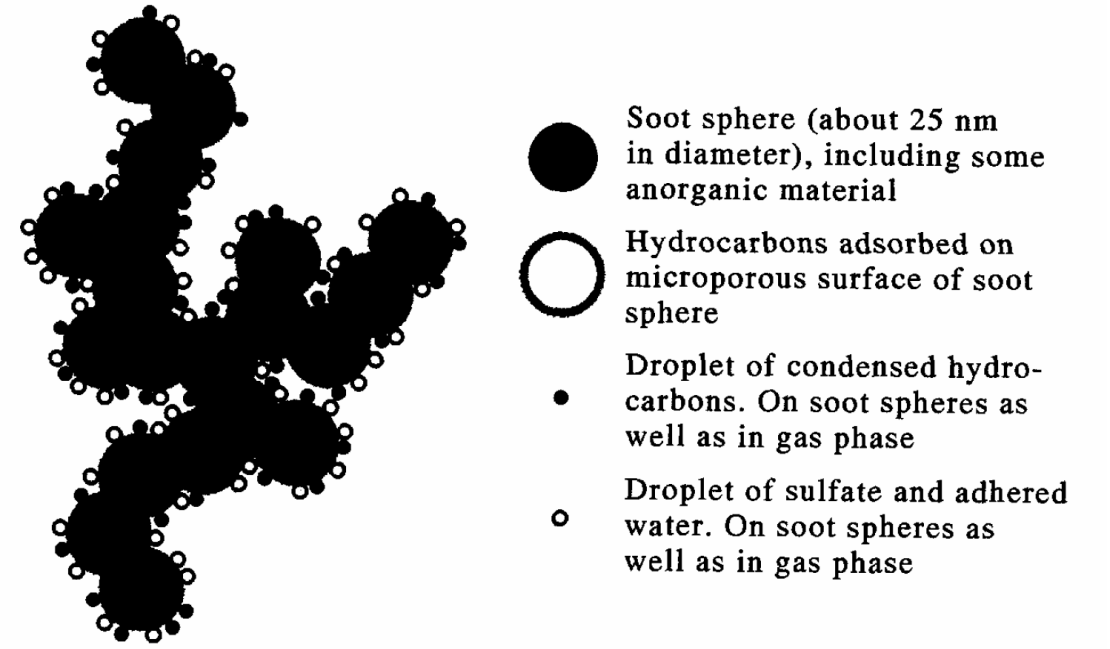

Figure 8. Schematic of Diesel particulates [Reproduced from Neeft et al. (1996)]

Soot formation occurs in the high temperature, fuel-rich reaction zone around individual fuel droplets, where fuel hydrocarbons are oxidized under substoichiometric oxygen conditions [Neeft et al., 1996]. In this reaction zone the oxidation reaction is limited by the oxygen concentration. Oxygen transport occurs by diffusion through the flame front for diffusion flames. Conversely, for premixed flames there is the combustion of a premixed amount of fuel and air. Temperatures in premixed flames are higher than in diffusion flames. As NO, formation depends strongly upon temperature and oxygen concentration [see, e.g., Seinfeld 1986; Bosch and Janssen 1987], premixed flames give rise to much larger NO, emissions than diffusion flames.

The formation of soot is thought to take place via a number of elemental steps: pyrolysis, nucleation, surface growth and coagulation, aggregation and oxidation.

These processes take place on different time scales, ranging from a few microseconds (initial nucleation processes) to some milliseconds (completion of soot formation, oxidation, and cooling by cylinder expansion). Pyrolysis is the process in which gas-phase molecules form soot precursor molecules by free radical mechanisms. Nucleation is the process in which soot precursor molecules grow into small soot nuclei. Surface growth is the process in which the precursor molecules grow from some l-2 nm to l0-30 nm. Aggregation or chain-firming coagulation, which starts at 0.02-0.07 ms after nucleation [Smith et al, 2001a], accounts for the formation of the well-known “fractal” structure of soot. Oxidation of soot also takes place, lowering the soot tail-pipe emission.

The composition of particles from the exhausts depends on where and how the sampling takes place. At the tailpipe, where high temperatures occur, most of the volatile material is in gaseous form. The details of the dilution and cooling processes determine the relative quantity of materials either adsorbing or condensing onto existing particles or nucleate to form new particles [Kittelson, 1998]. These issues are better described in the par.2.3.

2.3. ULTRAFINE PARTICLES

The internal combustion engine emits large amounts of submicrometer PM into the atmosphere. Particles emitted from engines, especially diesel, were firstly categorized by Kittelson (1998) into three general size ranges for steady-state operation. The so-called nuclei-mode (D_p <50 nm) contains as much as 90% of the emitted particles, although due to their small size only up to 20% of the total mass. Nuclei-mode particles are formed primarily of volatile organics and sulfur compounds that nucleate during post-engine dilution and cooling. Metallic compounds and elemental carbon make up some of these particles as well. The so-called accumulation-mode (50 nm < D_p < 500 nm) is made up of fewer particles, but their larger diameters result in the largest mass percentage of the emitted particles. Accumulation-mode particles are formed from carbonaceous agglomerates and through condensation and coagulation of volatile material. The larger particle mode (D_p > 500nm) contributes the least number and mass to particulate emissions (especially diesel) and is comprised of accumulation mode particles that have agglomerated while deposited on engine and exhaust surfaces. Engine pulse, vibration, and exhaust flow re-entrain these particles, resulting

in coarse mode emissions. These three groups of particles form trimodal distributions. In principle, it may be assumed that exhausts come out of the tailpipe with a single log-normal aerosol size distribution (combustion-induced, [Zhang and Wexler, 2004]). It takes 1-3 sec to reach a dilution ratio of 1000. Assuming C_{crit} as the gas-phase concentration of sulphuric acid required for binary nucleation to take place [Wexler et al., 1994], when the critical ratio $H_2SO_4(g)/C_{crit}$ becomes greater than 1, nucleation occurs instantaneously giving birth to fresh nuclei in another log-normal distribution (dilution-induced, [Zhang and Wexler, 2004]). Nucleation results when partial pressure is much greater than vapour pressure for nucleating species[1]. The partial pressure is simply proportional to the dilution factor. The vapour pressure is a function of temperature, which in turn is a function of dilution factor, f. As f decreases rapidly upon dilution immediately after emission, the supersaturation ratio may become high enough to induce nucleation. At the same time, due to their volatility and the existence of large surface areas of particles in the plume, sulphuric acid and many organic compounds condense quickly on the particles, which may or may not suppress

[1] All solids and liquids have a tendency to evaporate to a gaseous form, and all gases have a tendency to condense back. At any given temperature, for a particular substance, there is a partial pressure (that is the pressure which the gas would have in a mix of gases if it alone occupied the volume) at which the gas of that substance is in dynamic equilibrium with its liquid or solid forms. This is the vapor pressure of that substance at that temperature (that is the pressure of a vapor in equilibrium with its non-vapor phases). Vapor pressure is an indication of a liquid's evaporation rate. It relates to the tendency of molecules and atoms to escape from a liquid or a solid. A substance with a high vapor pressure at normal temperatures is often referred to as volatile. The vapor pressure of any substance increases non-linearly with temperature according to the Clausius-Clapeyron relation. Creation of liquid droplets in saturated vapour is also characterised by nucleation. (Source: http://en.wikipedia.org/wiki/Vapor_pressure)

the nucleation. Since nucleation favors compounds with both low volatility and low-molar volume in the condensed phase, high-carbon number organics which usually possess very low vapor pressure but have significantly larger condense-phased molar volume, are less likely to be the nucleating species than sulfuric acid, which may take a binary form (with water) or ternary form (with water and ammonia). Extremely rapid dilution is crucial for obtaining supersaturation where nucleation is possible. Decreases of temperature lead to exponential decreases in vapor pressures. The dilution profile mainly dependent on vehicle types and traffic conditions may also affect the occurrence of nucleation.

Knowledge of the detailed PM size distribution of an engine's emissions is crucial for the development of emission control devices. Nuclei-mode particles are most responsive to diffusion forces, and coarse-mode particles are most responsive to interception and inertial impaction. However, the majority of accumulation-mode particles is only marginally responsive to any of the aforementioned forces and is often responsible for the minimum efficiency of each of the currently existing filter types [Hinds, 1982]. Although PM size distributions have been generalized for steady-state conditions, subsequent studies have shown that during transient operation, changing engine parameters strongly affect both the size distribution and the concentration of emitted particles [Liu et al., 2005]. As after-treatment devices are integrated into diesel exhaust systems, the transient emission response could alter their effectiveness. Measurement of an engine operating transiently is more difficult, however, because both the speed and the load of the engine change as a function of time. These factors result in changing the air/fuel ratio, mixing pattern, and in-cylinder temperature, which in turn influence the formation and composition of PM inside of the engine [Heywood, 1988]. Additionally, the dilution and cooling of the exhaust are effected by the changing engine conditions, thus altering the particles in the exhaust stream.

2.3.1. DIESEL ENGINE

The particle size distribution of diesel exhaust typically displays two modes, accumulation and nucleation modes [e.g.: Ronkko et al., 2006; Kittelson, 1998]. The accumulation mode in the vehicle exhaust is not sensitive to dilution conditions [Kittelson et al., 2002; Maricq et al., 2002]. Liquid nucleation mode particles are usually smaller than 50nm in diameter and form during dilution of exhaust gas. Thus

the formation is sensitive to dilution parameters such as dilution ratio, temperature and relative humidity of the dilution air, and the exact development of temperature and instantaneous partial pressures of vapours during dilution. The tendency of nucleation has been connected with high sulphur or high hydrocarbon content in exhaust gas. Therefore, the formation of nucleation mode particles indirectly depends on engine parameters, fuel and lubricant oil properties, and after-treatment systems. A number of studies report enhanced nucleation mode formation with increasing engine load [Vogt et al., 2003; Mathis et al., 2004a; Giechaskiel et al., 2005]. Giechaskiel et al. (2005) and Vogt et al. (2003) have linked higher nucleation mode concentrations at high engine loads to higher exhaust gas temperatures and thus to enhanced SO_2 to SO_3 conversion in oxidation catalysts [Maricq et al., 2002]. Also sulphur content of fuel affects the nucleation [Khalek et al., 2003; Vogt et al., 2003; Ntziachristos et al., 2004]. On the other hand, Kittelson et al. (2002), Saito et al. (2002) and Lehmann et al. (2003) have reported increased tendency of nucleation at low loads. Vaaraslahti et al. (2004) found nucleation mode with a catalyst and a particle filter at high load, but without after-treatment at low load. They proposed the two cases represent two different processes of nucleation mode formation. At high load the process is sulphur dominated, while at low load the hydrocarbon species are important. At low loads the hydrocarbon concentration in exhaust gas is high and the SO_3 concentration low. The high air-fuel ratio at low loads keeps temperatures low and combustion inefficient, favouring hydrocarbon formation. At low exhaust gas temperatures the possible oxidation catalyst is inefficient in oxidizing hydrocarbons and SO_2. In addition, Mathis et al. (2004b) have shown by laboratory experiments that hydrocarbons have a clear effect on nucleation mode concentration.

New particle formation is very likely in the first-stage dilution of diesel exhaust and occurs when the dilution ratio is around 30–80; the growth of nucleation mode particles could be significant and is very sensitive to the amount of condensable materials remaining in the gas phase at tailpipe exit; coagulation is usually too slow to significantly change aerosol size distributions in this stage.

Liu et al. (*2003*) also explained that low exhaust gas temperatures, occurring during idle and declining loads, create favorable conditions for the formation of nuclei-mode particles. In addition to exhaust conditions, previous studies [Vaaraslahti et al., 2004; Shi et al, 1999; Ronkko et al., 2006] have positively correlated the formation of nuclei-mode particles to unburned hydrocarbon emissions during low and declining

load conditions. Finally, Liu et al. (2007) have also seen nuclei-mode particles occasionally forming during accelerations. Heywood (*1988*) explained that if over-fueling occurs during acceleration, hydrocarbon emissions will be increased. As the engine load and EGT increase, volatile compounds have less opportunity to nucleate, and more accumulation-mode particles are emitted due to higher fuel consumption inside of the cylinder [Kittelson, 1998 ;Heywood,1988]. This is especially true for increasing load conditions such as accelerations, which do not exist in steady-state analyses. Finally, several bimodal distributions have appeared throughout the FTP cycle of a Diesel engine and are usually seen during quickly changing engine conditions (Figure 9). When the engine is accelerating, decelerating, or the load and EGT are changing from increasing to decreasing, or vise versa, conditions are often favorable for both types of particles to form.

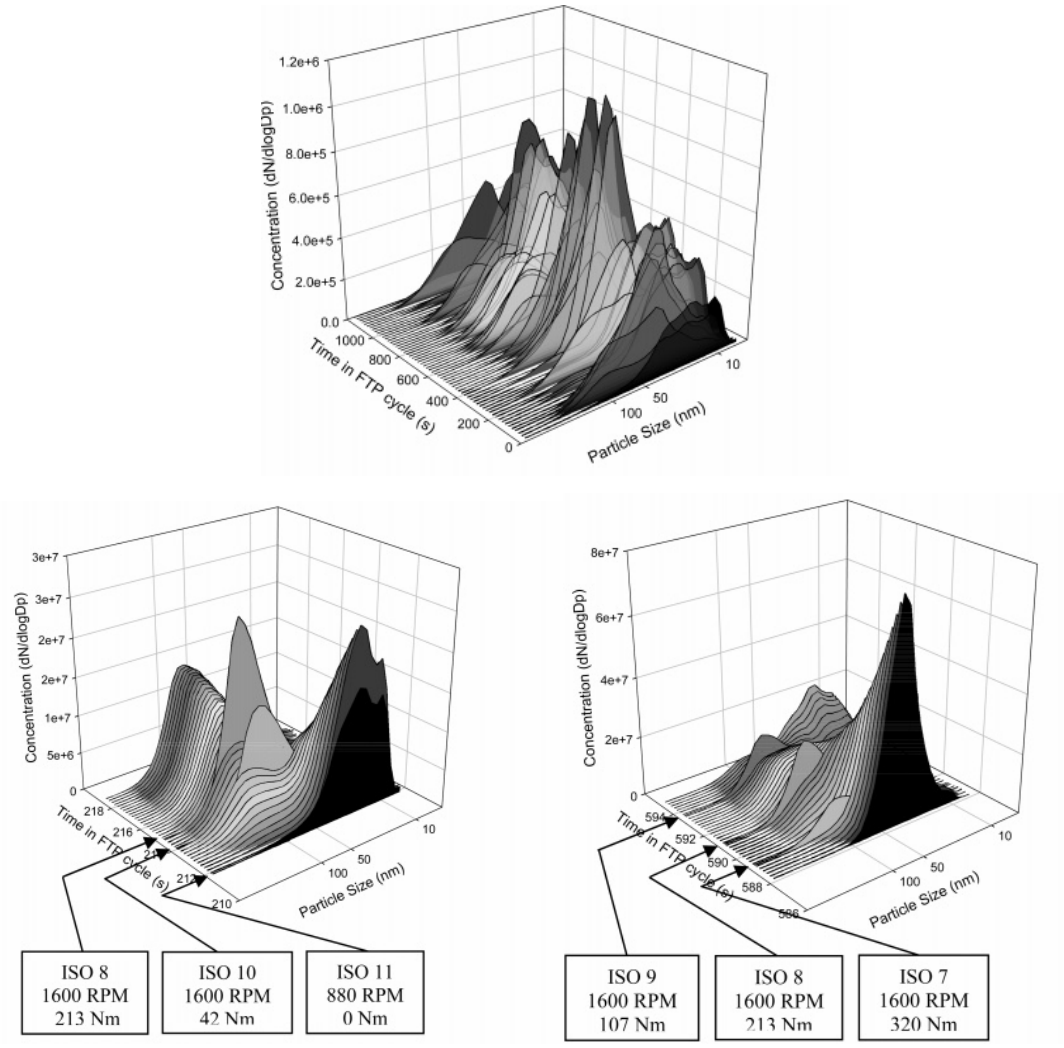

Figure 9. Particle size distribution of a Diesel engine throughout the FTP HD cycle (top), during an acceleration (bottom left) and during a deceleration (bottom right) for transient 2 test as compared to the particle size distributions produced from steady-state testing (a-c) [Reproduced from Liu et al., 2007]

The relative magnitudes of these modes then depend on the precise load, speed, fuel consumption, and EGT at the time of particle formation. The results of these quickly changing conditions rarely can be seen during steady-state testing.

2.3.2. SI ENGINE

Laboratory studies [CONCAWE, 1998; Graskow et al.,1998; Greenwood et al.,1996; Hall et al., 1998; Maricq et al., 1999a,b; Rickeard et al., 1996] have shown that nanoparticle emissions from SI engines are much more speed-and load-dependent than diesel engines. Gasoline engine exhaust particles are thought to be usually smaller than those emitted by diesel engines, mainly in the nuclei mode region [e.g., Kittelson et al., 2006a,b; Graskow et al., 1998]. They are often composed primarily of volatile and semivolatile materials, although ash may be the major constituent in some cases. Lube oil may play an important role in their formation.

The mechanism of particle formation in gasoline engines is very different from that in diesels and not as well understood. In a gasoline engine, fuel and air are premixed before combustion and combustion takes place under chemically correct conditions. In a diesel engine combustion initially takes place in a fuel-rich jet that subsequently continues to oxidize as it mixes with air. The primary combustion process in a gasoline engine should not make particles. Particle formation in a gasoline engine results from local inhomogeneous conditions – fuel pooling, big droplets, cracks, crevices, etc. Formation is much more dependent on operating conditions than with diesel engines, increasing strongly at high loads. During cold starts, the fuel-air mixture in a gasoline engine is very rich, leading to significant EC formation. Gasoline “high emitters” with some combination of high oil consumption and rich operation may produce particles much like those from older diesel engines.

There have been several studies on gasoline engine exhausts conducted by various researchers and no convincing evidences of nucleation have been found yet [Maricq et al., 2002; Zhang and Wexler, 2002b]. It has been arising thus questions whether there are nucleation events in gasoline exhaust at all. Zhang and Wexler (2004) showed that in terms of sulfuric acid concentrations, gasoline engine exhausts still favour nucleation. So very likely nucleation is occurring, but probably the fresh nuclei cannot grow to the detectable size under experimental or real-world conditions. Zhang and Wexler (2002b) proposed the hypothesis that these fresh nuclei have been fully

neutralized by ammonia produced by the catalyst system so that the acid-catalyzed chemical reactions, which are crucial to the early growth of these nuclei, are precluded. Then those small nuclei are easily subject to scavenging by larger particles. So unlike diesel exhaust, the characteristic particle size distributions measured in gasoline exhaust were usually mono-modal with a possible ‘hidden mode’ below the particle size detection limit.

CHAPTER 3.
ULTRA-FINE PARTICLES IN AMBIENT AIR

Whilst PM_{10} (mass of particles with an aerodynamic diameter less than 10 μm) emissions are regulated and there are plans to include regulation of $PM_{2.5}$ (mass of particles with an aerodynamic diameter less than 2.5 μm) in several countries, no regulations exist with respect to submicrometer particles (d<1 μm) or ultrafine particles (UFPs, d<100nm) in terms of particle number (see par.3.1). These particles in ambient air usually show the following modes: “fresh” nucleation mode (3-9 nm) ; “aged” nucleation mode (9-30nm) ; Aitken mode, 30-110nm; accumulation mode, 110-800nm [e.g., Birmili et al., 2001] (Figure 3). Recent health studies [e.g., Sioutas et al., 2005; Oberdorster, 2000, 2001] have shown that UFPs can have a greater adverse effect on men health than larger particles of the same composition since they are capable of penetrating deeper into the respiratory tract (see par.3.2). Furthermore, particle dynamics and lifetime in atmosphere can influence visibility, radiative balance, climate change, with the extent dependent on the size distribution and nature of the aerosols; a better understanding of these effects requires knowledge of the mechanisms by which new particles nucleate and grow in the atmosphere [Kulmala, 2003] (see par. 3.3). These issues are better discussed in the followings.

3.1. LEGISLATION

The COUNCIL DIRECTIVE of 15 July 1980 (80/779/EEC) refers to the determination of black smoke and its conversion into gravimetric units in Annex I. Alternatively, Annex IV refers to gravimetric measurements without specifying the size fraction to be sampled. During the following years, more data on health effects emerged suggesting smaller particles to be more important. The COUNCIL DIRECTIVE 96/62/EC of 27 September 1996 on ambient air quality assessment and management (Framework Directive) listed fine particulate matter such as soot (including PM_{10}), and Suspended particulate matter among the atmospheric pollutants to be taken into consideration. The COUNCIL DIRECTIVE 1999/30/EC of 22 April 1999 (First Daughter Directive) defined limit values for PM_{10} with a Stage 1 to be met by January 2005 and indicative limit values in Stage 2 foreseen to be met by 2010, but

to be reviewed in the light of further information on health and environmental effects, technical feasibility and experience in the application of Stage 1 limit values in the Member States. The scientific background was described in the Position Paper Ambient Air Pollution by Particulate Matter (1997). It stated: "*There is increasing evidence that health effects occur at very low levels of PM, and without an apparent threshold. This evidence arises from studies, initially in the US, but which have more recently been carried out in Europe and elsewhere with similar conclusions. These studies have, in general, used different measures of particles, but the majority have used* PM_{10} *and the Group felt that this was the most appropriate measure for a limit value for particles at the present time*." "*Good reasons might be given for considering other fractions rather than just* PM_{10}*, e.g.,* $PM_{2.5}$*, and there might be an increasing need of such kind of measurements in the future. At present knowledge on health effects of particle fractions is insufficient, and sufficiently standardised measurement methods are not available to provide a sound basis for limit values for particle fractions smaller than* PM_{10}*. As this will probably change in the future, limit values set for* PM_{10} *now may have to undergo revision at a later stage*" [e.g., see Englert, 2004]. WHO (2004) summarizes the results of the Systematic Review of Health Aspects of Air Pollution in Europe as follows: "*Nevertheless, there is sufficient concern to consider reducing exposure to coarse particles as well as to fine particles. Up to now, coarse and fine particles have been evaluated and regulated together, as the focus has been on* PM_{10}*. However, the two types have different sources and may have different effects, and tend to be poorly correlated in the air. The systematic review therefore recommended that consideration be given to assessing and controlling coarse as well as fine PM. Similarly, ultrafine particles are different in composition, and probably to some extent in effect, from fine and coarse particles. Nevertheless, their effect on human health has been insufficiently studied to permit a quantitative evaluation of the risks to health of exposure to such particles*.".

The results of research conducted in the last decade have, therefore, significantly increased the evidence on health impacts of particulate matter (PM). This newly accumulated evidence was used to review and update the WHO Air Quality Guidelines, completed in 2006 and resulting in a set of guidelines for PM_{10} and $PM_{2.5}$ [WHO 2006]. The research data for PM indicate that there are risks to health at concentrations currently found in many cities in developing and developed countries. Moreover, the research has not identified thresholds below which adverse effects do

not occur. In addition to $PM_{2.5}$ and PM_{10}, ultrafine particles have recently attracted significant scientific and medical attention. The Guidelines conclude that, "*while there is considerable toxicological evidence of potential detrimental effects of ultrafine particles on human health, the existing body of epidemiological evidence is insufficient to reach a conclusion on the exposure–response relationship to ultrafine particles. Therefore no recommendations can be provided at present as to guideline concentrations of ultrafine particles*" [WHO, 2006].

3.2. TOXICITY

The health burden due to PM air pollution is one of the biggest environmental health concerns around the world [WHO, 2007]. Airborne particles are associated in epidemiological investigations with a range of adverse health outcomes including increased illness, hospitalizations, and mortality rates [e.g., Dockery et al., 1993; Burnett et al., 2000; Samet et al., 2000; Dockery, 2001; Pope et al., 1995, 2002; Schwartz et al., 2002; Brunekreef and Holgate, 2002; de Hartog et al., 2003]. A particularly vexing research challenge has been identifying the physical and chemical characteristics of PM to determine toxicity.

Adverse health outcomes have been associated with various size fractions within the PM range. Particle deposition in the respiratory tract is determined predominantly by three mechanisms that move particles out of the streams of inhaled and exhaled air towards the airway walls, where they are deposited [e.g., Fell et al., 1997] (Figure 10). These mechanisms are (1) sedimentation by gravitational forces acting on particles > 0.5 μm aerodynamic diameter, (2) impaction caused by their inertial mass in branching airways acting on particles > 1.5 μm aerodynamic diameter, and (3) diffusional motion of particles < 0.5 μm (thermodynamic diameter) by thermal motion of air molecules. Each mechanism becomes relevant for the given size range. The larger thoracic coarse particles are primarily deposited in the nose and in larger airways due to impaction, because they cannot follow the air stream at bifurcations; these particles are filtered out of the air stream and cannot penetrate down to the deep lung. Smaller particles can pass through the large airways and are deposited in the lung due to sedimentation (settlement of particles in resting air due to gravity). These fine particles may preferentially affect the cardiovascular system.

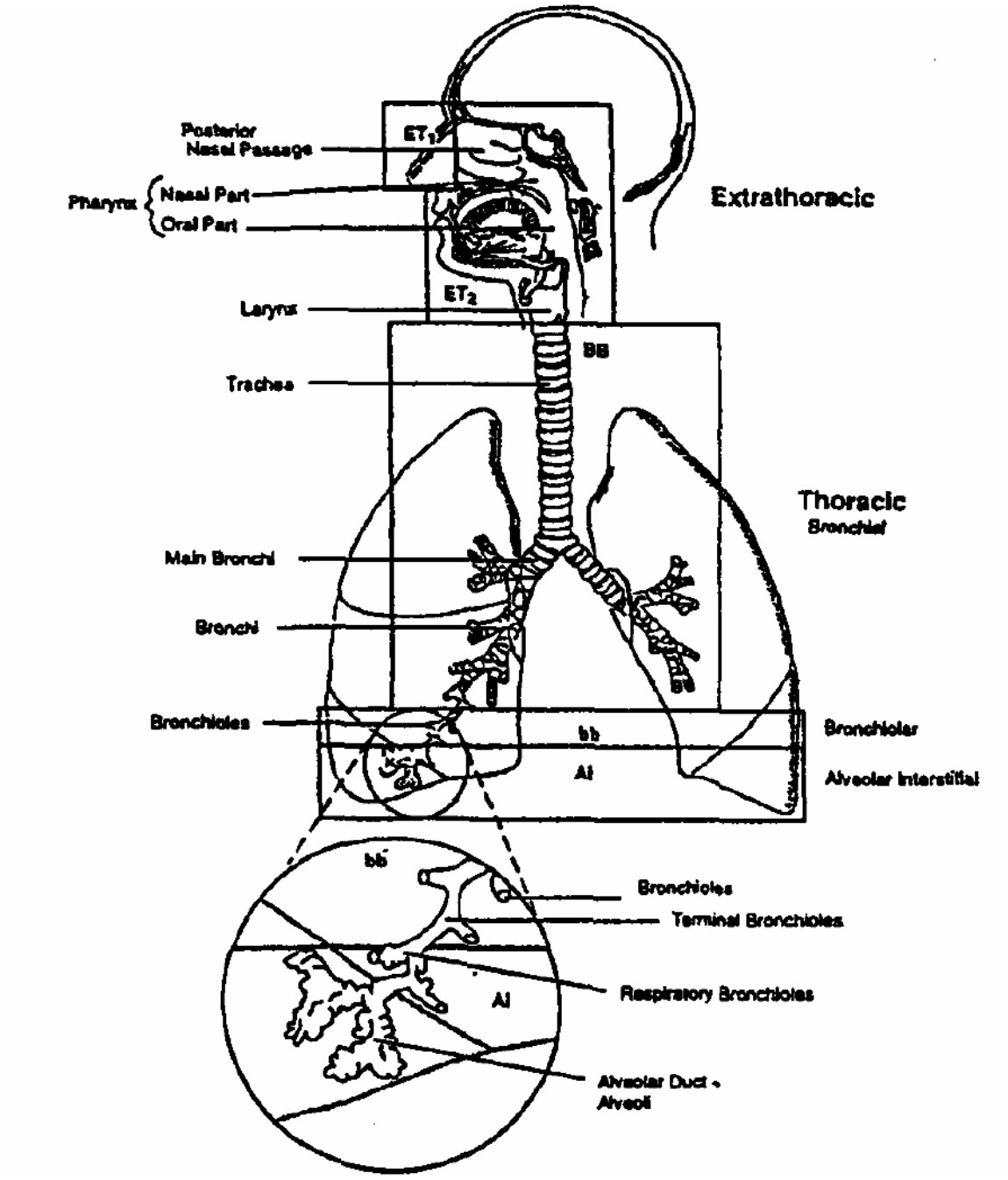

Figure 10. Respiratory tract regions defined in the ICRP publication 66 model [Reproduced from Fell et al., 1997]

Recent health studies have reported that ultrafine particles (UFP) may be responsible for some significant health outcomes, even though they account for a very small portion of total PM mass [Donaldson et al., 1998; Obersdörster et al., 2000; Obersdörster, 2001; Penttinen et al., 2001]. Ultrafine particles (UFP) behave like diffusing gas molecules and stochastically disperse due to Brownian motion (the smaller the particles, the more effective is Brownian motion). They have higher particle number concentration and surface area than larger particles, more insidious as

it can deeply penetrate and deposite much more efficiently than larger particles into the lung cavity [Brown et al., 2002; Jaques and Kim, 2000; Kim and Jaques, 2000; Smith et al., 2001a; Daigle et al., 2003], where they are not efficiently removed by macrophage clearance mechanisms, and may cause mechanical damage to lung tissue [Donaldson et al., 1998; Hughes et al., 1998; Utell and Framptom, 2000; Seaton and Dennekamp, 2003]. UFPs may also migrate via the lung to other locations transported through the blood stream to the heart, brain, liver, spleen, placenta and fetus [Nemmar et al., 2002; Obersdörster et al., 2002]. Another route of internal exposure is translocation of UFP via the olfactory nerve system to the brain [WHO, 2007]..
The health implications of these observations remain unknown, and intensive research continues [WHO, 2007].

3.3. DYNAMICS IN ATMOSPHERE

The study of number distribution can be traced back to the derivation of the general dynamic equation [Gelbard and Seinfeld, 1979] describing the number distribution of an internal mixed aerosol over time. In an Eulerian frame of reference, this equation can be written as (Eq.3) [Zhang and Wexler, 2002b]:

$$
\begin{aligned}
&\frac{\partial n(D_P,x,t)}{\partial t}\langle \text{local rate of change}\rangle \\
&+[V(x,t)-V_s(D_P)k]\cdot\nabla n(D_P,x,t)\langle \text{spatial avvection and gravitational settling}\rangle \\
&=-\frac{\partial}{\partial D_P}[I(D_P,x,t)n(D_P,x,t)]\langle \text{condensation/evaporation}\rangle \\
&+\frac{D_P^2}{2}\int_0^{\infty}\frac{\beta[(D_P^3-D_P'^3),D_p',x,t]}{(D_P^3-D_P'^3)^{2/3}}\times n[(D_P^3-D_P'^3)^{1/3},x,t]n(D_p',x,t)dD_p'\,\langle \text{coagulation in}\rangle \\
&-n(D_P,x,t)\int_0^{\infty}\beta(D_P,D_p',x,t)n(D_p',x,t)dD_p'\,\langle \text{coagulation out}\rangle \qquad \text{[Eq.3]} \\
&+\nabla\cdot[K(x,t)\nabla n(D_P,x,t)]\langle \text{spatial diffusion}\rangle \\
&+N(D_P,x,t)\langle \text{nucleation}\rangle \\
&+E(D_P,x,t)\langle \text{emission}\rangle \\
&+R(D_P,x,t)\langle \text{chemical reaction}\rangle
\end{aligned}
$$

where:

- $n(D_P,x,t)$ = number distribution
- $n(D_P,x,t)dD_P$ = number concentration of particles in the range [D_P, D_P+dD_P]

- $I(D_P,x,t)$ = rate of change of particle diameter (dD_P/dt) due to condensation and evaporation
- $\beta(D_P, D'_P)$ = coagulation coefficient for particles with diameter D_P and D'_P
- x= spatial coordinate vector
- t=time
- V=wind velocity vector
- V_s=settling velocity
- k=unit vector in the vertical direction
- K(x,t)=turbulent diffusivity tensor
- N=nucleation rate of particles in the range $[D_P, D_P+dD_P]$
- E=emission rate of particles in the range $[D_P, D_P+dD_P]$
- R=reaction rate of particles in the range $[D_P, D_P+dD_P]$

In this framework, the dynamics of aerosol in atmosphere, and the lifetime can be analysed in terms of three important steps: [Holmes, 2007; Zhang andWexler 2002a; Kerminen 1999]:

(i) formation of an initial nucleus. New particles, about 1 nm in diameter, are formed by nucleation through a number of different mechanisms (see par.3.3.1)

(ii) Growth of the particles to larger sizes. These particles grow as a result of coagulation with other particles or condensation of gas-phase constituents at a rate dependent on factors including particle size, chemical composition, concentration and temperature (see par.3.3.2).

(iii) Loss. Particle loss occurs through deposition. Settling velocity becomes important when particles are larger than about 1 μm. Vertical transport of aerosol particles is governed by turbulent diffusion, advection and gravitational settling. It is expected that for the smallest particles settling will be negligible compared to vertical turbulent diffusion, but for particles sufficiently large it will be significant. Their spatial distribution (see par. 3.3.3) comes to be a fundamental issue.

3.3.1. PARTICLE FORMATION

The two major processes introducing new particles into the atmosphere are:

- in situ production (nucleation)
- direct emission from sources such as combustion, sea spray, dust, etc.

Particle nucleation in the atmosphere has exercised the minds of scientists since John Aitken built the first apparatus to measure the number of dust and fog particles in the late 19th century. Although several mechanisms for particle nucleation have been proposed, it remains unclear which of them dominates in the atmosphere [Kulmala, 2003; Jung et al., 2006]. Several mechanisms have been proposed including:

(i) homogeneous nucleation involving binary mixtures of sulphuric acid and water [Nilsson and Kulmala, 1998; Vehkamäki et al., 2002],

(ii) homogeneous ternary nucleation (sulfuric acid-ammonia-water) [Kulmala et al., 2000],

(iii) nucleation of organic vapors [Marti et al., 1997; Zhang et al., 2004b],

(iv) ion induced nucleation of binary, ternary, or organic vapors [Laakso et al., 2002],

(v) halogen-oxide nucleation [Hoffmann et al., 2001].

Spontaneous nucleation can occur when the vapor pressure of sulphuric acid exceeds the saturation vapour pressure of the sulphuric acid– water mixture (binary nucleation). However, the rates of nucleation are often much smaller than the observed production, therefore, in the majority of cases new particle formation is dominated by processes other than binary nucleation. However, under certain conditions (industrial plumes) binary nucleation rates of sulphuric acid and water mixtures can still be significant. Classical theory suggests that sulphuric acid cannot exist in free form and is either bound in ammonium bisulphate or ammonium sulphate cluster or hydrates [Holmes, 2007]. Therefore, because of its high concentration in the troposphere and ability to decrease the vapour pressure of sulphuric acid above a solution it has been proposed that the enhanced nucleation rate is a result of a ternary reaction between H_2O/H_2SO_4 and NH3 (ternary nucleation). However, the comparison of the results of the new ternary model with particle formation observations clearly suggests that there must be other so far unknown mechanisms operating. Ionic charge in particles can increase the formation of larger particle as a result of enhanced stability of the charge clusters and higher growth rates due to the electrostatic forces (Ion induced-nucleation, IIN). The mechanism of IIN is still not clear and model simulations are generally based on the assumption that the core consists of negative bisulphate ions and the critical cluster is stabilised by ammonia. All schemes are based on the classical nucleation theory, on which the nucleating molecular clusters are treated as macroscopic droplets—a questionable approach given that the clusters

often contain fewer than 20 molecules; ideally, the nucleation process should be investigated with molecular dynamics [Kulmala, 2003].

3.3.2. PARTICLE GROWTH

Another important issue is what species are involved in the growth of these nuclei. This step is also uncertain [e.g., Stanier et al., 2004]. These particles have been proposed to grow by condensation of sulfuric acid, and self-coagulation. However, these processes are relatively inefficient: the condensation of sulfuric acid alone is often not sufficient to grow these nuclei to detectable sizes, since these particles have a very short lifetime before being lost through coagulation with larger existing particles [Gaydos et al., 2005]. To aid in the growth of these particles, additional growth mechanisms have been proposed, such as the condensation of organic species [Kerminen et al., 2000], heterogeneous reactions [Zhang and Wexler, 2002a], ion-enhanced condensation, heterogeneous nucleation of organic insoluble vapors on ternary clusters [e.g., Kulmala, 2003], activation of the clusters for condensation of soluble organic vapors, chemical reactions at the surfaces of small clusters [Zhang and Wexler, 2002a], multicomponent condensation of organic and inorganic vapors (Figure 2). The limited experimental evidence indicates a potential role for organic compounds [Novakov and Penner 1993; Rivera-Carpio et al. 1996]. Recent work considers the potential for heterogenous reactions of SO_2 [Kerminen 1999] and organic compounds [Kerminen 1999; Jang and Kamens 2001; Zhang and Wexler 2002a] to significantly contribute to growth.

The nucleation and growth of new particles seem to occur almost everywhere in the atmosphere. Ion clusters are always present , and the nucleation of new aerosol particles seems to be controlled by the very initial steps of growth and the competition between condensation and coagulation. The more rapid the condensation growth, the larger the fraction of nucleated particles that will survive. Chemical reactions in the particle phase cannot form new particles, but may cause them to grow or shrink similar to condensation and evaporation.

Coagulation results in the formation of a single particle following a collision between two aerosols. Two physically different cases should be considered: intermodal coagulation and intramodal coagulation. Intramodal coagulation can hardly be important for number distributions except in the case of the extremely high number concentration, such as near emissions or just after a nucleation event. Intermodal

Brownian coagulation may be important for the number distribution of sufficiently small particles (smaller than 0.05 μm)

Coagulation of small particles with large ones will not change the number of large particles, but will reduce the number of small particles. In addition, coagulation onto large particles is similar to condensation in that it may result in significant 'growth' and 'shift'. The diameter of a new particle, D_n, after small particles with diameter D_s coagulating with large particles with diameter D_l, is roughly [Zhang and Wexler, 2002b]:

$$D_n = \sqrt[3]{D_s^3 + D_l^3}\ .$$

Being often $D_l^3 >> D_s^3$, small particles coagulating with large ones will not substantially alter the diameter of the larger particles, which means the shifting speeds are very slow. This 'growth' term can be neglected and coagulation does not significantly affect the size distribution of large particles. The time scale for depletion of the number of small particles due to Brownian coagulation is [Zhang and Wexler, 2002b]:

$$\tau_{coag} = \left| \frac{n^s}{\left(\frac{dn_s}{dt} \right)} \right|$$

Large diffusivities promote coagulation, but the deposition velocity will also become larger. Tiny nuclei are subject to scavenging by preexisting particles and their surface depositions can be neglected. Volatile gases readily condense on particles to make them grow. When particles grow larger, their diffusivities decrease, and so do the coagulation rates, i.e., condensation may suppress coagulation.

The rate at which small particles coagulate with larger ones ($t_{c,g}$) is proportional to the small particle diffusivity, Ds:

$$\tau_{c,g}^{-1} = \frac{1}{D_s} \left| \frac{dD_s}{dt} \right|$$

If $\tau_{c,g}$ is bigger or the same magnitude as τ_{coag} , small particles coagulate before they grow too large and coagulation is important. Otherwise, coagulation can be ignored.

Due to the rate of the process, coagulation is not an efficient mechanism for particle growth under typical urban conditions. It can hardly occur before condensation grows particles too large to efficiently coagulate. Particles tend to coagulate on particles

larger than about 0.05 μm and particles larger than about 0.05 μm do not coagulate onto even larger ones.

Condensation is typically the partitioning of species between the gas and particle phases as the result of concentration differences between the ambient and equilibrium concentrations [Holmes, 2007]. However, due to similarity between the size of the nanometer-sized particles and the gas molecules condensation onto the new particles is best determined by the rate of collisions between the gas molecules and the particles [Lehtinen and Kulmala, 2003].

The term in (Eq.3) describing the condensation can be written by (Eq.4) [Zhang and Wexler, 2002b]:

$$-\frac{\partial}{\partial D_P}[I(D_P,x,t)n(D_P,x,t)]=\left(-\frac{\partial I}{\partial D_P}n\right)+\left(-\frac{\partial n}{\partial D_P}I\right)= \\ =\left(-\frac{\partial I(D_P,x,t)}{\partial D_P}n(D_P,x,t)\right)+\left(-\frac{\partial n(D_P,x,t)}{\partial D_P}I(D_P,x,t)\right) \quad \text{[Eq.4]}$$

The first term on the right-hand side of Eq.2 is the ‘growth’ term, which is caused by a gradient in I over D_p, $\frac{\partial I}{\partial D_P}\neq 0$.The second term on the right-hand side of Eq.2 represents the ‘shift’ in the distribution due to condensation and evaporation. As condensation proceeds, the particle diameter becomes larger and the distribution ‘shifts’ to the right. In case of evaporation, the curve ‘shifts’ to the left.

Condensation and evaporation do not change the total number of particles in an aerosol population, but they may alter the distribution, leading to “growth” of number distribution.

Volatile gases tend to evaporate from the surfaces of small particles and condense on larger ones. Particles larger than about 2 μm are not affected significantly by condensation and evaporation.

3.3.3. SPATIAL DISTRIBUTIONS

Particles typically form during the late morning and then grow throughout the day, reaching growth rates of 1 to 20 nm/hour [Kulmala, 2003]. Various field measurements have been conducted to measure the particle number concentrations near roadways and dilution is found to be the dominant mechanism that alters particle number concentrations [Shi et al., 1999; Zhu et al., 2002; Zhang et al., 2004]. When a plume dilutes, every small parcel of air contains a certain fraction *f* of the original

exhaust, and *1-f* of the ambient, being *dilution factor=f*, and *dilution ratio=1/f* [Zhang and Wexler, 2004]. The plume concentration for inert species [Kerminen and Wexler, 1995] and the aerosol number concentration experiencing a dilution process [Zhang and Wexler, 2004], can be given by:

$$C_i = C_{i,A} + f \cdot (C_{i,E} - C_{i,A})$$

and

$$\frac{1}{f} = \frac{C_{i,E} - C_{i,A}}{C_i - C_{i,A}}$$

Similar equations govern aerosol number concentration, *n(Dp, t)*, experiencing a dilution process:

$$n(D_p,t) = n_A(D_p,t) + f \cdot [n_E(D_p,t) - n_A(D_p,t)]$$

and

$$\frac{1}{f} = \frac{n_E(D_p,t) - n_A(D_p,t)}{n(D_p,t) - n_A(D_p,t)}$$

where:

C_i = plume concentration for inert species,

$n(D_p,t) = n$= aerosol number concentration,

A=ambient,

E= exhaust.

Turbulence dilutes the exhaust. Consider an exhaust parcel emitted from the tailpipe (dilution stage 0), dispersing to the background; this parcel experiences two very distinct dilution processes [Zhang and Wexler, 2004]: first it is diluted by the strong turbulence generated by moving traffic, moving it from tailpipe to roadside (dilution stage 1: tailpipe-to-road), and then by atmospheric turbulence induced mainly by wind and atmospheric instability, moving it from roadside to the ambient (dilution stage 2: road-to-ambient). Although dilution is the most important mechanism in altering pollutant concentrations in both stages, the magnitudes are conspicuously different (Table 1). The relative dilution magnitudes can be quantified by comparing turbulence dissipation rates in the two stages, namely ε_{mt} and ε_{atm}, respectively. Dissipation is characterized by u^3/l, where u is the characteristic speed and l the characteristic length scale. For turbulence generated by moving traffic, the characteristic speed and the length scale are the speed and the height of moving vehicles, respectively. For

atmospheric turbulence, wind speed is the characteristic speed and the integral length scale of atmospheric turbulence close to the ground is about 50–100m [Baker, 2001].

First stage dilution (indicated by 1/f and ε) is much stronger than the second one so that the first stage dilution is almost independent of atmospheric conditions, while mainly depending on traffic speed and road conditions. This traffic-generated turbulence dominates dispersion near highways and its importance for initial dispersion of pollutants has been recognised [Rao et al., 2002].

Previous field studies and laboratory experiments have analysed such distinct dilution stages. At stage 1, it has been found (i) dilution ratio ~ 1000 or more reached 1-2 sec behind tailpipe [Kittelson, 1998]; (ii) dilution ratio increased exponentially to 350 within 2.54 m downwind exhaust outlet in wind tunnel simulation of HD trucks, within 0.5 sec [Kim et al., 2001]; (iii) dilution ratio=1000-4000, 2-3 m away from passing vehicles in less than 1 sec [Shi et al., 2002]. At stage 2, (i) particle concentrations at 10 m from highway <3.5 times as much as those 700 m from highway [Kittelson et al., 2004]; (ii) particle concentrations 2m from curbside ~4 times higher than 30-100m away [Shi et al., 1999]. It is worth mentioning that, however, processes other than dilution often affect the spatial variation of concentration from exhausts to ambient. This, therefore, result in a more complicated relationship. The analysis of this issue is the major objective of this work, and is discussed in the followings.

CHAPTER 4.
ROAD-TO-AMBIENT: AIR POLLUTION SPATIAL DISTRIBUTIONS[2]

4.1. INTRODUCTION

During the last decades a growing body of research has investigated worldwide the extremely vast subject of urban air quality [e.g.: Fenger, 1999]. Monitoring any potential effect of any urban air pollutant requires a high number of joint measurements. Diffusive sampling technique has been proposed for multiple purposes [e.g.: Ferm and Svanberg, 1998; Fagundez et al., 2001; Kimmel and Kaasik, 2003; Cox, 2003] including traffic-related pollutant evaluation [e.g.: Lebret et al., 2000; Janssen et al., 2001], and spatial distribution (*mapping*) of air pollutants [e.g.: Atkins and Lee, 1995; Krochmal and Kalina, 1997]. However only a few of all these studies has been conducted in urban environments, often limited to deployment of low sampling-density measurement sites and to determination of only one to three species (mostly NO_2, SO_2).

Urban air pollution is usually represented as time series of the pollutant concentrations. In this respect, pollutant frequency distributions (FD) have been intensely studied since 70ties [e.g.: Choch et al., 1975; Bencala and Seinfeld, 1976].

[2] This chapter was published in the paper: Costabile et al., 2006 / Atmospheric Environment 40 (33), 6380-6395. The text was rearranged to fit the format of this dissertation.

Many types of probability distributions have been used to fit air pollutant concentration data: lognormal [Mage and Ott, 1984; Kao and Friedlander, 1995], Weibull [Georgopoulos and Seinfeld, 1982], pseudo-log-normal [Mage, 1984] and Type V Pearson [Morel et al., 1999]. As time series, air pollutant concentration data collected at each station are usually characterized by a strongly right-skewed uni-modal FD [Georgopoulos and Seinfel, 1982]. Consequently, even if no one FD is always the best data representation, the log-normal is clearly a useful one and is selected most often [Bencala and Seinfeld, 1976; Georgopoulos and Seinfel, 1982; Ott, 1990]. Nevertheless, systematic studies concerning FD of space series of air pollutants [Lee, 2002; Orlinski, 2002], and particularly the Normal distribution (NFD), are scarce in literature.

This chapter reports some of the results of a work carried out in Suzhou (2.07 million people), one of the top-ten cities of China [Costabile et al., 2006a] with the objective to preliminary assess major air pollutants in an urban environment in order to infer source contributions and frequency distributions.

4.2. METHODOLOGY

The sampling was carried out during August and October 2003. 900 samplers of SO_2, NO_x , NO_2 and 300 samplers of BTX were taken for this work by using Analyst® diffusive samplers. They were located around 100 sampling locations systematically selected over the study area with a protocol that mainly defines how representative these sites are. Sites located near known sources reflect the impact of these sources on the locations [Costabile et al., 2006b]. Statistical data processing was performed using SigmaStat 3.0 and SigmaPlot 9.0 software packages. The data set, consisting of n elements (n=1.200), was treated as a 3-dimensional statistical sample defined by Eq.5:

$$x = x_{ijk};\begin{cases} i \in [NO_2; NOx; SO_2, Benzene, Toluene, Xylene] \\ j \in [0 \ldots 99] \\ k \in [1...3] \end{cases} \qquad \text{(Eq.5)}$$

where: i = air pollutant; j = site ID; k = campaign ID; x = concentration of the air pollutant i at site j during the k^{th} campaign. Frequency distribution (FD) were calculated for each $\bar{i}$ and $\bar{k}$ fixed varying j. R, the correlation coefficient (covariance divided by the product of the sample standard deviations) was calculated for each fixed $\bar{k}$ to measure the relationship between each couple of columns

$x_{i1,\bar{k}} = \left(x_{i1,0,\bar{k}} \ldots x_{i1,1,\bar{k}} \ldots . x_{i1,99,\bar{k}}\right)^T$ and $x_{i2,\bar{k}} = \left(x_{i2,0,\bar{k}} \ldots x_{i2,1,\bar{k}} \ldots . x_{i2,99,\bar{k}}\right)^T$ of the variable x_{ijk} (eq.1), for each i_1 and $i_2 \in \left[NO_2; NOx; SO_2, Benzene, Toluene, Xylene\right]$. To secure a correct form of statistical evaluation, 15-days averaged data were tested for frequency and normality of distribution. The Kolmogorov-Smirnov test was used to investigate the data Normality [Pardo-Iguzquiza and Dowd, 2004]. According to this test: (1) K-S distance represents the maximum cumulative distance between the histogram of measured data and the Gaussian distribution curve of data; (2) *P* value is the probability that the population of data measured is Normally distributed, namely P values for the significance level are used to determine whether there is a statistically significant difference in the mean values of the measured data and normal distribution. If the *P* computed by the test is greater than an acceptable level of significance $\overline{P}$, the data can be considered Normal. The value of $\overline{P}$ was set to 0.05 [Lu and Fang, 2002], where α=0.05 is the acceptable probability and $100 \cdot (1-\alpha)$=95% the confidence interval, assuming no significant discrepancy at the 5% significance level between the estimated and measured distributions of pollutants. The same procedure was used to investigate the Lognormal distribution (LnFD). It is important to note that this *P* value does not affect the value of K-S distance but explains if the difference in the mean values of the groups is due to chance or due to random sampling variation.

Air pollutant concentrations $x=x_{ijk}$ (Eq.1) are presented for each pollutant i broken down by exposure type of sampling locations in the form of box plot graphs (Figure 11). The results of the Kolmogorv-Smirnov normality test are shown in Table 2.

Three important points should be kept in mind when one reads the experimental data discussion that follows below. First of all, all of the sampling sites were located in proximity of significant emission sources of the urban area due to our aim to investigate the source-receptor relationship. The closer is the sampling site to a local emission source, the clearer is the influence of such source upon the related air pollutant concentration field. Therefore, the data showed give information on whether the location of these sources or the impact they make in their immediate environment. Secondly, diffusive samplers can only integrate exposures to give a cumulative value of all the hourly fluctuations in pollutant gas concentrations. Therefore, they are suitable to describe the spatial distribution of air pollutants even though temporal trend inside the integration time cannot be directly determined. Finally, the seasonal

variability certainly showed up in the data is however limited because based on campaigns over only three adjacent periods.

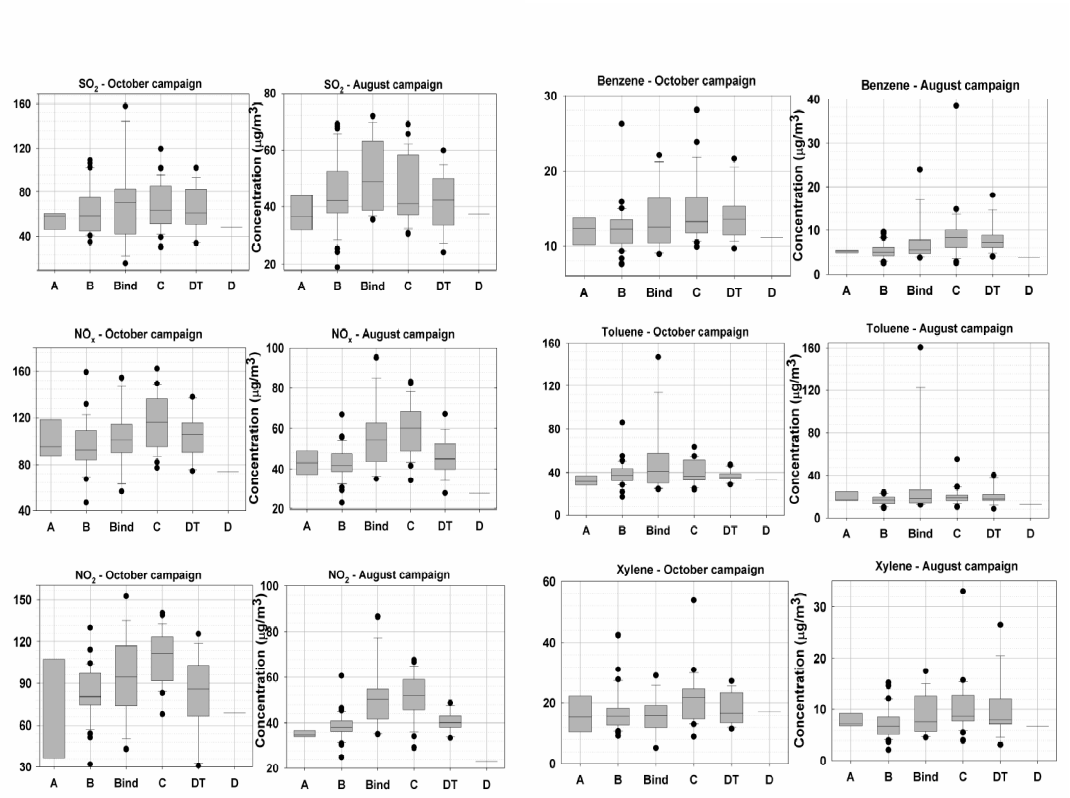

Figure 11. Boxplot graph of NO_2, NO_x, SO_2, and BTX concentration data (in $\mu g/m^3$) measured in Suzhou in 2003 broken down by type of sampling stations exposure in October (third campaign) and August (average of first and second campaign). A= urban background; B=residential area; Bind=industrial area; C= heavy traffic; DT= downtown area; D=non urban background [Reproduced from Costabile et al., 2006a].

4.3. FACTORS RELEVANT FOR THE VARIABILITY OF CONCENTRATIONS

Among the common factors to whom spatial concentration variations should be attributed are, first of all, dispersion and diffusion conditions of pollutant concentrations. The variable wind direction in October caused the concentrations to be more spatially diffused than in summer (when wind direction was constant); on the contrary, the higher wind speed in August should have caused each emission to be more dispersed contributing to the local lowering of concentrations (particularly evident for BTX). The enhanced diffusion is likely the reason why K-S distance of the NFD Kolmogorov-Smirnov test (Table 2) was lower for all the pollutants in October;

the exception of SO_2 was likely due to the combination of increased number of emission sources (in-building use of coal) and decreased dispersion of each source (as better discussed below).

Campaign ID	Pollutant	NORMAL FD			Ln-NORMAL FD		
		K-S DISTANCE	P VALUE	TEST RESULT ($\overline{P} = 0{,}05$)	K-S DISTANCE	P VALUE	TEST RESULT ($\overline{P} = 0{,}05$)
1		0,160	< 0,001	Failed	0,125	<0,001	Failed
2	**NO_2**	0,125	< 0,001	Failed	**0,080**	**0,136**	**Passed**
3		**0,074**	**> 0,200**	**Passed**	0,136	<0,001	Failed
1		0,099	0,023	Failed	**0,038**	**>0,200**	**Passed**
2	**NO_x**	0,118	0,003	Failed	**0,068**	**>0,200**	**Passed**
3		**0,078**	**0,175**	**Passed**	**0,078**	**0,168**	**Passed**
1		**0,081**	**0,151**	**Passed**	**0,046**	**>0,200**	**Passed**
2	**SO_2**	**0,087**	**0,082**	**Passed**	**0,050**	**>0,200**	**Passed**
3		0,118	0,003	Failed	**0,055**	**>0,200**	**Passed**
1		0,266	< 0,001	Failed	0,107	0,010	Failed
2	Benzene	0,205	< 0,001	Failed	0,123	0,001	Failed
3		0,159	< 0,001	Failed	0,102	0,018	Failed
1		0,328	< 0,001	Failed	0,172	<0,001	Failed
2	Toluene	0,324	< 0,001	Failed	0,168	<0,001	Failed
3		0,184	< 0,001	Failed	0,103	0,016	Failed
1		0,372	<0,001	Failed	0,120	0,002	Failed
2	Xylene	0,173	< 0,001	Failed	0,096	0,028	Failed
3		0,125	< 0,001	Failed	**0,061**	**>0,200**	**Passed**

Table 2. Results of the Kolmogorov-Smironov test for normality of data measured in Suzhou in 2003

Different chemical processes due to different meteorology should also have relevantly influenced FDs, particularly for NO_2 and Xylene, being further causes of the differences among their Summer and October FDs relative to both NFD and LnFD. Additionally, in this respect, it may also be explained the FD dissimilarity of NO_2 among the two summer campaigns, which had meteorological conditions slightly different: slightly higher wind speed during the second one and different range of ambient temperature that are very important in facilitating the quick transformation of these compounds [Abdul-Wahab and Al-Alawi, 2002]. The Benzene temporal variation rather different from Xylene and Toluene during the second summer campaign, as well: it may likely be attributed to a Benzene enrichment due to the increased solar radiation, wind speed and air mixing that enhanced Xylene and Toluene reactivity. After being photo-destructed, Toluene and even more the isomers of Xylene may have reacted with other atmospheric constituents; Xylene, particularly,

may have exhibited intense photochemical activity due to its ability to give stable free radicals by photolysis [Pilidis et al., 2005]. As a results they were less abundant in relation to Benzene, the less reactive molecule due to its stable structure [Heywood, 1988]. Finally, the topography of sampling points (street canyons, enclosed yards, open space, etc.) should be considered, since it should have also strongly influenced the concentration fields.

4.4. VARIATION OF AIR POLLUTANT CONCENTRATIONS

Sulphur dioxide

As likely expected [Bencala and Seinfeld, 1976], the LnFD always fits the data (Table 2). However, the fit with the Normal distribution is acceptable for both the August campaigns, as well. On the contrary, in October the FD is more peaked (Kurtosis higher) and asymmetric (Skeweness > 0), tailed on the right with a greater number of outliers, and the IQ increased 1.5 times. The change in "normality" behavior between October and August may be explained considering that SO_2 emissions vary by season as the consumption of fossil fuel products changes with ambient weather conditions [Smith et al., 2001b]. Seasonality is important since the conversion of sulfur dioxide into sulfate aerosol vary by season due to changes in the chemical composition of the atmosphere, level of solar radiation, and climate. These changes can lead to a much higher sulfate burden in summer months, even though emissions are generally higher in winter. China has a significant contribution to emissions from the direct use of coal in buildings. These emissions together with the fraction of electricity used in buildings can be assumed to be temperature-dependent. As a consequence, inconstant seasonality results in variable annual-average sulfate burden in the atmosphere. The concentrations were broken down by district and analysed with respect to nearby industrial emission sources: no statistical evidence of higher concentrations in one or more districts was found. On the contrary when the concentrations are broken down by representativeness of emission sources (Figure 11) a clear tendency is evidenced. Maximum values were obtained at industrial locations. The contribution of residential areas, heavy-traffic streets and downtown locations depends on the micrositing parameters of each sampling station, and it's not clear which is the second emission source in order of importance.

Nitrogen oxides (NO2 and NOx)

Contrarily to August, in October both NO_2 and NO_x FDs may be assumed to be Normal (even if LnFD is acceptable for NO_x, its P value is lower than the NFD, Table 2). In fact, the FD asymmetry with small tails on the right showed in August (characteristic of LnFDs) was not shown in October, when Skeweness and Kurtosis were ~0. Additionally, the negative Skeweness of NO_2 (the only case) didn't allow for the Lognormality. The enhanced October FD symmetry may be associated to a bigger tail on the left represented by the lowest concentrations measured at either urban/non-urban background or residential locations. The increased spatial diffusion of concentrations during the third campaign, due to the increased wind direction variability above all, was likely the reason why FDs were Normal. The highest concentrations were measured at high-traffic streets, followed by industrial and downtown locations (Figure 11). These findings may probably explain the diversity of causes generating seasonality of SO_2 and Nitrogen oxides concentrations, and FDs as well, as evidenced by the Normality tests (tab.3): the former showed a NFD in Summer, the latter in October. The seasonal variability of Nitrogen oxides in atmosphere is a general phenomenon [Atkins and Lee, 1995] and was also measured in our study (though limited, as said): a clear seasonal cycle is particularly evident if one considers concentration medians and ranges. The seasonality in emissions from power stations should also be considered: their plumes may be emitted above the boundary layer, generally higher in summer, causing them to reach the ground. Also the increased fuel consumption in buildings with decreased temperature is likely to partially contribute to the higher October concentrations. However, this small seasonality in emissions cannot explain alone whether the lower summer concentrations or the differences between NO_2 and NO_x FDs or the LnFD unacceptability for NO_2, as well . Thus, some other factors should have contributed. Lower wind speed, rainfall, temperature and solar radiation in October were certainly an important factor leading to the higher Nitrogen oxides concentrations; however, seasonal variability in the chemical removal of NO_2 should also be considered. This aspect is complex because of the interaction between photochemistry and dry and wet removal processes of oxidised nitrogen, and HNO_3 formed in the atmosphere from the reaction of NO_2 with OH radicals, which are at higher concentration in the summer. The reduced photochemical activity expected in October due to the lower OH radicals concentrations was probably a further factor that contributed to the higher and more diffused concentrations measured in this month, as well as to the decreased

asymmetry and "peakedness" of their FDs fitting the NFD. The only four sites where the concentrations of NO_2 decreased in October are associated with high ozone concentrations measured: the reaction of NO_2 with O_3 became much more important at those sites. Likely such processes (less relevant for NO_x) may also have influenced the LnFD unacceptability for NO_2 during all the campaigns, with the exception (though the low P value) of the second one characterised by the highest wind speed, namely the highest dilution of air pollutants.

Toluene

Toluene is a ubiquitous aromatic compound in urban air emitted from fuel evaporation, combustion processes, architectural surface coatings, graphic arts, industrial solvents and chemical feedstock [Monod et al., 2001]. Probably that's the reason why its FD is very peaked (Kurtosis 20÷30, much greater than inorganic compounds), especially in August (tab.3) when the diffusion was lower. FDs of all the sampling campaigns are highly asymmetric with a greater number of values smaller than the mean (Skewness 4÷5) and are far from both NFD and LnFD found for Nitrogen oxides and Sulphur dioxide, sampling conditions being equal. The non Normality indicates the presence of one or more predominant factors that influenced the spatial concentration distributions. They are likely correlated to the presence of significant emission sources that produced at least the three frequency classes lying out of NFD and LnFD. The highest class was measured around a fine chemical industry. The second one is represented by heavy-traffic emissions. These two frequency classes were found for all the sampling periods. The anomalous frequency class (70÷86 $\mu g/m^3$) found in October were likely due to the fact that wherever at the north-east side of the urban area toluene concentrations were highly influenced from the industrial emission source. However, due to the toluene atmospheric lifetime (1.9 days) [Monod et al., 2001] and to the continuous sampler exposure for 15 consecutive days, a significant fraction of the air sampled didn't contain freshly emitted pollutants. These air samples have had the time to accommodate all possible kinds of chemical reactions among BTX compounds [Pilidis et al., 2005] and manifest their potential photochemical activity [Vardoulakis et al., 2002], especially considering that the sampling points were not very far from the emission source. That should be carefully considered in evaluating the real influence of this industrial emission source upon the concentrations of whether Toluene or Benzene and Xylene (nevertheless significantly lower).

Benzene

Benzene showed data not much spatially distributed: the variation range of 90% of the exposed samplers was up to 10 $\mu g/m^3$ with a few, but important, much higher values making the FD different from the NFD indeed (tab.3). These highest concentrations were measured at high-traffic sites like in summer. The impact of industrial emissions though relevant (Figure 11) was less important during this campaign: no peak value was measured close to such sources. And this may likely have contributed, among the other factors, to the lowering of the K-S distance in October compared to August (Table 2): the FD is much less peaked (Kurtosis value is a fifth), more symmetric around the mean (Skeweness value is a third) and distributed around higher values. Meteorology strongly influenced its Normality behaviour indeed, so as for the other pollutants. However, Benzene value relative to the hydrocarbons reactivity scale is 0 [Heywood, 1988]. Thus, its concentration ubiquitous in urban air so as for Toluene [e.g. Monod et al., 2001] more depends on meteorological conditions, all other factors (emission source strength, distance between source and receptor, topography) being equal. Meteorology changes from August to October, particularly wind direction, should have caused the concentrations to increase at high-traffic sites, and decrease close to a crossroad as well. The highest concentrations largely measured close to high-traffic emissions (Figure 11) clearly indicates that the main source of Benzene in the urban area of Suzhou comes from motor vehicles, though industrial sources were also relevant. A further evidence of that is likely provided by the high values measured at downtown locations and assumed to be generated by the same source.

Xylene

The highest values of all the campaigns were measured at sites close to traffic emissions (Figure 11) mainly in the middle of the city; on the contrary, the lowest values were measured out of the urban area and far from traffic roads. Thus, xylene behaved in a way similar to benzene, its main emissions coming at Suzhou from traffic sources (high values also measured at downtown locations, Figure 11). The Normality behaviour of its FD is comparable to Benzene as well (Table 2), even if the evident differences were likely due to a further factor being considered: photochemistry. Far from local source influence, in urban and suburban areas, Xylene was lower compared to benzene; moreover, its concentrations spread over a range larger than Benzene indicating as they decay at different rates due to OH-oxidation in

the atmosphere [Monod et al., 2001]. This may have influenced the acceptability of the LnFD found in October only for Xylene and not for Benzene (or Toluene). The comparison between Xylene R with Nitrogen oxides and BT (they are almost the same only in October) may be whether a further evidence of the shared traffic sources or an indication of causes generating such xylene LnFD. Considering its very short atmospheric lifetime (less than 24 hours [Monod et al., 2001]), the high concentrations measured at some sites only for xylenes should have been emitted unavoidably by a local source (combustion processes or evaporation of fuel or others [Sigsby et al., 1987]) not emitting Benzene and Toluene indeed. If compared to NO_x and NO_2, this is a further indication of the higher variability (type and number) of BTX sources in Suzhou that may have influenced their FDs deviating from the Normality.

4.5. NORMALITY OF FREQUENCY DISTRIBUTIONS

In principle, since extreme high concentrations are possible but negative values are not, air pollutant FD is always non-Normal and tends to be log-normal, as explained by the theory of successive random dilution [Ott, 1990]. However, the FD type of air pollutant concentration is a special case in every area [Lu, 2002] being influenced by several factors, such as emission levels, meteorological conditions, chemistry, geography and local morphology. LnFD was not always suitable to fit FDs of our study (Table 2): except SO_2 and NO_x, it was never fitting for BT and only once for the most reactive compounds, namely NO_2 and Xylene. In contrast, FDs of both NO_2 and NO_x in October and SO_2 in both the Summer campaigns were significantly fitted (95% confidence interval) by the NFD. Different seasonality of different emission sources and different chemical removal processes may likely be considered as primary reasons of the dissimilar spatial diffusion (and thus FDs) of SO_x and Nitrogen Oxides, all the other factors being equal. The presence of relevant emission sources of Toluene (the fine chemical industry above all) and Benzene, not sufficiently diffused by the weaker wind speed in October and the constant wind direction in August, may likely explain why BTX presented a most peculiar distribution around the mean rather different to a NFD. Similar results for BTX were obtained by Pilidis et al. (2005) in Europe.

The findings relative to FD Normality may be important in understanding the spatial characteristics of these pollutants. The long integration time (15 days) may be

considered likely to explain it. Moreover, air pollutant concentrations are expressed in this work as space series at different time periods rather than time series at different locations; thus, the predominant factors influencing their FD may likely be associated to the diffusion mechanisms in atmosphere, rather than mixing and diluting of source emissions (relevant for LnFD [Ott, 1990]). Every process where the pollutant space series show a NFD, in fact, should satisfy the diffusion equation and thus may likely represent such a mechanism [Buccianti et al., 2003].

4.6. REPRESENTATIVENESS OF MEASUREMENTS

Most epidemiological studies have used ambient air monitoring data as surrogate for the exposure of the population of interest [e.g., Cyrys et al., 2004]. Exposure has been often characterized with one city average concentration, by using the air pollution data from a single monitoring site or the average of observations from a few monitoring sites to represent the whole population of the study area [e.g., Chen et al., 2007]. A common assumption is that certain pollutants are homogeneously distributed in space within a large urban area. However, several recent studies have found that, in some areas, there may be greater variation within a city than previously reported [Briggs, 2000; Zhu et al., 2002; Ito et al., 2004; Kim et al., 2005; Pinto et al., 2004; Wilson et al., 2005; Costabile et al., 2006a]. The validity of ambient concentrations as an accurate estimate of exposure has, therefore, raised concerns because exposure misclassification could lead to substantial bias in exposure response relationships [Hoek et al., 2002; Monn, 2001]. However, the issue of representativeness of air quality measurements has been overlooked in the past, and the lack of a quantitative method to describe this concept results often in inconsistent comparison for air quality data among different sites [e.g., Costabile et al., 2006b]. Before considering a field measurement, a broader scientific understanding of the behaviour of the spatial variability of air pollutants in an urban atmosphere is probably required.

This paragraph focuses on a work [Costabile et al., 2006d; Allegrini and Costabile, 2008] carried out in the city of Lanzhou (about 3 million inhabitants, West China), one of the most seriously polluted cities in the world due to its special geographical location, weather conditions and large amount of emissions from coal-fired factories [e.g., Xia et al., 2008; Qi et al., 2001; Xu, 2003; Ta et al., 2004]. The major objective was to investigate intra-urban variations of the major gaseous pollutants in both space

and time, and in relation to the representativeness of locations where to measure air quality. With reference to the work previously described in Suzhou, the aim was here to test the influence of seasonality through a yearly period, as well as the use of the effective sample size to test the data normality instead of the total number of observations [Costabile et al., 2006a]. Almost 800 samplers of SO2, NOx, NO2 and BTX were taken by using Analysts diffusive samplers, along with four seasonal campaigns on a yearly basis (2005-2006). The data set comprised between the maximum and minimum values (thus not including the outliers) were tested for statistical Normality of the FD in order to evaluate the statistical model describing it (Table 3). The outliers values were calculated by the equation 6 [Buccianti et al., 2003]:

$$\text{Outlier} = \begin{cases} IF > 75_{th} + 1{,}5 \bullet IQ \\ IF < 25_{th} - 1{,}5 \bullet IQ \end{cases} \qquad \text{[Eq.6]}$$

where IQ indicates the interquartile range, that is:

$$IQ = 75^{th} \text{ percentile} - 25^{th} \text{ percentile.}$$

With only one exception, all the space-series passed the Normality test indicating that the dataset matches the pattern expected if the data was drawn from a population with a Normal distribution. The only exception of Benzene in Spring should be due to those elements conditioning air pollutant diffusion, and thus FD and its Normality:, such as meteorology, relevant emission sources, emission seasonality , and photochemistry [Costabile et al. (2006]. This result is very important in understanding the characteristic of the spatial trend of the main air pollutants in an urban area. Known the Normality of the pollutants' FDs, the concentrations measured at the fixed stations can, therefore, be used to reconstruct the spatial variations in concentration levels occurring for each pollutants along the study area (Figure 12).

For Normally distributed pollutants in space the choice of the site where to monitor air quality for health-effects studies may be less critical [Monn, 2001]. Mean and median values (quite same) can correctly be used to represent the concentration values of these pollutants all over the city for air quality management purposes. Another obvious benefit of understanding of the spatial variation of pollution concentration is to use this knowledge for the assessment of the efficiency of the urban monitoring network and for the modification of the network to improve the efficiency. The very high correlation between concentration levels of pollutants measured at different

locations and lying on a Normal FD let to identify areas of the city representative of different concentration levels.

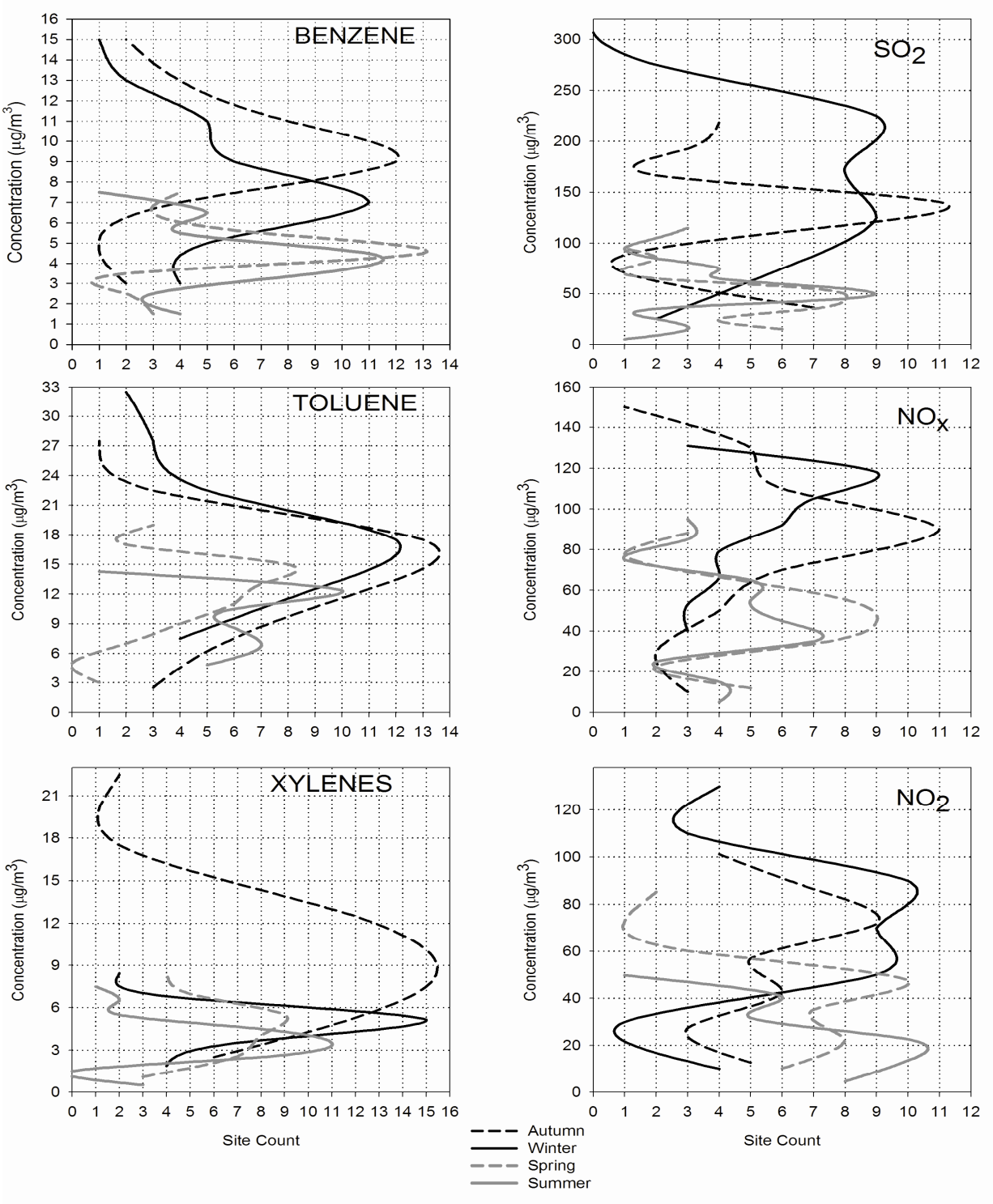

Figure 12. Frequency distributions in space measured during the four seasonal campaigns in Lanzhou

Therefore, the knowing of the pollutants' spatial distribution model can significantly enhance the understanding of the representativeness of measurements, and consequently the process of designing the locations for field measurements.

Table 3.Normality Test for the total data without outlier in Lanzhou

Pollutant	campaign ID	K-S Distribution	Probability	Test result
Benzene	I	0,122	> 0,200	Passed
	II	0,099	> 0,200	Passed
	III	0,152	= 0,046	Failed
	IV	0,086	> 0,200	Passed
Toluene	I	0,071	> 0,200	Passed
	II	0,132	= 0,120	Passed
	III	0,089	> 0,200	Passed
	IV	0,118	> 0,200	Passed
Xylenes	I	0,084	> 0,200	Passed
	II	0,124	> 0,200	Passed
	III	0,085	> 0,200	Passed
	IV	0,088	> 0,200	Passed
SO_2	I	0,115	> 0,200	Passed
	II	0,078	> 0,200	Passed
	III	0,079	> 0,200	Passed
	IV	0,114	> 0,200	Passed
NO_x	I	0,100	> 0,200	Passed
	II	0,136	= 0,068	Passed
	III	0,075	> 0,200	Passed
	IV	0,095	> 0,200	Passed
NO_2	I	0,117	= 0,195	Passed
	II	0,071	> 0,200	Passed
	III	0,088	> 0,200	Passed
	IV	0,083	> 0,200	Passed

CHAPTER 5.
ROAD TO AMBIENT: LINKING AIR QUALITY TO TRAFFIC EMISSIONS[3]

5.1. INTRODUCTION

In the design of cost effective abatement strategies it must be realized that the relations between emissions and resulting concentrations are by no means simple. A lot of research has been done to investigate this issue. Most of the emission factors used by the emission inventories to quantify traffic contribution upon total emissions originate from laboratory measurements carried out according to specific measure and driving protocols [e.g. Hausberger et al., 2003]. On the opposite, pollutant concentrations have been measured on the road to infer emission profiles and rates [Querol et al., 2002; Shi et al., 1999]: besides temperature and humidity, these results strongly depend on wind speed and direction, and, therefore, on the temporal variation of dilution rate; they account for a mix of vehicles indeed. To remove the effect of wind, measurement stations inside tunnels have been used. However, distribution profiles of not all the pollutants measured in such a way can represent ambient air conditions [Sturm et al.,2003]. In order to solve these issues and obtain also results that can discriminate emitting vehicle type, whether chasing experiments on the road

[3] This charter was entirely published in the paper: Costabile et al., 2008/ Environmental Modelling & Software, 23 (3), 258-267. The text was rearranged to fit the format of this dissertation.

[e.g.: Kittelson et al., 2002; Vogt et al., 2003] or simulation of exhaust dilution in ambient air [e.g.: Sasaki and Nakajima, 2002; Maricq et al., 2002] have been carried out. However, a further improvement in the knowing of this relationship is needed. Measurements are still the foundation of our understanding, but application of mathematical and physical modeling is of increasing importance in urban air pollution management [Fenger, 1999]. Such models can be further developed to form full decision support systems [e.g., Dennis et al., 1996] to be integrated with measurements [e.g.: Carras et al., 2002; Schmidt et al., 1998].

This chapter reports some of the results of a big project on-going in Beijing (China) aimed at analysing the relationship between urban traffic and air quality [Costabile et al., 2008]. The objective was to assess a new framework which allows the communication between transport emissions and air pollutant concentrations, as well as address a need of continue research. It would also provide policy-makers with valuable lessons learned regarding transportation programs which promote economic development while reducing pollution impacts.

The methodology developed was based on the analysis of the source-receptor relationship relative to traffic air pollution and can be broadly divided in four stages, namely, requirement analysis, system design, system implementation, and system testing. That is detailed in the paragraph 5.2. Five are the main operation strategies: (1) set up of a transportation and dispersion model simulating the mobility of different scenarios and calculating motor vehicle emissions and air quality; (2) measurement of pollutant concentrations in ambient air; (3) measurement of traffic-generated emissions; (4) monitoring of traffic sources; (5) management of public transport. The final result is an integrated system, which would link traffic and air quality measurements through different modeling modules in order to automate transport-related air pollution assessment. The essentiality of each stand-alone component relative to all the others, its clear functionalities and targets, as well as the integration of measurement and modelling tools result in the key-feature of the system. That is detailed in the paragraph 5.3.

5.2. SYSTEM DESIGN, IMPLEMENTATION AND TESTING

The main system components are: (1) a Data Centre (DC) for the integrated management of the system which incorporates a traffic-environmental modelling tool

(TEM); (2) a network of air quality monitoring stations (AQMS); (3) a network of private traffic monitoring stations (TMS); (4) a Public Transport Management Subsystem (PTMS). The modelling tool, TEM, runs air quality calculations aimed at identifying strategies and actions to manage private and public transport.

The measurement data are provided by the integration of TMS and AQMS. TMS is composed of sensors for the measurement of traffic flow (both private and public) and composition (type of vehicle, polluting labels, number of plate, etc.), as well as traffic emissions (on the road remote sensors and analysers); thus, in case of traffic restrictions TMS could identify grossly polluting vehicles [Costabile et al., 2008] and record the plates of vehicles entering sensible areas. The AQMS core-module measures the air pollutant concentrations to input the whole system; it is composed of monitoring stations representative of traffic air pollution equipped with automatic and manual apparatuses for the measurement of selected gaseous and particulate air pollutants and meteorological parameters [Costabile et al., 2006b]. The spatial representativeness of the AQMS, requested to guarantee the reliability of air quality measurements, is mainly defined by the protocol used to select its measurement locations (network design): the sites are located in relation to known traffic sources to reflect their impact on the measurements [Costabile et al., 2006a]. Finally, the PTMS seeks to optimize the public transport fleet management (optimization of operational tasks, routes and vehicles allocation, bus load optimization) and improve the service quality by sharing of information, over and above service planning and dispatching procedures, real time fleet management of public transport service (via GPS localization of buses) and real time information to the public. The four components form the basic structure of the system, but there are a number of interface modules within each components providing the link between the various air quality and transportation tools; the number of interface modules may vary between the components and a future development of the framework can easily accommodate more of them.

The relationship between these components mainly defines the framework to link transport and air quality. The measured data of both air quality and public/private traffic flows input the TEM where the transportation model calculates the traffic-generated emissions and the dispersion model calculates the concentrations throughout the interested areas. Should the system determines pollution levels which exceed the target values, sensible areas of the city can be banned to pollutant vehicles

and transformed in low emission zones where to provide extra public transportation. Therefore, the system would allow competent authorities to perform the following action scheme (Figure 13): (1) to receive air quality data through the integration of measurements (AQMS, TMS) and modelling (TEM) tools; (2) in case of high level of pollution to ask the local authorities to authorize traffic restrictions for polluting vehicles; (3) to manage the TMS to control that polluting private vehicles do not enter the restricted areas; (4) to provide extra public transportation by the PTMS to compensate for private traffic restrictions. By keeping track of date, time and other relevant data generated every time such a scheme is activated, it would be possible to create the basis for a scientific study on the relationship between air pollution and traffic restrictions countermeasures.

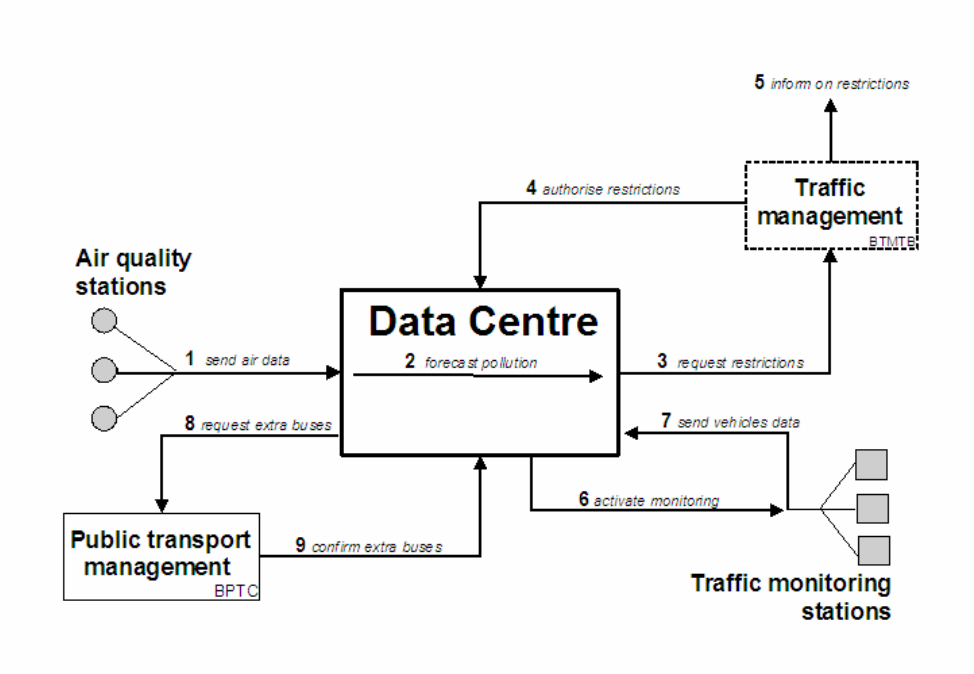

Figure 13. Action scheme of the Beijing ITS-TAP project [Reproduced from Costabile et al., 2008a]

System testing was performed from 2003 to 2004 through a feasibility study for the mega-city of Beijing whose main outcome was the planning of an Intelligent Transport System based on the control of Traffic Air Pollution (ITS-TAP).

5.3. RUNTIME INTEGRATION OF MODELLING AND MEASUREMENTS

In view of the complications and uncertainties remaining in the high-resolution urban air quality modelling, most of the assessments of human exposure to date have used measurements, not modelling. Software has been developed to integrate transportation

and dispersion models [Lim et al., 2005]; some applications have been designed for specific models [Namdeo et al., 2002] while others require considerable computing resources on a client-server architecture [Schmidt and Schafer, 1998]. However, only measurements cannot solve the air pollutant concentration field of an urban environment. The system implementing the methodology presented in this paper seeks to provide high time and space resolution measurements of both air pollutant concentrations and traffic emissions, as well as real-time transportation and dispersion modelling of those data. The traffic flows measured are continuously elaborated by the transportation model to generate known linear emission sources; the emissions calculated are diffused by the dispersion model to simulate the air pollutant concentration field that is continuously compared with the real-time measurements provided by the AQMS in order to train and validate the models with a back-propagation scheme. In such a way the system would be able to foreseen pollutant concentrations and analyse the concentration field with good accuracy. Thus, the key advantage of the system would be the runtime integration of measurements and modelling. Moreover, since the dispersion modelling is known to be time-consuming (particularly in the data preparation and analysis stages), our methodology would significantly reduce the pre- and post-processing time (especially for the model validation) by the integration with the measurements. Different traffic scenarios can be quickly evaluated to screen out those that may be unfeasible; conversely, beneficial scenarios can be identified and then fully tested using whether air pollution or congestion targets, or rather a combination of them.

As described in the previous chapter, the approach to input models with air pollutant concentration data measured by a single air quality station as a surrogate for the daily level of air pollution of a city can be highly misleading. Each urban areas is characterised by several air pollution exposure zones, and each pollutant by different spatial distributions. Thus, at least one monitoring station representative of each of the above mentioned zones must be included in the AQMS module [e.g.: Costabile et al., 2006a,b; Costabile et al., 2008]. Furthermore, besides emissions and meteorology the air pollutant concentration field of each exposure zone depends on its particular urban topography and morphology, and relative atmospheric chemistry; thus, more measurement points should be selected in each exposure zone. It is worth mention that an accurate assessment can’t consider all the monitored pollutants at the same time, but a different analysis should be performed for each pollutant. Our system seeks to

address such micro-design criteria including more monitoring stations differently equipped for the measurement of different pollutants to be representative of different zones.

Road transport is distinguished from other sources of air pollution in that the emissions are released in very close proximity to human receptors [Colvile et al, 2001]. This reduces the opportunity for the atmosphere to dilute the emissions which would render them less likely to damage human health. Furthermore, in most city centre atmospheres, the vehicle exhaust concentrations are significantly enhanced by the fact that many roads have buildings alongside; the effect of such buildings is to shelter the road reducing the wind speed at the source of emissions by as much as an order of magnitude relative to that on an open road [e.g.: Costabile et al., 2006c]. The contribution of emissions from traffic on that road to the kerbside pollutant concentrations is increased by approximately the same factor. Thus, it seems necessary to monitor on the road by the TMS the pollutant emissions to be compared with the pollutant concentrations measured by the AQMS. Despite the very large uncertainties in all evaluations of air quality impacts, the traffic source monitoring is an essential item of such kind of systems since, as before said, the pollutant concentrations from road traffic sources tend to exhibit much more spatial variability than those from non-road networks. Therefore, one of the main outcome of the integrated system here discussed is its suitability to give detailed information about traffic emissions and sources to determine which combination of fuel type, engine type and end-of-pipe emissions abatement technology is likely to be most effective at reducing impacts on human health [Colvile et al, 2001].

CHAPTER 6.
ROAD TO AMBIENT: ULTRAFINE PARTICLES AT URBAN SCALE

6.1. INTRODUCTION

The major objective of this part of the work was to collect and analyse a data-set of UFP number concentration in a middle-size urban area of Italy (Parma) with the aim to study valuable connections with local traffic sources [Costabile et al., 2007b].

A Water-Condensation Particle Counter (WCPC,TSI Mod. 3781, Figure 14 and Figure 15) [e.g., Petäjä et al., 2006; Hering et al., 2005; Hering and Stolzenburg, 2005; Biswas et al., 2005] was used to measure the number concentration of particles in air with diameter larger than 6 nm (and smaller than 3 μm), $N_{6,}$

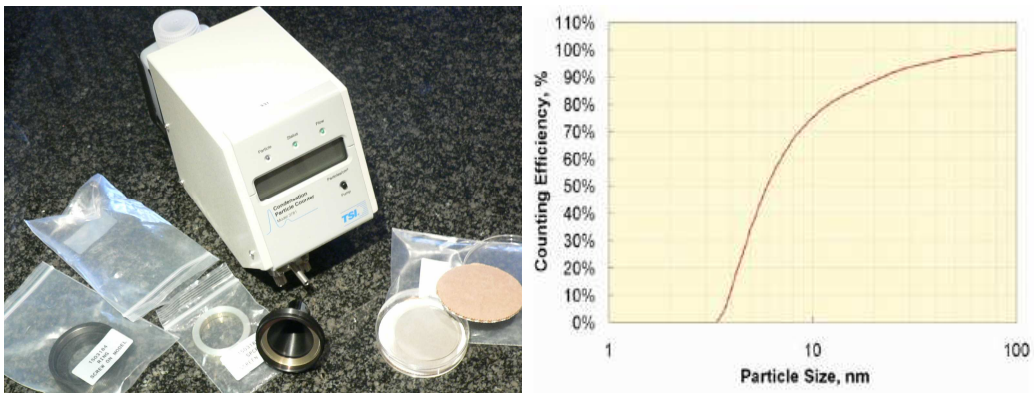

Figure 14. Picture and counting efficiency of the Water-Condensation Particle Counter (WCPC,TSI, Modello 3781) [Reproduced by: TSI, operating manual, 2006]

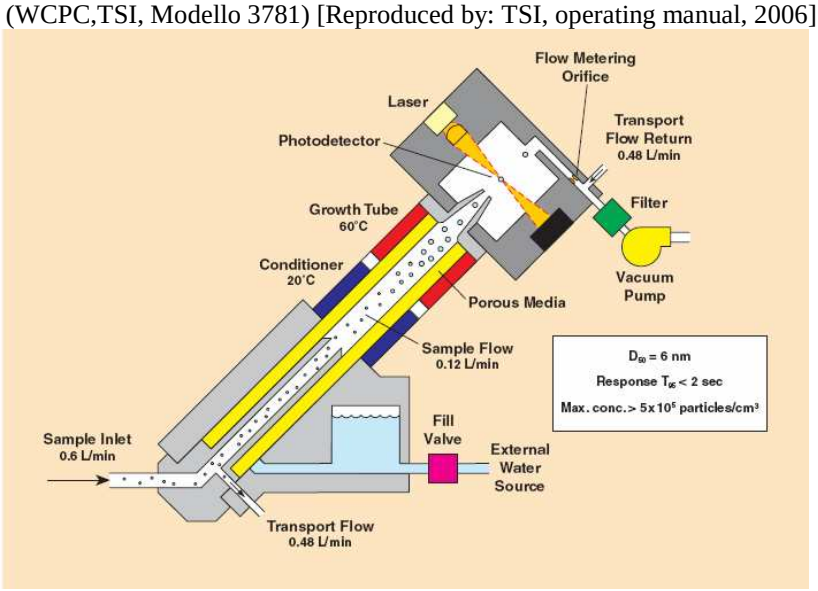

Figure 15. Working principle of the Water-Condensation Particle Counter (WCPC,TSI, Modello 3781) [[Reproduced by: TSI, operating manual, 2006]

Data were collected every 2 seconds, and then averaged to generate 1-minute values. Measurements were taken during winter (January, February and March) and summer (July, August, September) time of 2007 (both week-days and week-ends). Instruments were located at two urban sites, 740 meters far each other in Parma downtown: via Montebello, and Parco della Cittadella (Figure 16, Figure 17).

Figure 16. Picture by Google Earth of the two measurement sites in Parma: Parco della Cittadella (top) and via Montebello (bottom).

Figure 17. Details by Google Earth of the two measurement sites in Parma: Parco della Cittadella (left) and via Montebello (right).

Representativeness criteria with respect to emission sources drove the selection of these two sites [Costabile et al., 2006a,b]. Parco della Cittadella was selected as representative of urban background concentrations, the closest traffic emission source being around 100 meters far. Conversely, the traffic site in Via Montebello would reflect pollution concentrations strongly influenced by urban traffic emissions;

measurements were taken less than 1 meter from the road (the road is south of the measurement point, Figure 17). The sampling probe was made by a straight stainless steel tube, with 7 mm internal diameter and lenght < 15 cm, in order the sampling losses to be neglectable. A small cyclone was used at the traffic site (where the concentrations were expected to be higher) to avoid particle larger than 1 μm to either block or damage the system.

6.2. FROM TRAFFIC SITE TO URBAN BACKGROUND

UFPs concentrations measured (Figure 18, Figure 19, Figure 20, Figure 21) were found to be low, but comparable to similar works (e.g., Harrison et al., 1999): urban background locations have usually average concentrations of 10.000 #/cm^3, whereas traffic locations exhibit 30.000-50.000 #/cm^3. Since the particle number is generally dominated by local emissions, it is particularly affected by primary particles generated by vehicle exhausts. Therefore, as found in previous studies (e.g., Zhang et al., 2004), UFP number concentrations measured at Via Montebello - close to traffic emissions - showed tendencies significantly different from the concentrations measured just 700 meters far away in the park, representative of the urban background. Differences related mainly to two factors. The traffic site showed UFP number with both much higher concentrations, and much more rapid fluctuations (Figure 18, Figure 19, Figure 20, Figure 21). Much faster and more intensive dilution processes could result in a more rapid reduction of UFP number, as well as a trigger for other physical processes (such as nucleation) in connection to other parameters, such as solar radiation. Concentrations are comparable only at night-time, from midnight to 4.00 a.m., when both the traffic flow and the concentration fluctuations at Montebello station were very low.

Contrary to the urban background site, concentrations at the traffic location showed a daytime trend shaped by two peaks (Figure 23). They can be likely related to traffic rush hours (7.00 a.m. and 18:00), and were also showed by other gaseous pollutants [not shown here]. This finding clearly indicates traffic emissions to be the prevailing source of UFP number [e.g. Shi et al., 1999].

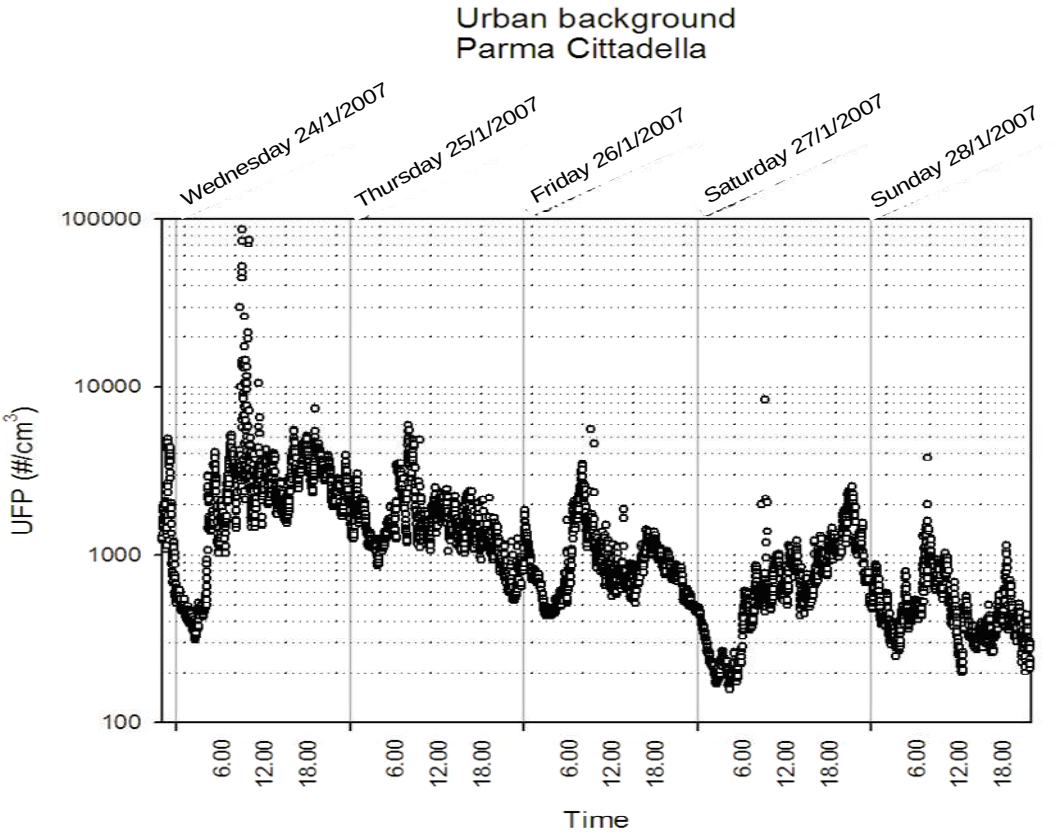

Figure 18. UFP number concentration during the winter campaign at an urban background station in Parma. [Reproduced from Costabile et al., 2007b]

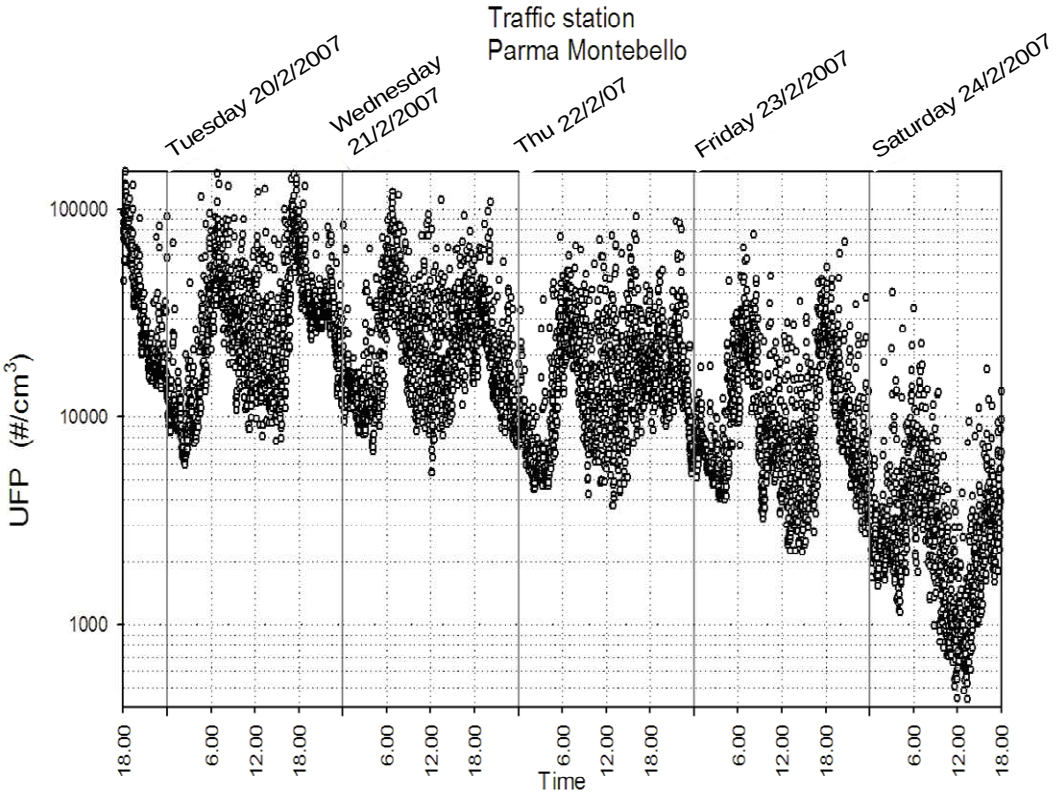

Figure 19. UFP number concentration during the winter campaign at a traffic station in Parma [Reproduced from Costabile et al., 2007b].

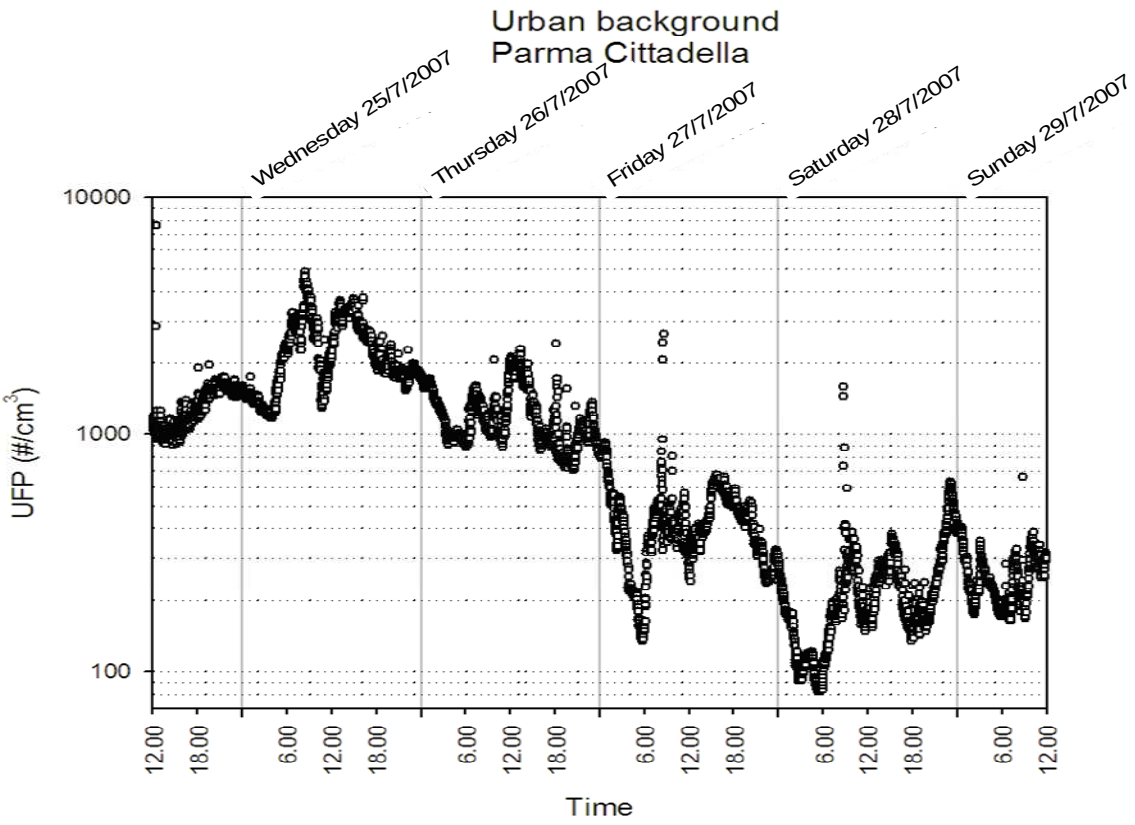

Figure 20. UFP number concentration during the summer campaign at the background station in Parma [Reproduced from Costabile et al., 2007b].

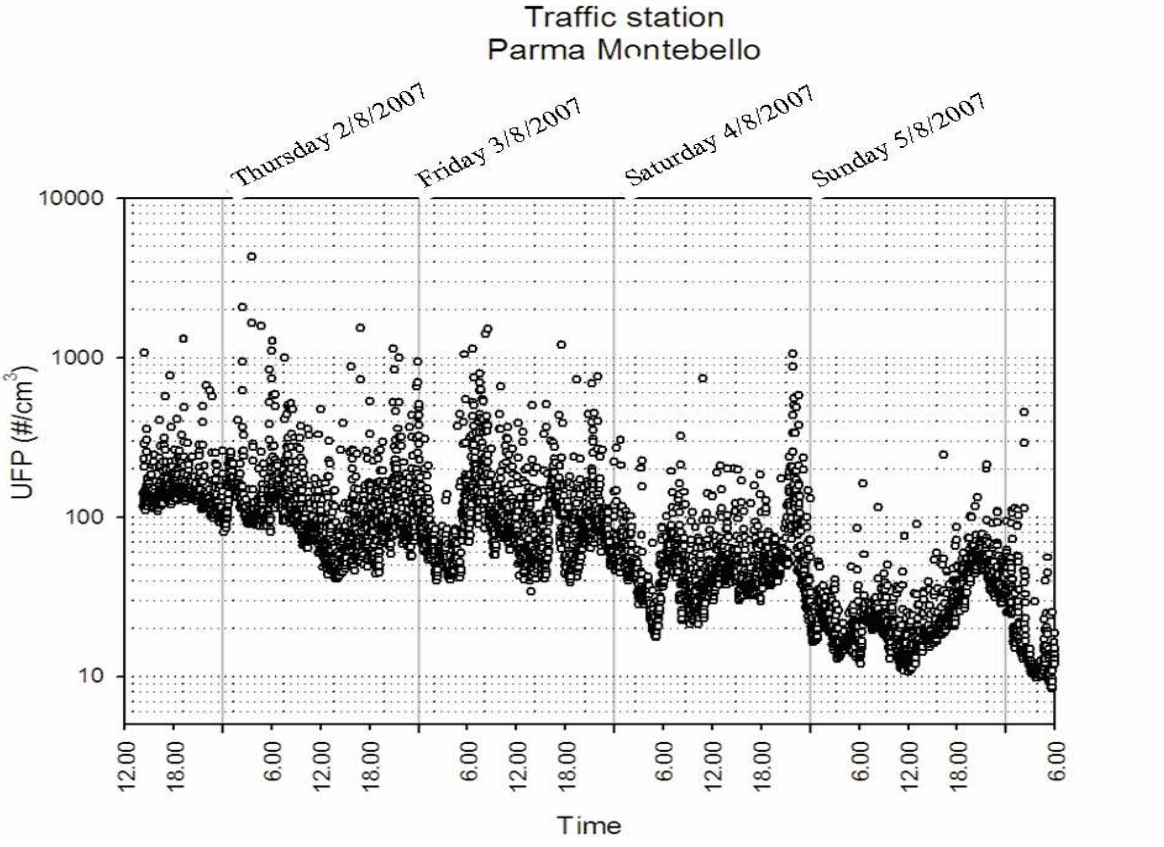

Figure 21. UFP number concentration during the summer campaign at a traffic station in Parma [Reproduced from Costabile et al., 2007b].

6.3. COUPLING WITH METEOROLOGY AND GASEOUS POLLUTANTS

Variations due to meteorology can be more easily analysed at the urban background site, where traffic flows influence can, however, also be recognised. UFP peaks (either relative or absolute) measured in the Cittadella often corresponded to (noon) solar radiation peaks (Figure 18, Figure 20). This suggests that the solar radiation probably induced an increase in the number of particles (in the nucleation mode) due to gas-to-particle conversion [e.g., Harrison et al., 1999]. The highest value of UFP number concentration (not including spikes) at this site was measured on January 19 (Figure 22). This was a week-day (Friday) with high solar radiation, temperature and wind speed, and low relative humidity.

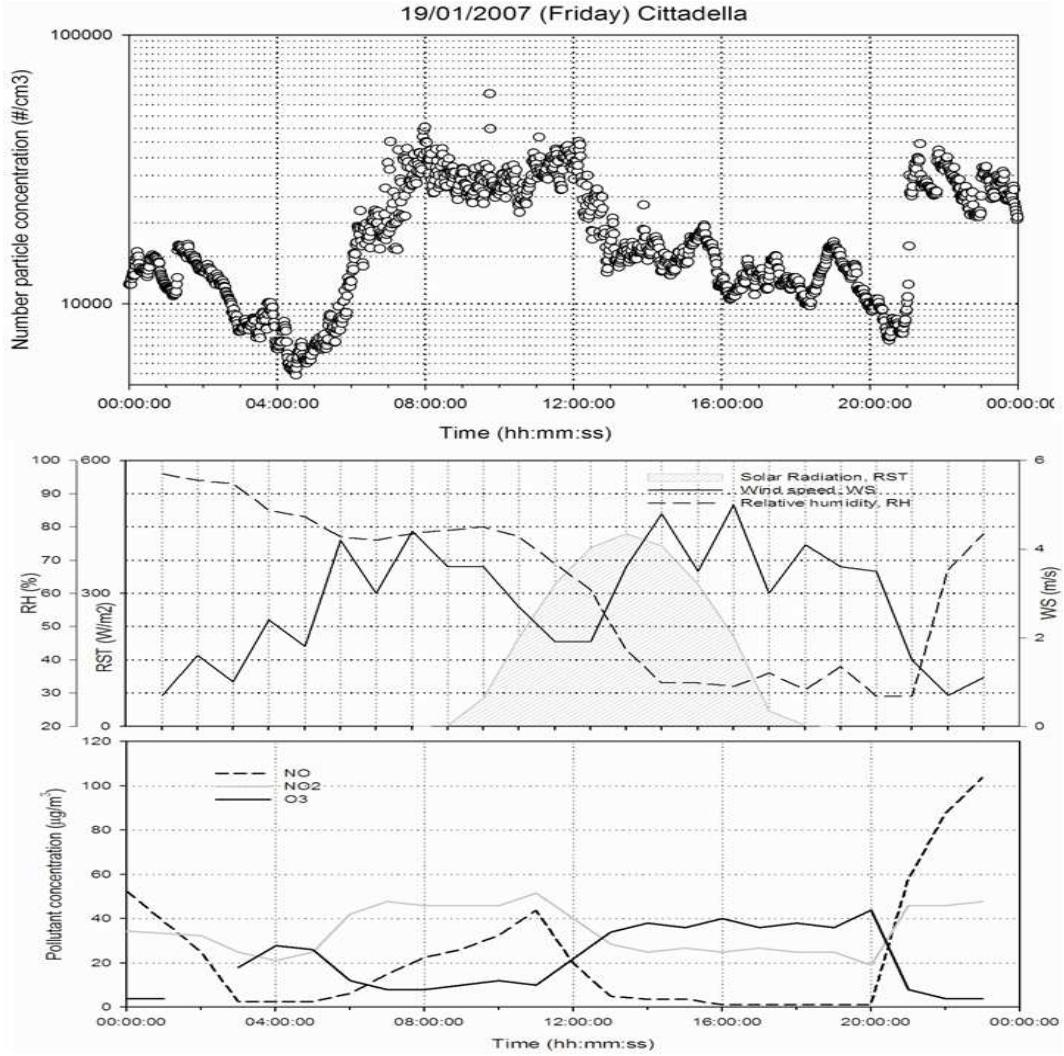

Figure 22. Concentrazione di particelle ultrafini misurata nel Parco della Cittadella il 19 Gennaio 2007 e Variabili meteorologiche e concentrazione di inquinanti gassosi misurata nel Parco della Cittadella dall'ARPA di Parma il 19 Gennaio 2007

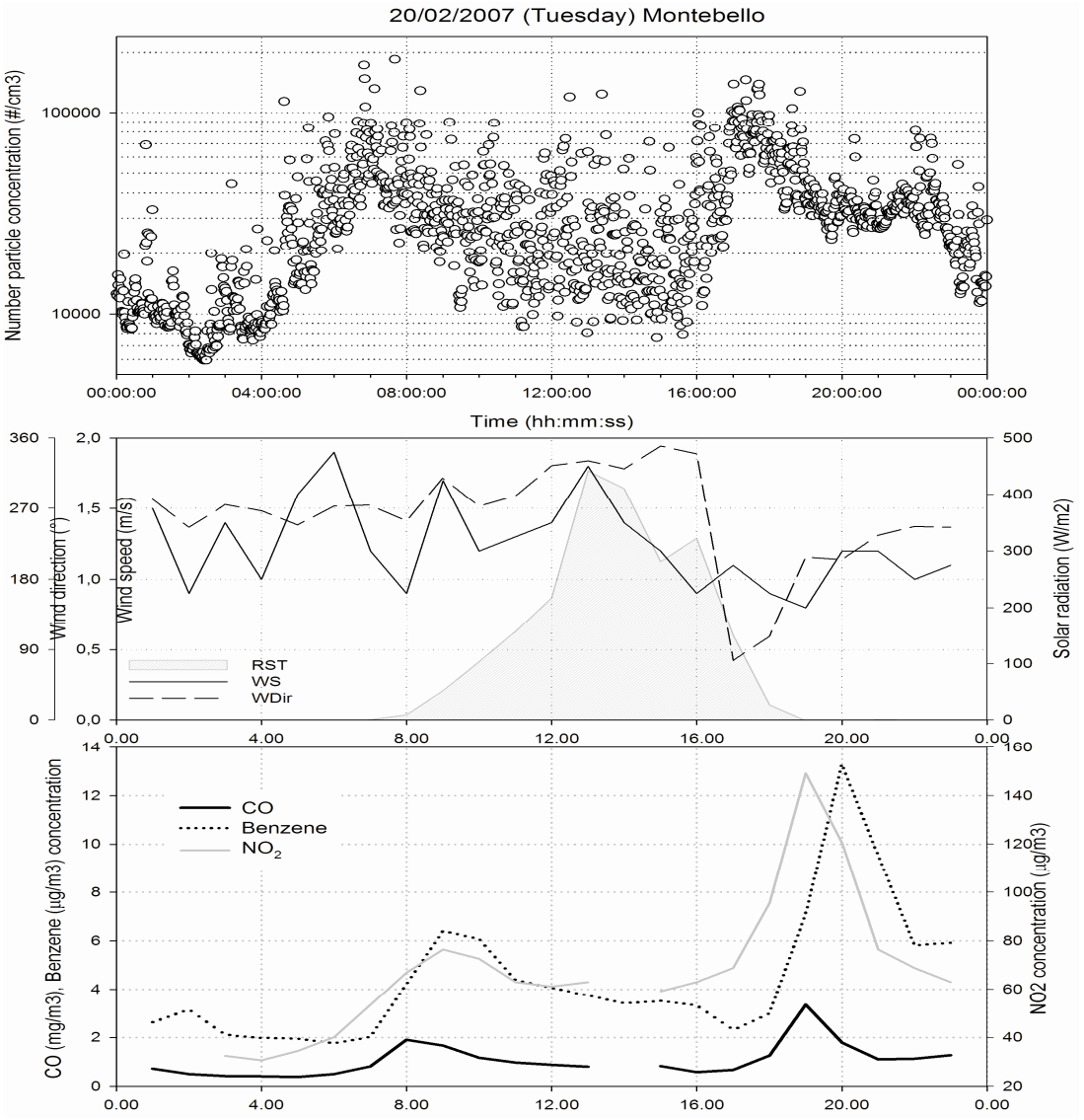

Figure 23. Concentrazione del numero di particelle ultrafini (dati al minuto) e concentrazione di inquinanti gassosi e variabili meteorologiche (dati orari) misurata il 20 Febbraio 2007 in via Montebello

Though less clear, these noon-time peaks can also be seen at the traffic site (Figure 19, Figure 21, Figure 23).

Beyond this effect, a correlation with wind speed was also found (Figure 22, Figure 23), suggesting that increased wind speeds can induce significant transport phenomena of UFPs either emitted or formed by nearby traffic sources [Shi et al., 1999]. This effect was less evident at the traffic site, probably due to the traffic-induced turbulence: local emitted particles effectively dominated measurements even when the site was upwind to the near road. It is not clear if the afternoon peak measured for both UFPs and gaseous pollutants on February, 20 in Montebello (Figure 23) should be related either to the wind direction change, or (more likely) to

the lower wind speed (wind calm, <1m/s) , the rush hours, and increased atmospheric stability.

Interestingly enough, diurnal trends of both UFPs and primary gaseous pollutants (particularly NO and CO) were found to be quite similar (Figure 22, Figure 23) [e.g., Kittelson et al., 2006a,b]. Different time resolutions of data collected (1min versus 1h) are likely the major reason for the differences in the fluctuations, and the related time shifts. These findings indicate UFP number as a valuable marker of fresh emissions, significantly correlated with combustion-generated pollutants.

Finally, the comparison between the frequency distributions of UFPs measured at the two sites (Figure 24) shows a double FD mode only at the urban background location. This could likely suggest the existence of an (extremely low) urban background level (the lowest mode, 1000#/cm^3, which can be recognised at both the sites). The second mode in the background location could be related to UFPs concentrations (extremely diluted) transported from nearby sources and already aged because of meteorology-induced transformations. The FD at the traffic site looks like a Ln-FD, suggesting mixing and dilution of local traffic source emissions to be the prevailing process over time [e.g., Ott et al. 1990, Costabile et al., 2006a]

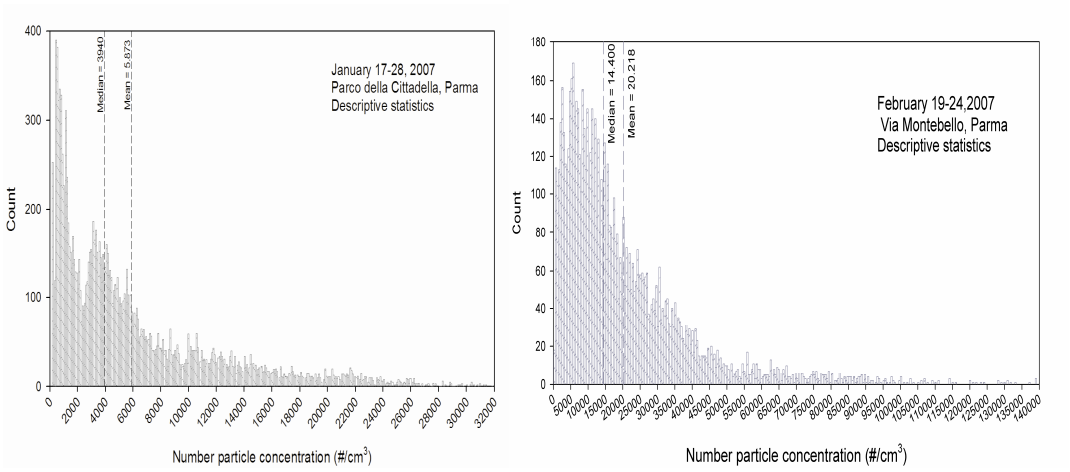

Figure 24. Distribuzione di frequenza misurata della concentrazione di particelle ultrafini misurata nel Parco della Cittadella e in Via Montebello

CHAPTER 7.
FROM TAILPIPE-TO-ROAD: VARIATIONS INTO STREET-CANYONS[4]

7.1. INTRODUCTION

During the last few years, more and more attention is being focussed upon street canyon levels of urban air pollution [e.g.: Vardoulakis et al., 2003]. There are usually strong gradients of gaseous and particulate pollutants both in the vertical and horizontal direction, and pollutants may accumulate in small side-cavities (such as enclosed spaces, small streets or yard) where additional recirculation regions occur [Boddy et al., 2005].

Several studies have investigated this topic. Qin and Kot (1993) found an average vertical difference of approximately a factor of two for both CO and NO_x between street level and the 25 m level. Vakeva et al. (1999) observed the dilution factor to be on average 5 between street and rooftop (22 m) levels for CO and Nitrogen Oxides; the formation of secondary pollutants was found to significantly change the gradient of NO, NO_2 and O_3 from that due to the dilution only. Ziv et al. (2002) stated the differences found for the pollutant concentrations at two levels could be attributed

[4] This charter was entirely published in the paper: Costabile et al., 2007/ Atmospheric Environment, Vol 41 (31) pp 6637- 6647. The text was rearranged to fit the format of this dissertation.

probably to the fact that in case of NO_x the contribution of sources located outside the street is more significant, and that the differences are also due likely to the "sink-effect" of the enclosed yard relative to NO and ozone.

However, there is very little information available for both street level concentrations and vertical gradients. Moreover, direct field measurements of the wind flow in street canyons are rare [Kukkonnen et al., 2001]. Whilst there is some evidence of vertical dilution, further studies are required at heights up to and including the rooftop, in order to fully understand the degree of mixing along vertical gradients within street canyons [Vakeva et al., 1999]. Additionally, experimental determinations of pollutant behaviour within urban street canyons have been, relative to measurements at urban free spaces and rooftops, scarcely reported in the literature [Kourtidis et al., 2002]. The coupling between different pollutants is also a very complicated issue [e.g. Meng et al., 1997]. Despite the range of idealised numerical studies, few full-scale experiments have been conducted which provide data from simultaneous measurements of in-canyon wind flow and pollutant concentrations, relative to a suitable background wind measurement [Boddy et al., 2005].

In order to investigate these issues, a field study was undertaken in an open urban street canyon, in the Chinese city of Suzhou. Measurements of pollutants concentrations (NO_x, NO, NO_2, SO_2, CO, BTX, O_3, PM_{10}), traffic flows, meteorological parameters and wind flow field were taken at a 25 m-high rooftop and into an open yard at street level. Due to the very short distances between sources and receptors, only very fast chemical reactions have a significant influence on the measured concentrations within street canyons [e.g.: Berkowicz et al., 1997]. Therefore, most traffic-related pollutants (e.g. CO and hydrocarbons) can be considered as practically inert species within these distances [e.g. Vardoulakis et al., 2003]. This is not the case either for NO_2 or for NO: the time scales of their chemical reactions are of the order of tens of seconds, thus comparable with residence times of the pollutants in a street canyon [e.g.: Palmgren et al., 1996]. For this reason this work focused on Ozone and Nitrogen Oxides compounds, with the primary objective of exploring their vertical distributions in urban conditions associated with canyons and enclosed spaces.

The measurement area was located in an open street-canyon with a W/H ratio of 1.8~2, in the middle of the city, along a 40-meter wide road with average traffic flow of 1.800 veh/hour [Costabile et al., 2006a]. Measurements were taken at two points

(Figure 25): in a street-level yard (site B) and on the rooftop of a 22 meters high building (site A), sampling inlets 3 meters higher.

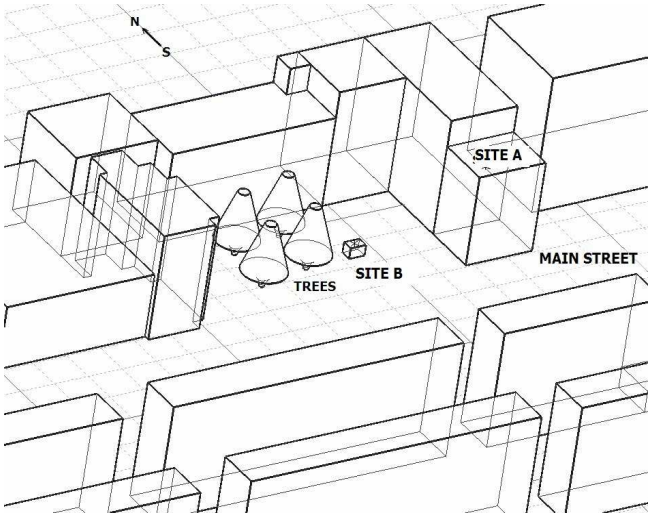

Figure 25. Schematic of 3D view of the street-canyon. The two measurement sites are indicated: on the roof (site A) and in the yard (site B) [Reproduced from Costabile et al., 2007a].

The concentrations in ambient air of O_3, NO_x, NO_2, NO, BTX (Benzene, Toluene and Xylene), the wind field and others meteorological factors (ambient air temperature, relative humidity and total solar radiation) were continuously measured for one week from June the 29th to July the 5th, 2005 (Table 4).

Table 4. Measurement protocol of the one-week field in Suzhou: measured items, measurement methods, sampling frequency, measurement site, and response time and detection limits of the instrument.

Measured item	*Measurement method*	*Sampling Frequency*	*Measurement site*	*Response time*	*Detection limit*
NO_x,NO_2,NO	Chemiluminescence NO_x analyser (API 200 A)	5 minutes	Yard & Roof	<60 s	0.4 ppb
Ozone	UV absorption ozone analyzer (API 400 A)	5 minutes	Yard & Roof	<20 s	0.6 ppb
BTX	Gas Chromaograph POPC analyser (SYNSPEC GC955)	30 minutes	Roof	30 min	<10 ppt
Horizontal Wind speed and direction	Optoelectronic and Potentiometer sensor (LASTEM C500D-S)	5 minutes	Yard	<3 s	<0.25 m/s, <0.4°
Horizontal (WS) and vertical (WS-z) Wind speed and direction	Sonic anemometer (OPSIS Gill WS/520)	5 minutes	Roof	39 impulses/sec	0.01 m/s, 0.1°
Relative Humidity (RH) and Total solar radiation (TSR)	1/3 DIN Pt 100 (LASTEM C502TH)	5 minutes	Yard & Roof	10 s	0.1°, 2%

The monitors were calibrated on site at the beginning of the measurement campaign and inter-calibrated against each other to ensure comparability of results.

7.2. SPATIAL DIFFUSION OF POLLUTANTS

The results of the one week field (Figure 26 and Figure 27) give evidence for relevant vertical variations of the measurements from roof to yard.

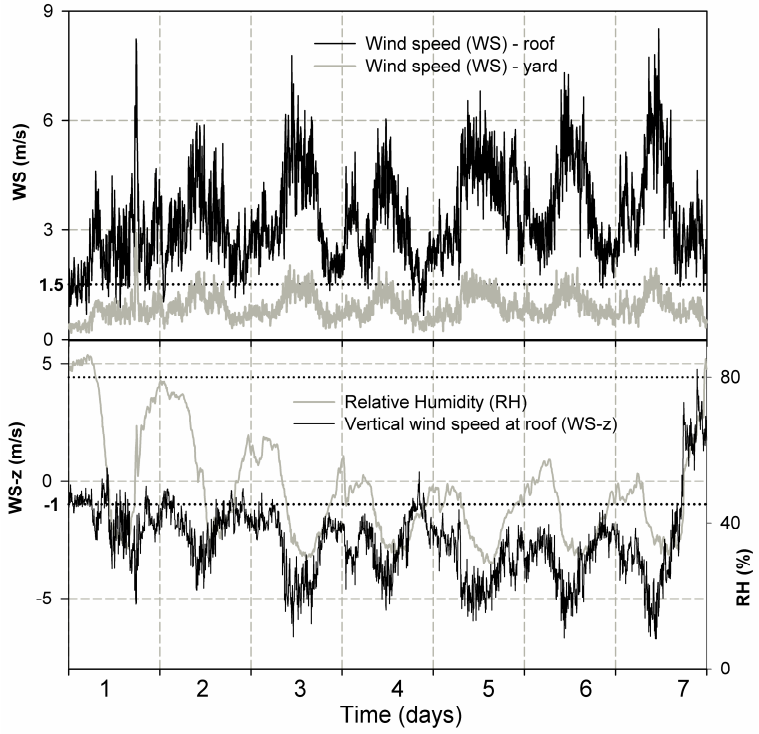

Figure 26. Measured meteorological variables during the 7-days field vs. time: (TOP) wind speed (WS) measured on the roof (black line) and in the yard (grey line); (BOTTOM) vertical wind speed, WS-z (black line, left axis) and relative humidity, RH (grey line, right axis) measured on the roof. References (dotted lines) are indicated: (TOP) WS=1.5 m/s; (BOTTOM) WS-z=-1 m/s and RH=80%. [Reproduced from Costabile et al., 2007a]

Ozone measurements show significant smaller amounts of this pollutant at street level (in the yard), even if there is a high (positive) correlation with the roof values ($R^{ozone_{yard}\text{-}ozone_{roof}}$=0.728) likely indicating common sources. Similar results were obtained e.g. from Vakeva et al. (1999), which found at street level on average 8 times smaller amounts of ozone than at rooftop (25 meters), and from Baker et al. (2004) reporting on the windward side of the canyon a ground ozone concentration 5 times lower than at 25 meters.

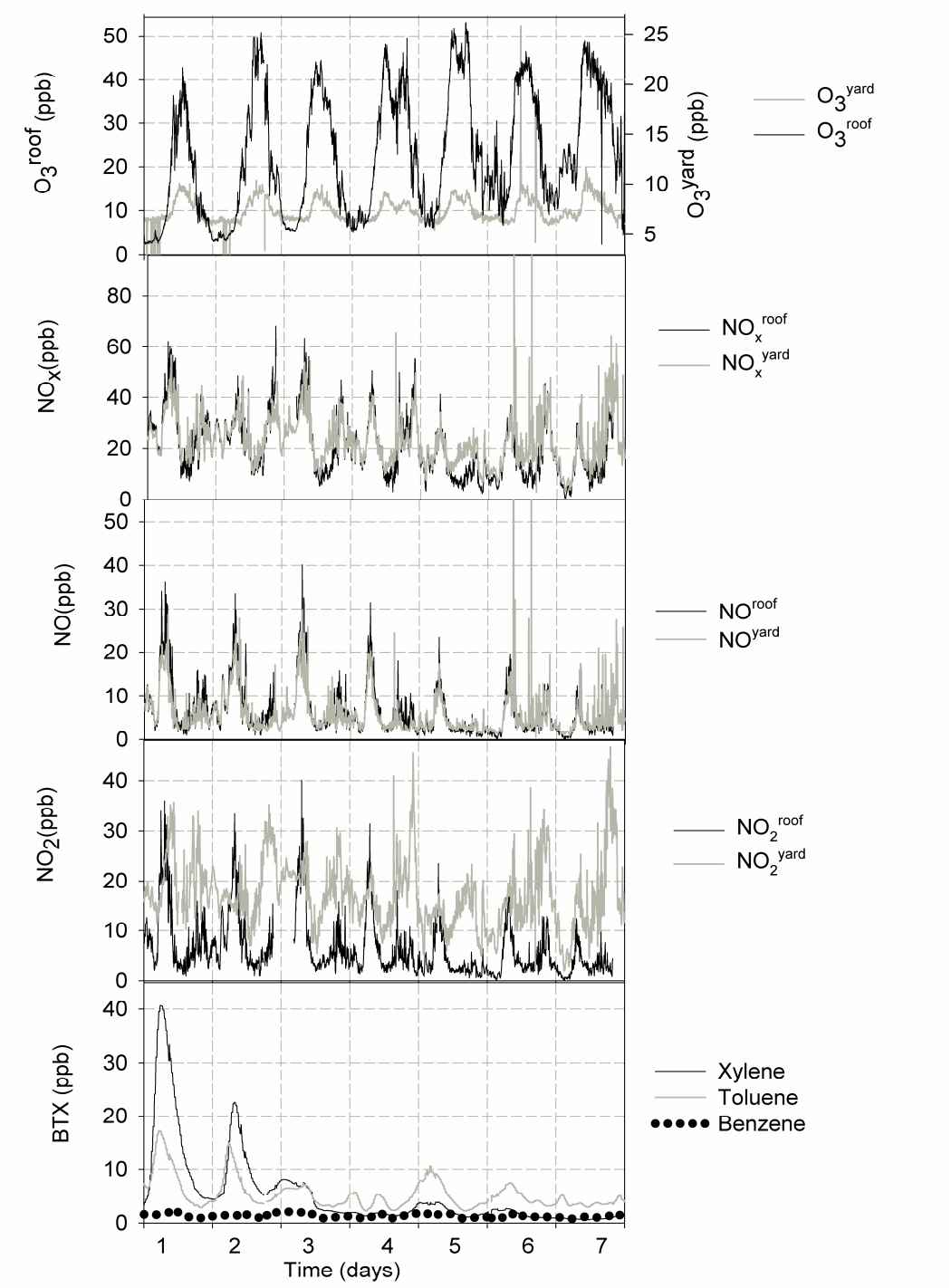

Figure 27. Pollutant concentrations measured during 7-days field vs. time: (from top to down) (1) ozone measured on the roof (black line, left axis) and in the yard (grey line, right axis); (2) NO_x measured on the roof (black line) and in the yard (grey line); (3) NO measured on the roof (black line) and in the yard (grey line); (4) NO_2 measured on the roof (black line) and in the yard (grey line); (5) Benzene (dotted line), Toluene (grey line) and Xylene (black line) measured on the roof [Reproduced from Costabile et al., 2007a].

The variable Δ_i was defined as:

$$\Delta_i = \Delta_i(t) = X_i^{yard}(t) - X_i^{roof}(t); \{i \in [NO; NO_2; O_3]\} \quad (1)$$

where X_i^{yard} and X_i^{roof} are the concentrations of the air pollutant *i* measured in the yard and on the roof, respectively. Δ_i would reflect (for each pollutant) the (spatial) differences between the two measured (time) concentrations. The analysis of the Frequency Distribution (FD) of Δ_i may be used to understand how this variable distributes in regard to the major factors influencing it [e.g. Buccianti et al., 2003]. Particularly, it could give insights into the pollutant diffusion mechanisms in atmosphere [Costabile et al., 2006b]. The FDs of Δ_{NO} (Figure 28a) and Δ_{NO2} (Figure 28b) measured along the one week field were found to be significantly fitted by the Gaussian curve (the coefficients of regression , R^2, between the measured FD of Δ_i and the Gaussian distribution are 0.99 and 0.94, respectively). These findings suggest that the Δ_{NO} and Δ_{NO2} defined by Eq. (1) were determined by many small and unrelated random factors [e.g. Buccianti et al., 2003].

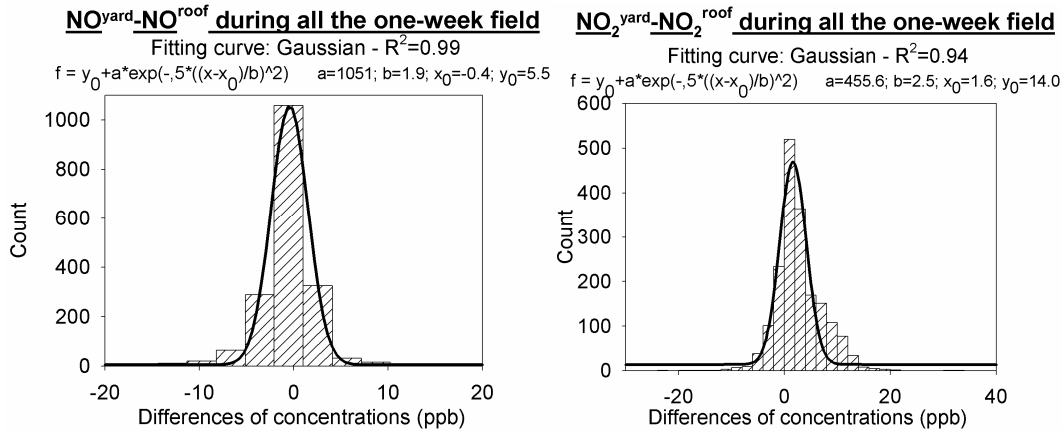

(a) (b)

Figure 28. The measured frequency distributions, FD (histogram filled with diagonal pattern) and the fitting curves (black solid line) of (a) Δ_{NO} and (b) Δ_{NO2}. On the top are indicated: (1) the better type of distribution fitting the measured FD, (2) the coefficient of regression R^2 between the measured FD and its analytical fitting, and (3) the equation of the fitting [Reproduced from Costabile et al., 2007a]

The slightly worse fit found for Δ_{NO2} (lower R^2), related to the tail on the right of its FD, indicates the statistical prevalence of $\Delta_{NO2}>0$, and then the existence of some small "systematic" factors (not measured for NO) generating it. Several and more relevant should have been, on the contrary, the "systematic" factors deviating the FD of Δ_{O3} (Eq.1) from Normality: the FD was bimodal and not Gaussian, indeed (Figure 29). To identify these factors, the time scales responsible for ozone transformations were analysed and the FD of Δ_{O3} was split in a daytime- and a nighttime- FDs. Both of them were found to conform very well to the Weibull distribution. In effect, the

Weibull FD has been shown to fit to oxidant data of air quality [Seinfeld and Pandis, 1998], especially for ozone [Cox and Chu, 1993]. These findings provide a twofold evidence. On one hand, as known [e.g. Sillman, 1999; Emmerson et al., 2005; Trainer, 2000] different processes governed the daytime and night-time ozone concentrations. On the other hand, different factors primarily influenced the Δ_{O3} , Δ_{NO}, and Δ_{NO2} defined in Eq. (1) (and thus their vertical diffusion [Costabile et al., 2006-b]) in atmosphere.

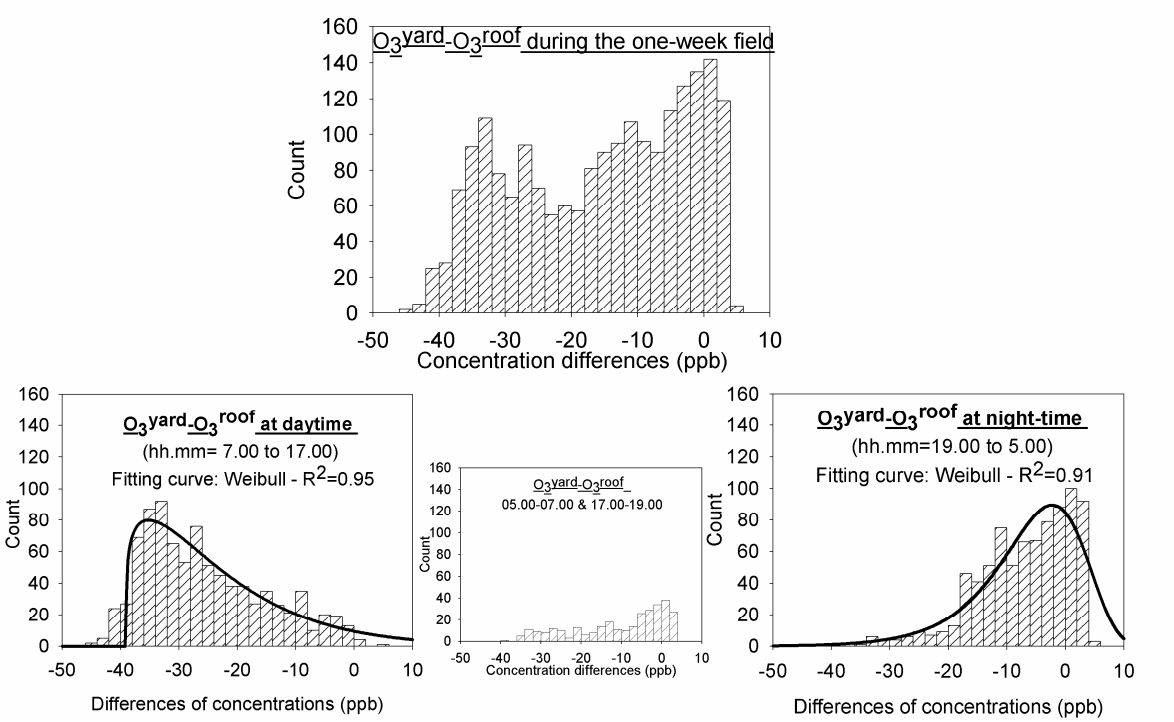

Figure 29. The measured frequency distributions, FD (histogram filled with diagonal pattern) and the fitting curves (black solid line) of Δ_{O3} : (i) during the 7-days field (TOP), (ii) only from 7.00 a.m. to 5:00 p.m. (LEFT, BOTTOM), (iii) only from 7:00 p.m. to 5:00 a.m. (RIGHT, BOTTOM), (iv) during the remaining time. On the top of two charts are also indicated: (1) the better type of distribution fitting the measured FD, (2) the coefficient of regression R^2 between the measured FD and its analytical fitting [Reproduced from Costabile et al., 2007a].

In particular, these factors were even significantly different for ozone and NO_2, both secondary pollutants. Emission levels, chemistry, meteorological conditions, geography and local morphology are though to be the main factors affecting these FDs [e.g. Lu, 2002]. In this experiment the last three factors were equal at both yard and roof. Therefore, different chemical processes and emission levels can be assumed to be the predominant "systematic" factors causing the measured vertical differences of NO, NO_2 and O_3. The accurate evaluation of these factors involving fluid-dynamic effects, heterogeneous removal on surfaces and in the aerosol phases, and ozone chemical production and loss relative to its precursors [e.g., Trainer et al., 2000] is

beyond our current capabilities; however, their analysis could provide further insights and is presented in the followings.

7.3. FLUID-DYNAMIC EFFECTS

The yard-roof pollutant ratios were found to increase together with the background wind speed (measured on the roof, Table 5).

Table 5. Coefficients of correlation calculated between the wind speed (WS), and the ratios of ozone and NOx measured on the roof and in the yard during the one-week field in Suzhou.

	O_3^{roof} / O_3^{Yard}	NO_x^{yard}/NO_x^{roof}	WS^{yard}
WS^{roof}	0,491	0,373	0,814
O_3^{roof} / O_3^{Yard}		0,453	0,472
NO_x^{yard}/NO_x^{roof}			0,284

Their relationship is shown in Figure 30 where the raw data of O_3^{roof}/O_3^{yard}, NO_x^{yard}/NO_x^{roof}, and background wind speed were smoothed by a (locally weighted) regression. It can be seen that the higher the wind speed, the higher the pollutants' ratios (and vice versa). In effect, in this work, the roof is representative of an open space where winds and pollutants measured are urban-background related. Conversely, the yard is representative of an enclosed space at street-level where locally-emitted pollutants, micro-meteorological effects, and local wind flow take place [e.g. Hunter et al., 1992]. This caused the wind to be always higher on the roof than in the yard (where wind was most of the time lower than 1.5 m/s, Figure 26); therefore, under the same background winds, a better diffusion situation of locally emitted pollutants and thus decreased concentrations along with height can be assumed [e.g. Qin and Kot, 1993] .

This could explain the increase of NO_x^{yard}/NO_x^{roof} for increasing wind speed. Contrary to ozone, NO_x ratios were always greater than 1 (Figure 30) highlighting as NO_x was influenced more by local emissions than by emissions transported from surrounding areas, the former being less wind-dependant than the latter. This probably explain also the reason why NO_x ratios correlate less to wind speed than O_3 ratios do (Table 5). The increase of O_3^{roof}/O_3^{yard} for increasing wind (Figure 30) can be likely explained by a twofold mechanism, indeed. In the yard the higher the wind speed, the larger the entrapment of air masses due to the formation of stable vortices [e.g. Kukkonnen et al., 2001]: this likely enhanced there the consumption of ozone by the locally-emitted NO. On the roof the higher the wind speed, the greater the advection of ozone-rich air from the surrounding areas [e.g. Vardoulakis et al., 2003]. Finally,

the wind-dependant influence of the big Cedars (low-emitter trees [e.g.Taha, 1996]) into the enclosed yard (Figure 25) should also be considered.

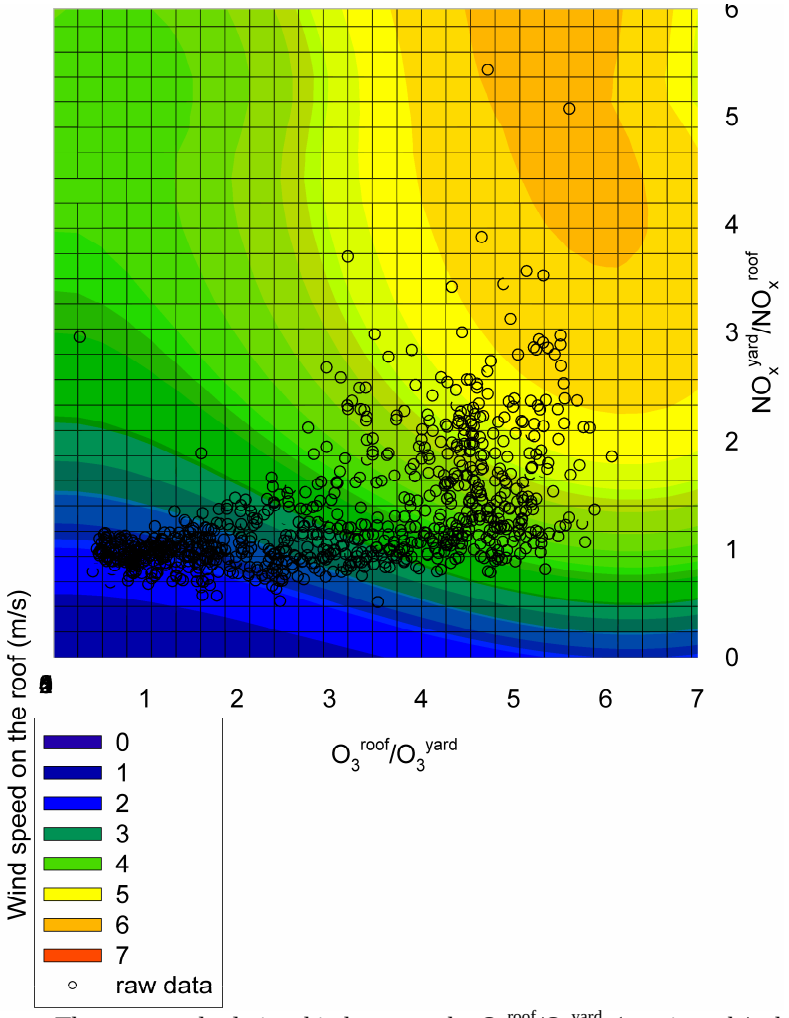

Figure 30. The measured relationship between the O_3^{roof}/O_3^{yard} (x-axis, ppb/ppb), NO_x^{yard}/NO_x^{roof} (y-axis, ppb/ppb) and roof wind speed (z-axis, m/s, colours). Triplets of raw data (circles) are smoothed by a tricube weigh function to weight the data, and a polynomial regression of degree 3 is used as smoother. Each point along the smooth curve is obtained from a regression of data points close to the curve point with the closest points more heavily weighted. All data points were used for each regression. Outliers were rejected to reduce their effects on the smoothed values [Reproduced from Costabile et al., 2007a]

These trees had the potential to further decrease ozone concentration in the yard in relation to the roof by means of (i) reduction of vertical mixing [Theurer, 1999] (and thus increased titration of ozone by NO), (ii) increased pollutants deposition and changed micro-meteorology [Nowak et al., 2000], and (iii) increased pollutants scavenging [Taha, 1996]. Therefore, it can be likely assumed that wind variations produced processes of ozone production and/or consumption complex and different on the roof and in the yard, as better discussed in the following paragraph.

7.4. OZONE CHEMICAL PROCESSES RELATIVE TO ITS PRECURSORS

The relation between ozone and one of its two main precursors, NO_x, is usually roughly simplified to only two reactions [e.g.Palmgren et al., 1996]:

$NO+O_3 \rightarrow NO_2 + O_2$ [R1]

$NO_2+h\nu \rightarrow NO + O$ [R2]

Typically, NO and NO_2 adjust to establish a near-steady state between reactions (R1) and (R2). However, there are several situations in which these reactions may results in different regimes [e.g. Sillman, 1999]. To analyse this point the NO_2/NO_x ratios and the NO were plotted against each other (Figure 31) [e.g. Soltic, Weilenman, 2003]. The same Eq. (2) gives the linear regression of the entire field data at both the measurement sites:

$$\frac{NO_2}{NO_x} = 1 - 0{,}03 \cdot NO \,. \qquad (2)$$

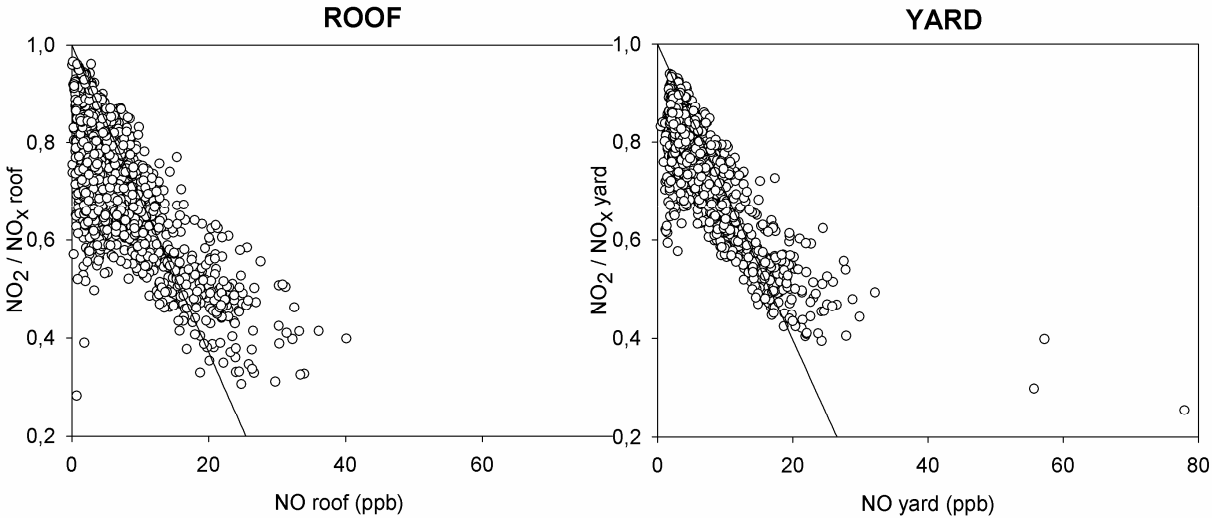

(a) (b)

Figure 31. NO_x partitioning versus the NO concentrations (a) on the roof and (b) in the yard [Reproduced from Costabile et al., 2007a].

However, the coefficients of correlation (R) are higher in the yard (R_{roof}=-0,729, R_{yard}=-0,814). This finding suggests a common measure of transformation $NO \rightarrow NO_2$, but likely more depending on NO in the yard than on the roof. That is, in the yard the higher amount of fresh emissions (richer in NO) locally generated and entrapped likely induced a greater $NO \rightarrow NO_2$ transformation, and thus a greater NO consumption. This could explain the small Δ_{NO} (Eq.1) found (Figure 27, Figure 28) although the NO^{yard} was measured closer to the emission source. Consequently, ozone

was more effectively destroyed in the yard [e.g. Molina and Molina, 2002] where its concentrations were kept up to 15 ppb for almost daytime (Figure 27). Accordingly, the NO_2/O_3 ratios were found to be generally higher in the yard (Figure 32a). At night as there were no photolysis and low emissions, and thus no reforming of NO, once the NO emitted had been used up, the ozone concentration was mainly due to the mixing down of ozone-rich air from aloft and Δ_{O3} (Eq.1) were lower (Figure 27, Figure 29). Beyond the larger ozone consumption in the yard by the locally-emitted (and entrapped) NO, the $\Delta_{pollutants}$ (Eq.1) were probably also influenced by a different daytime ozone production relative to NO_x. A production larger on the roof than in the yard is suggested by both (i) the steady rise in the roof ozone levels (partly caused by the already discussed ozone advection) observed at daytime for decreasing NO_2 concentrations (fig.3) and (ii) the greater negative correlation between NO_2 and O_3 ($R_{roof}^{NO_2\text{-}O_3}$=-0.40, $R_{yard}^{NO_2\text{-}O_3}$=-0.11). Moreover, though no measurements are available in this study for either the radical concentrations due to the BTX or the yard BTX, the inverse correlation measured during all the campaign with ozone (stronger for toluene at roof, $R_{roof}^{toluene\text{-}ozone}$=-0.45, $R^{toluene_{roof}\text{-}ozone_{yard}}$=-0.34) and greater to that among ozone and NO_2 ($R_{roof}^{NO_2\text{-}Ozone}$=-0.40, $R_{yard}^{NO_2\text{-}ozone}$=-0.11) should likely suggest an influence of the BTX in the photochemical ozone production.

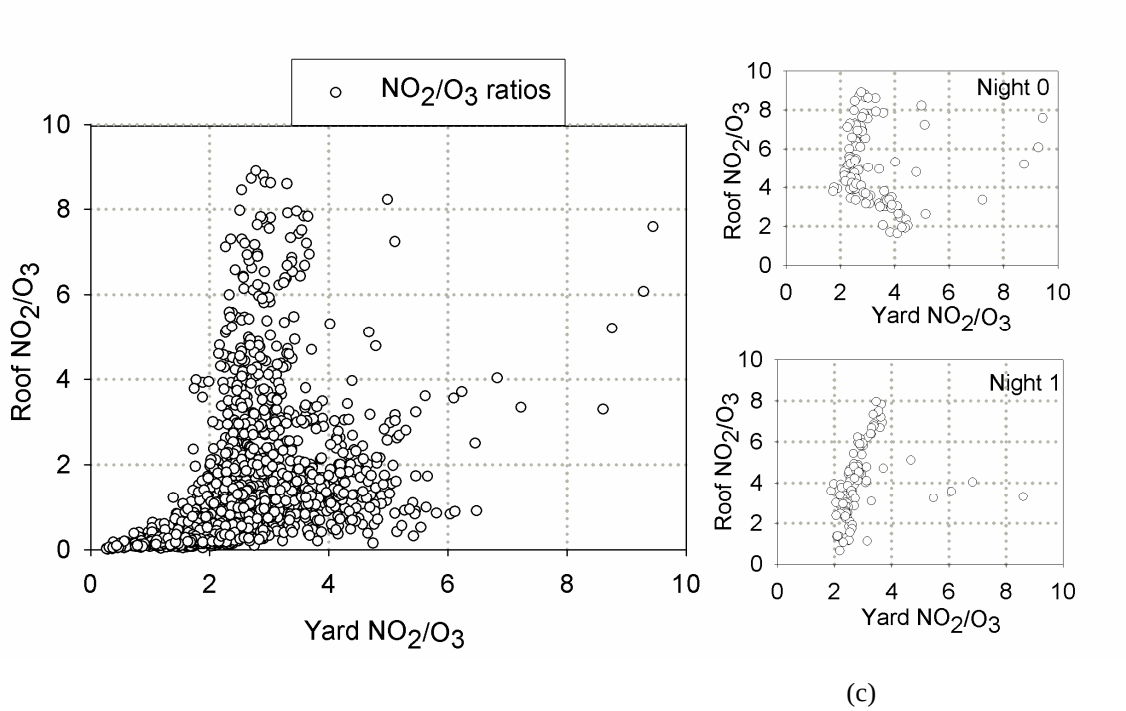

Figure 32. NO_2 to ozone ratios (ppb/ppb) measured in the yard (x axis) and on the roof (y axis) during: (a) the one-week field, (b) the night 0 and (c) the night 1 [Reproduced from Costabile et al., 2007a].

Interestingly enough, during the nights 0 and 1 (when the highest BTX were measured, Figure 27) the ozone, NO, Toluene and Xylene concentrations showed very similar behaviours (Figure 33). There is a positive correlation among them, contrary to the rest of the campaign (Table 6).

Table 6. Comparison between the correlation coefficients calculated during the one-week field and only during the nigh 0 and the night 1 for NO, BTX (Benzene, Toluene, Xylenes) and ozone measured on the roof

		NO	BTX
1-week field	ozone	-0.46	-0.35
Night 0		0.49	0.42
Night 1		0.62	0.62

Probably, at early morning for increasing emissions and solar radiation, as far as BTX increased also NO_x raised; the reaction (R1) enhancing the nocturnal removal of ozone [e.g. Sillman, 1999] was small compared to the rate of ozone production; thus, NO, Toluene, Xylene and ozone built-up all together. However, the positive correlation and the Δ_{O3} (Eq.1) >0 only during these nights suggest a further observation. On one hand, the values of NO_2/O_3 measured on the roof during these two nights (the highest of the field) were much higher than in the yard (Figure 32b,c) though Δ_{NO2} (Eq.1) was >0 (Figure 27). Additionally, NO_2^{roof} during these two nights was higher than during the other nights of the field (Figure 27).Therefore, an ozone destruction and a NO_2 increase (or not decrease) only on the roof can likely be assumed. On the other hand, the inverse correlation between ozone and relative humidity, RH (night 0: $R_{roof}^{RH\text{-}ozone}$=-0.95 and $R_{yard}^{RH\text{-}ozone}$=-0.27; night 1:$R_{roof}^{RH\text{-}ozone}$= -0.94 and $R_{yard}^{RH\text{-}ozone}$=-0.09) was much higher on the roof.

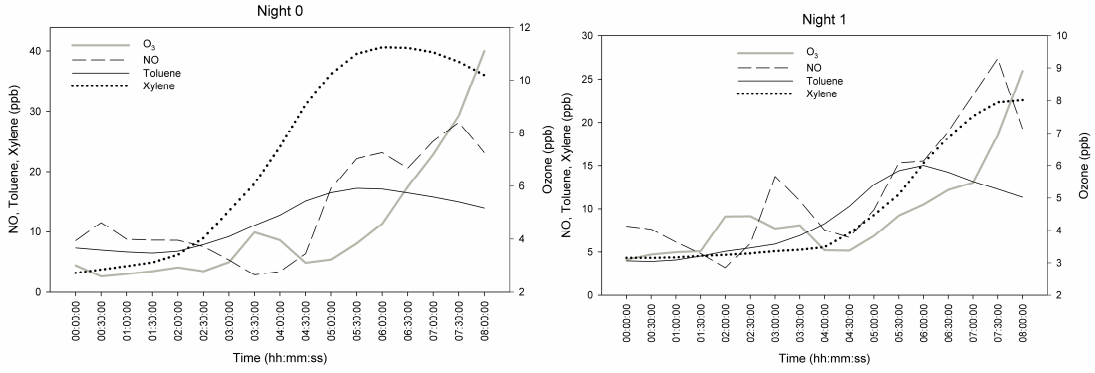

(a) (b)

Figure 33. The behaviours of ozone (solid grey line), NO (long dash black line), Toluene (solid black line) and Xylenes (dotted black line) vs.time measured on the roof during (a) the night 0 and (b) the night 1 [Reproduced from Costabile et al., 2007a].

Therefore, a destruction of ozone in relation to the high RH only on the roof can likely be assumed. In the absence of additional data, it can be only suggested a connection between these findings and the high toluene and xylene concentrations measured on the roof, likely transported from surrounding sources and poorly vertically mixed (vertical wind speed<1m/s and low wind [Vardoulakis et al., 2003], Figure 26). The group of reactions OH+aromatic could have been sourced on the roof by the OH radical in connection with the reaction (R3) [Lloyd et al., 1976]:

$O_3+H_2O \rightarrow OH+O_2$ [R3]

favouring the destruction of ozone, as well as the production of NO_2 by sourcing HO_2 and RO_2 in the reactions (R4) and (R5) [Sillman, 1999; Emmerson et al., 2005]:

$HO_2 + NO \xrightarrow{[O_2]} OH+NO_2$ [R4]

$RO_2 + NO \xrightarrow{[O_2]} R'CHO+HO_2+NO_2$ [R5].

While only tentative, this observation would indicate a further possible cause for the large Δ_{O3} (Eq. 1) found: Toluene and Xylene (whose high concentrations measured in Suzhou by Costabile et al. (2006b) were mainly apportioned to industrial emissions) likely influenced significantly the production of ozone on the roof at daytime, e.g. when followed by reaction (R2) where the O atom immediately combines with O_2 to reform O_3 .[e.g. Trainer et al., 2000])

CHAPTER 8.
FROM TAILPIPE TO ROAD: ULTRAFINE PARTICLES AT KERBSIDE[5]

8.1. INTRODUCTION

Internal combustion engines are known to be a major emission source of ultrafine particles [e.g., Weijers et al., 2004; Charron and Harrison, 2003; Alam et al., 2003; Kittelson et al., 2004; Morawska et al., 2003]. However, in spite of extensive laboratory studies on engine emissions, there are few investigations of how particle mobile emissions evolve and affect air quality establishing a link between sources and receptors [e.g., Abdul-Khalek et al., 1999; Scheer et al., 2005; Giechaskiel et al., 2005]. Moreover, there is little information on traffic-related particles smaller than 10 nm that have been regarded as evidence of particles either truly emitted [Giechaskiel et al., 2005] or newly formed in the atmosphere [Charron and Harrison, 2003; Shi et al., 2001; Alam et al., 2003]. Therefore, it is important to understand how particles transport and transform near roadways [Zhang, Wexler, 2004].

[5] This chapter was entirely submitted for publication as a manuscript: Costabile, F., Allegrini, I. Increase of particle number concentration at sunset time close to traffic emissions. Submitted to Science of the Total Environment (November 2007, Ms. Ref. No.: STOTEN-D-07-01887).

It has been shown that not only is total particle concentration important but also the particle size distribution [Holmes, 2007]. Recent field data have shown that the size distribution of emitted particles evolves substantially within a few hundred meters of emission [e.g., Shi et al., 2001; Zhu et al., 2002]. After release into the atmosphere, ultrafine particles are subjected to complex dilution and transformation processes. Neither current models nor those that will be available in the near future are tough to be able to cover all the spatial and temporal scales that are involved from the emission (centimetres, milliseconds) to the urban/regional scale (kilometres, hours) [Ketzel and Berkowicz, 2004]. Therefore, because the evolution of particle size and mixing state starts at the point of emission and proceeds rapidly, it is important to examine the evolution near the source [Jacobson, J.H. Seinfeld, 2004], and particularly for the relationships between the various particle sizes [Seinfield and Pandis, 2006; Westerdahl et al., 2005], and the mechanisms by which new particles nucleate and grow in the atmosphere [Kulmala, 2003].

Although previous studies have examined the relationship between fresh particle nucleation and pre-existing particle surface area (*S*), no clear correlation has been found [e.g., Clarke et al, 1992; Lowenthal et al.; 2002]. On one hand, coagulation of nanoparticles (<7nm) with the pre-existing *S* is though to be the major loss process [Shi et al., 2001]. On the other hand, *S* may be considered as a condensation sink since in case of high pre-existing *S* nucleation to form new particles is frequently less favourable than condensation of low volatility vapours onto existing particles (the competitive process) [Alam et al.,2003]. The contrasting opinions about coagulation and condensation indicates that these mechanisms are still the centre of much debate [Holmes, 2007; Jacobson and Seinfeld, 2004].

In this study, measurements were taken 30 km North of Rome (Italy) near three major traffic emission sources (a highway, a provincial road and a small road), and showed the total particle number concentration (N) to significantly increase at sunset time. The purpose of this work was to provide insights to this nightfall increase by concentrating on one of the five investigated days when the maximum reached 4 times the background level.

8.2. METHODOLOGY

Measurements were taken, from December 17 to December 21, 2006, 30 km north-east of the urban area of Rome, Italy (Figure 34), in a rural area, in proximity to three major roads: a highway (< 2km far), a provincial road (<500 m) and a small road (<1m). The measuring devices were installed inside an electric van equipped with an online data acquisition system (Table 7). A video camera mounted in the driver cab of the van was used to reconstruct the traffic flow on the nearest road. A weather station installed about 20 meters North-East of the measurement point provided the meteorological data (tab.1). The remaining equipment was located in the main van cab, branching off the sampling air from the same window with no additional probes. A Water-Condensation Particle Counter (WCPC) [e.g., Petäjä et al., 2006; Hering et al., 2005; Hering and Stolzenburg, 2005; Biswas et al., 2005] and a diffusion-screen-equipped WCPC [Stohl et al., 2007; Feldpausch, et al. , 2006] counted contemporarily N_6 and N_{26}, number concentration of particles in air with diameter larger than 6 nm and 26 nm, respectively.

Table 7. Measurement protocol: measured items, Instrument types, measurement frequency, Sample flows, and Resolution. Because of the different time resolution of the WCPCs and OPC; in case of measurements comparison the WCPC-data were averaged over 6s

Measured item	Instrument type	Time res.	Sample flow	Accuracy
Particle number concentration Min.particle size: 6nm Intermediate size cut: 26 nm Max.particle size: >3µm	Twin Condensation Particle Counters (WCPC3781,TSI) Condensing fluid: distilled Water Particle size selector (PSS376060, TSI): fine-mesh screen to remove particles smaller than 26 nm by diffusional capture	2 sec	Aerosol flow rate: 0.12 ± 0.012 L/min Inlet flow rate: 0.6 ± 0.12 L/min	± 10% at10^5 particles/cm^3 (maximum detectable concentration 5×10^5 particles/cm^3)
Particle number/surface concentration in 15 channels: 0.30 - 0.40 - 0.50 - 0.65 - 0.80 - 1.0 - 1.6 - 2.0 - 3.0 - 4.0 -5.0 - 7.5 - 10 - 15 - 20 µm	Aerosol Spectrometer (Optical particle counter OPC 1.108, GRIMM) by Laser light scattering	6 sec	Aerosol flow rate: 0.2 L/min Clean additional sheat air: 0.4 L/min	+- 5% µg/m3
Temperature and humidity	Hygroscopic polymer sensor + Platinum 1/3 Class DIN	1 min	-	± 0.3°C / ± 2%
Wind speed and direction	Wind sensor	1 min	-	
Traffic flows	Digital video camera	continuous	-	

The difference between N_{26} and N_6 was a rough measure of the nucleation mode particles (N_{6-26}) [Giechaskiel et al., 2005]. The size distribution of particle number and surface area in the size range 0.3–20 μm ($N_{0.3-20}$ and $S_{0.3-20}$, respectively) were measured in 15 size classes by an Optical Particle Counter (OPC) [e.g., Alastuey et al., 2004]. As the OPC measures N of particles bigger than 300nm and the diffusion-screen-equipped WCPC measures N_{26}, the difference was a measure of N_{26-300}, covering both some ultrafine and most of the accumulation mode particles. In analysing the results, it should be considered that the total S was underestimated since it was not measured for aerosol with diameters below 300 nm and their contribution may be quite relevant [e.g., Seinfield and Pandis, 2006]. As well, that the cut size of the WCPC is sensitive to the chemical composition of particles, especially their water-solubility, and this can matter at least for nanoparticles.

Measurements were processed by Principal Component Analysis (PCA) for data reduction and interpretation [e.g., Rencher, 1998; Henry and Hidy, 1979].

Figure 34. Image of the measurement location (30 km north-east of Rome, Italy) created by Google Earth. The highway at the left side, and the provincial road in the center can be recognised.

The data-set was standardized by the (Eq.1) [e.g., Henry and Hidy, 1979]:

$$\hat{x}_{ij} = \frac{(x_{ij} - \mu_j)}{\sigma_j} \qquad (1)$$

where μ_j and σ_j are mean and standard deviation values of the j^{th} variable, respectively. Then, data was transformed (using the correlation matrix [e.g.,Poissant et al., 1996]) into a new set of orthogonal variables (principal components, PCs) by using the orthogonal transformation method with Varimax rotation and retention of

PCs whose eigenvalue is greater than 0.65÷1 [e.g., Almeida et al., 2005; Eder, 1989; Thurston and Spengler, 1985]. The PCs were, then, arranged in decreasing order of importance with scores estimated by the (Eq. 2) [e.g., Verbeke et al., 1984]:

$$PC_{ij} = \sum_{k=1}^{m} w_{ik} x_{kj} \qquad (2)$$

where PC_{ij} is the PC score for the j^{th} object on the i^{th} component, w_{ik} is the loading of the k^{th} variable on the i^{th} component, and x_{kj} is the standardized value of the k^{th} variable for the j^{th} observation.

8.3. DAILY TRENDS AND IDENTIFICATION OF THE "EVENT"

Particle number concentration measured during five consecutive days showed similar daily tendencies (Figure 35), with lower and more constant nocturnal values, and three morning peaks [Costabile et al., 2007b]. The biggest increases of N with respect to the "background" level occurred at sunset time, after 16:00 (by roughly a factor 2). On only one of the five investigated days (20.12.2006), the maximum increase reached (between 16:00 and 17:00) 4 times the "background" level (Figure 35). During that day the meteorology was something different (Figure 36): higher solar radiation, higher temperature variation, no clouds, lower relative humidity, relatively constant wind speed and wind direction. The purpose of this work is to analyse the principal causes of this sunset "event" characterised by: (i) measurement site downwind the small closest road, and upwind the highway and the provincial road (fig.1, Figure 36); (ii) lower photochemical formation as there was little light at that time (even if photo-chemically formed particles might have formed a couple of hours before, reaching then sizes >6 nm slightly after 16:00, Figure 36).

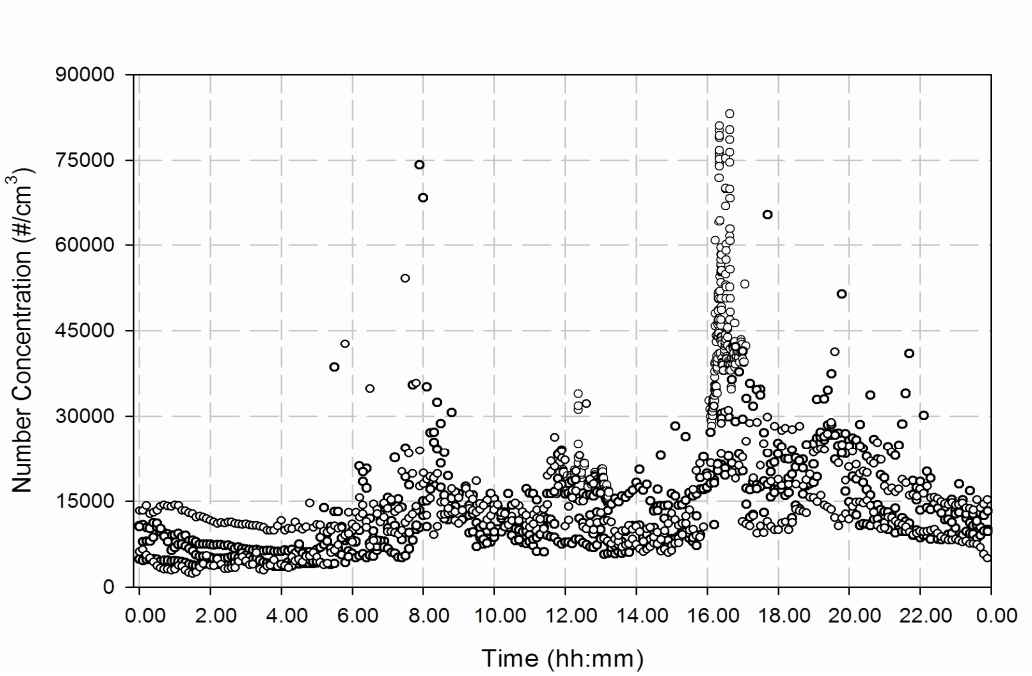

Figure 35. Daily particle number concentration (N_6) measured on December 17,18,19, 20,21 2006 and reported on the same time axis. The maximum peak from 16:00 to 17:00 was measured on December 20 [Reproduced from Costabile et al., 2008b].

Despite the known connections of N with temperature (T) [e.g., Meja et al., 2007; Virtanen et al., 2006; Voigtalnder et al., 2006; Giechaskiel et al., 2005], atmospheric stability [e.g., Imhof et al., 2005], traffic peaks [Kittelson et al., 2004; Shi et al. 2001; Wehner et al., 2002], and S [Charron and Harrison, 2003; Alam et al. , 2003], the selected event shows no direct relationship (Figure 36).

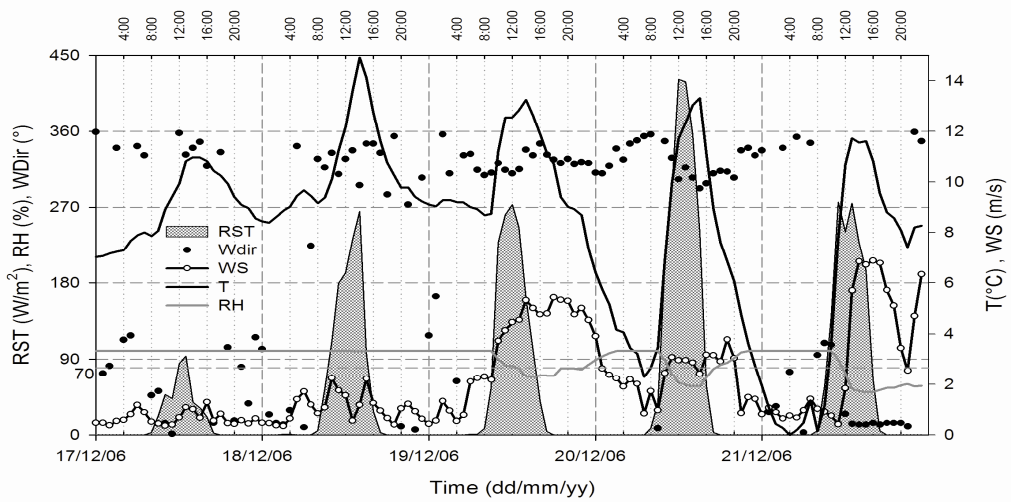

Figure 36. Meteorological variables measured on December 20, 2006. Right axis: total solar radiation (RST), relative humidity (RH) and wind direction (WDir, 0° correspond to North). Left axis: temperature (T) and wind speed (WS) [Reproduced from Costabile et al., 2008b].

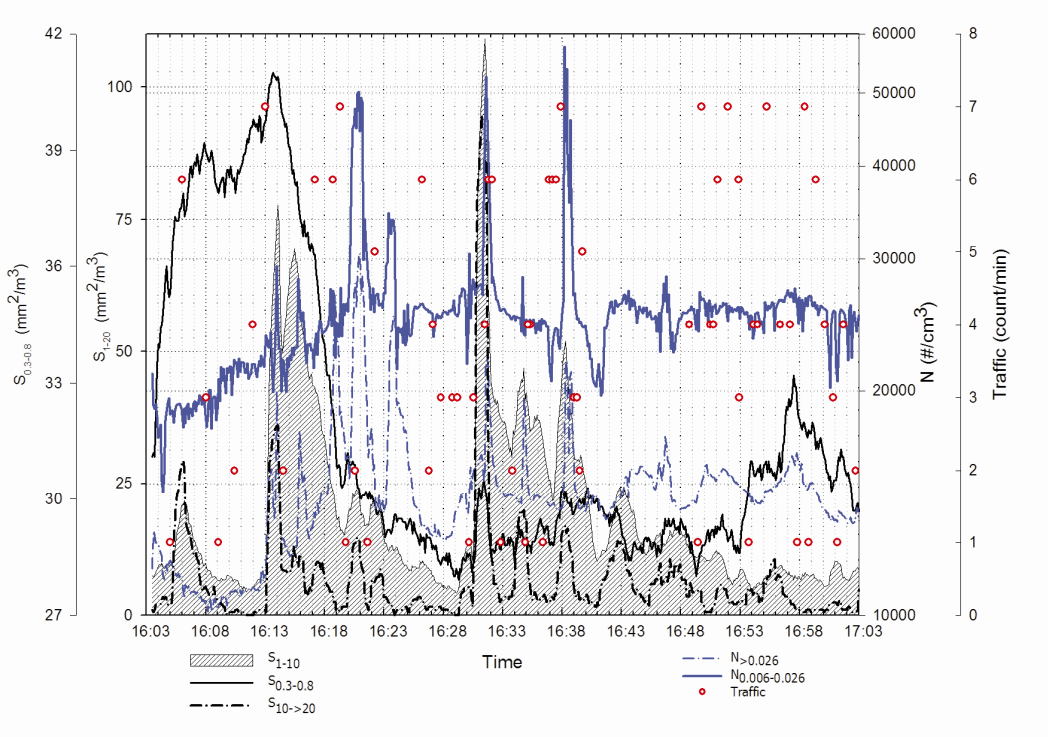

Figure 37. Time series measured during the selected event for: (i) number concentration of particles in the 6-26 ($N_{0.006-0.026}$, blue solid line) and 26-300 ($N_{0.026}$, blue dash dot line) nm size range; (ii) surface area (S) of particles in the 0.3-0.8 ($S_{0.3-0.8}$, dark solid line), 1-10 (S_{1-10}, filled curve), 10->20 ($S_{10->20}$, dark dash dot line) μm size range; (iii) traffic counts (red circles) [Reproduced from Costabile et al., 2008b].

To unravel the hidden variables governing N, PCA^I was run (Figure 38) as defined by (Eq.2) where x_{kj} is the value standardized by (Eq.1) of the k^{th} variable given by the (Eq.3):

$$x_{kj} = N_{\alpha-\beta} = N_\beta - N_\alpha, \begin{Bmatrix} \alpha,\beta \in \{(0.006,0.026,0.3,0.4,0.5,0.65,0.8,1,1.6,2,3,4,5,7.5,10,15,20)\mu m\} \\ \beta > \alpha \\ m = 16 \end{Bmatrix}$$

(3)

for the j^{th} observation taken during the event. PCA is a multivariate statistical technique commonly used for source apportionment of particulate matter [e.g., Vallius et al., 2003; Hopke et al., 1976]. In this work, particle modes and sizes were used as specific markers of source and process categories contributing to N [e.g., Birmili et al., 2001]. These categories were identified by examination of the variable loadings on the PCs (Figure 38), which indicated the correlation of each variables with each component [Almeida et al., 2005].

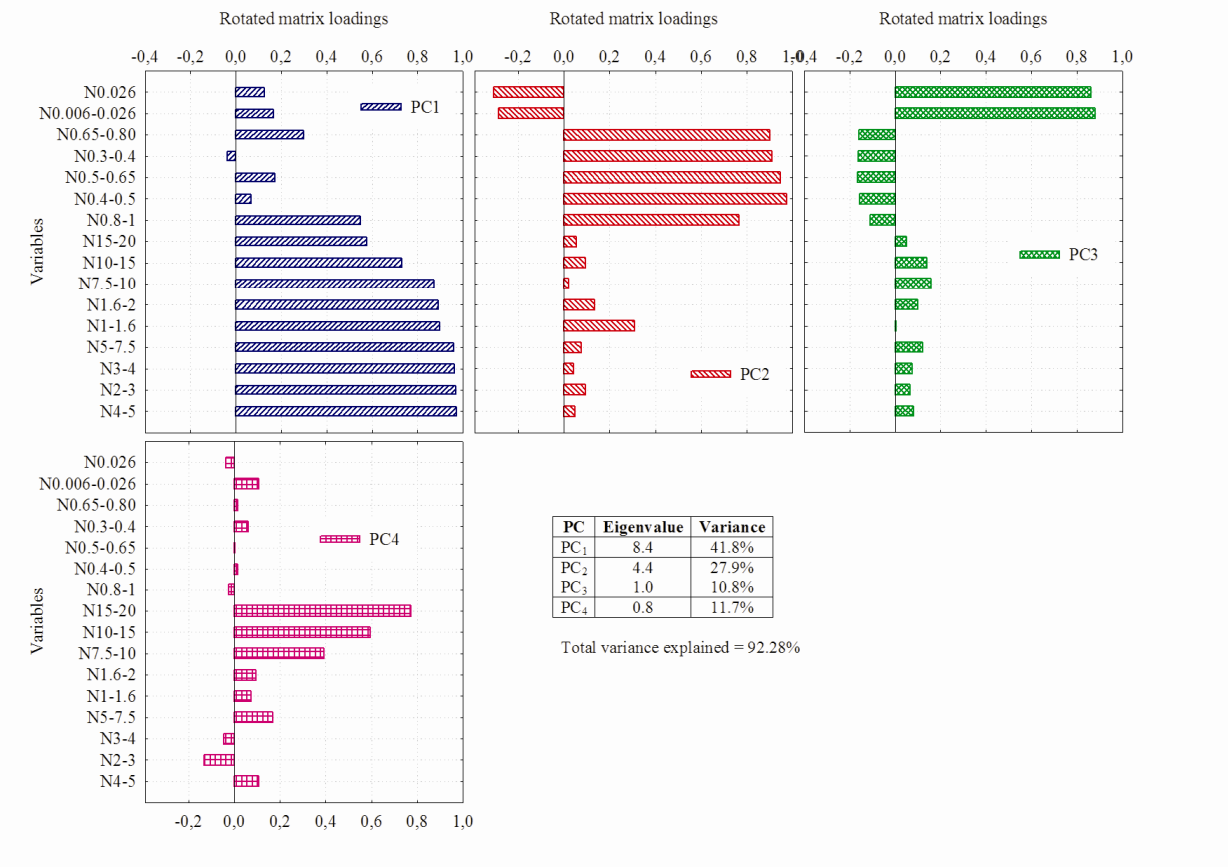

Figure 38. PCA^I as defined by (Eq.1,2,3) with 16 variables given by the number concentration N of particles spanning from 0.006 to 20 µm grouped in 16 size bins [Reproduced from Costabile et al., 2008b].

The particle number distribution (PND) analysed by PCA^I was found to be governed by the interaction of four components (eigenvalues>0.6) at 92.28% of total variance explained (Figure 38). this finding firstly shows as different modes of the size distribution behave differently to one another. However, their further analysis could likely provide insights to: (i) sources [e.g., Birmili et al., 2001] and aging processes of particles after the emission (i.e. dilution with background air, nucleation, coagulation, deposition and condensation [e.g., Zhang and Wexler, 2004]); (ii) other variables influencing the occurrence of these processes, such as available S and temperature [e.g., Kerminen et al., 2001; Voigtalnder et al., 2006]. Therefore, it is presented in the followings.

8.4. PARTICLE SOURCES AND AGING PROCESSES DURING THE EVENT

PC_1^I (Figure 38) reveals that all the size ranges of N correlate positively with each other with the exception of $N_{0.3\text{-}0.5,}$ which loads highly (in $N_{0.3\text{-}0.8}$) on PC_2^I. This could

indicate a common prevailing source for all the particle size ranges measured with the exception of the 0.3-0.5 μm channel. This source is likely attributable to the traffic emissions from the near roads [e.g., Wåhlin et al., 2006]. It dominated particles larger than 1 μm, likely attributable to tyre and brake abrasion and soot re-entrainment from the exhaust pipe [i.e., Imhof et al., 2005;Weijiers et al., 2004]. In contrast to the larger particles, the small combustion-generated particles ($N_{0.006\text{-}0.026}$, $N_{0.026\text{-}0.3}$) directly stemmed from the exhaust pipe [e.g., Pirjola et al., 2004; Zhu et al., 2002; Shi et al., 1999] could be linked to PC_3^I. Because of their singular variation into PC_1^I (Figure 38), emission sources of particles in the 0.3–0.5 μm size range (loading on PC_2^I) can be likely related to long-range transport [Birmili et al., 2001; Wåhlin et al., 2006] rather than to incomplete combustion emissions from the near road [Imhof et al., 2005]. As presented here PC_2^I is not a specific pollution component, but it is comprised of particles from various sources "aged" during the transport, e.g. diesel vehicle traffic [e.g., Kleeman et al., 2000], urban background, vegetation burning (around 0.06 μm) [Morawska et al., 2003], "droplets" (above 300nm) [Birmili et al., 2001]. Finally, particles larger than 10 μm showing a different pattern to the smaller ones [e.g., Charron and Harrison, 2003] and loading on PC_4^I can be probably linked to the re-suspension of road dust due to both traffic and wind [e.g.,Weijiers et al., 2004]. Data should be less meaningful for this size range due to the lower abundance of particles, and therefore poor counting statistics.

Beyond indicating that the PND resulted from the interaction of the four above mentioned sources, this analysis is, however, hampered by a lack of understanding of the different variances found for the PCs (Figure 38). To solve this issue, the findings were further analysed. It is known that PCA orthogonalizes the components of the input vectors, orders the resulting PCs so that those with the largest variation come first, and eliminates components that contribute the least to the variation in the data set [Jain and Dubes, 1998]. Since processes with the smallest time scales have most relevance in changing the concentrations of the particles [e.g., Ketzel and Berkowicz, 2004], the idea here is that the faster the process, the higher the variance, the higher the eigenvalue. Therefore, PC_1^I could likely indicate the fastest process (highest variance) influencing most of the size ranges of N and varying with particle diameters (Figure 38). At the concentration levels of this work, this process could likely be the

dilution of traffic emissions from the closest upwind road [e.g., Ketzel and Berkowicz, 2004; Jacobson and Seinfeld, 2004]. The higher loadings of the supermicron particles (Figure 38) are likely linked to the fact that the return to background levels is faster for particles larger than 1 μm removed faster due to sedimentation [e.g., Weijers et al. 2004]. In particular, for particles sufficiently large (10-20 μm size range) the dominant process (with the highest loadings) was likely the gravitational settling represented by the PC_4^I (Figure 38). Conversely, for submicron particles, remaining longer in the air, gravitational settling was ineffective when compared to the other faster processes associated to PC_2^I and PC_3^I [e.g., Weijers et al. 2004; Zhang and Wexler, 2002]. The former, PC_2^I, could likely indicate a process quite significant near road (second highest variance, Figure 38), but slower than dilution (lower variance and eigenvalue, Figure 38) in altering the PND. This process could have a time scale depending on particle sizes (Figure 38) and fastest in scavenging (as the major removal process) the smallest particles (D<300nm highest negative loadings). The removal of these smallest particles (D<300 nm) in PC_2^I (Figure 38) could be linked to the highest increase of submicron particles larger than about 0.05 μm (positive highest loadings), but not to even larger (supermicron) ones. All these findings could probably suggest [e.g., Holmes, 2007; Pohjola et al., 2003; Zhu et al., 2002; Ketzel and Berkowicz, 2004; Kerminen et al., 2001; Alam et al., 2003; Zhang and Wexler, 2002] that this component could be linked to coagulation processes.

Finally, PC_3^I could likely be linked to the mechanism of formation of the smallest particles, for whom it was found to be the dominant process (highest loadings) without influencing the other number concentrations [e.g., Holmes, 2007; Charron and Harrison, 2003; Zheng and Wexler, 2002], as better discussed below.

8.5. PRINCIPAL FACTORS INFLUENCING NUCLEATION MODE PARTICLES

To better understand the PC_3^I (Figure 38), PCA^{II} was calculated (Figure 39) including $N_{0.006\text{-}0.026}$, $N_{0.026\text{-}0.3}$ and other variables expected to influence it, such as ambient T and RH [Abdul-Khalek et al., 1999; Bukowiecki et al., 2003], available S [Holmes

2007; Zhang and Wexler, 2002], and traffic counts from the closest road. PCA^{II} is defined by (Eq.2) where x_{kj} is the value standardized by (Eq.1) of the k^{th} variable given by the (Eq.4):

$$\left\{\begin{array}{l} x\in\{N,SA,RH,T,WS,Wdir,VehN\} \\ x=N,SA\rightarrow x=x_{\alpha-\beta}=x_{\beta}-x_{\alpha}\left\{\begin{array}{l} x=N\rightarrow\alpha,\beta\in\{(0.006,0.026)\mu m\} \\ x=SA\rightarrow\alpha,\beta\in\{(0.3,0.4,0.5,0.65,0.8,1,1.6,2,3,4,5,7.5,10,15,20)\mu m\} \\ \beta>\alpha \end{array}\right\} \\ m=22 \end{array}\right\} \quad (4)$$

for the j^{th} observation taken during the event.

The variables were found to be governed by the interaction of five components (eigenvalues>1) at 84 % of total variance explained. PC_1^{II} and PC_3^{II} show meanings quite similar to PC_1^{I} and PC_4^{I} (Figure 38, Figure 39). PC_4^{II} seems to be linked predominantly to the meteorology. PC_5^{II} (with the lowest variance) is likely associated to the dilution of exhaust plumes due to the mechanically-induced turbulence produced by the passing vehicles on the near road (Figure 39).

On the contrary, the explanation of PC_2^{II} is not so straight forward. As suggested by PC_2^{I}, PC_2^{II} reveals a singular relationship between three variables (Figure 39): $N_{6\text{-}26}$, $S_{300\text{-}800}$, and ambient T (and the associated RH), whose scatter plot is reported in Figure 40.

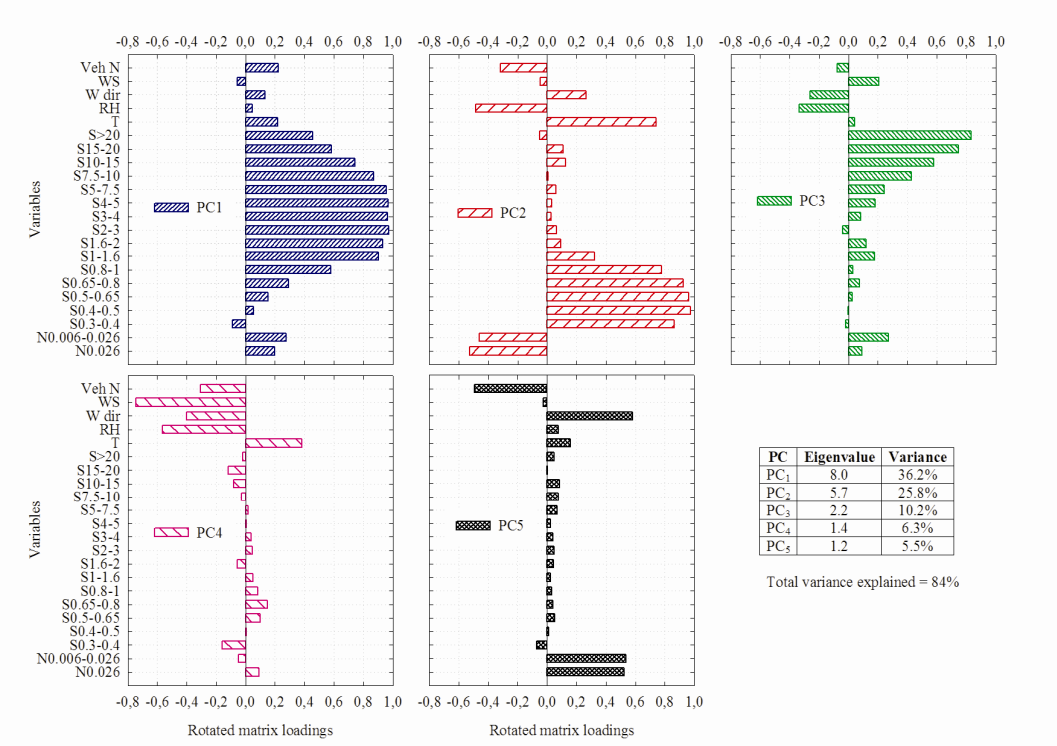

Figure 39. PCA^{II} as defined by (Eq.1,2,4) with 22 variables: (i) number concentration of particles in the 6-26 ($N_{0.006-0.026}$) and 26-300 ($N_{0.026}$) nm size range; (ii) surface area (S) of particles spanning from 0.3 to> 20 µm grouped in 15 size bins; (iii) meteorological variables (relative humidity, RH, temperature, T, wind speed and direction, WS, Wdir); and (iv) vehicle number (Veh_N) [Reproduced from Costabile et al., 2008b].

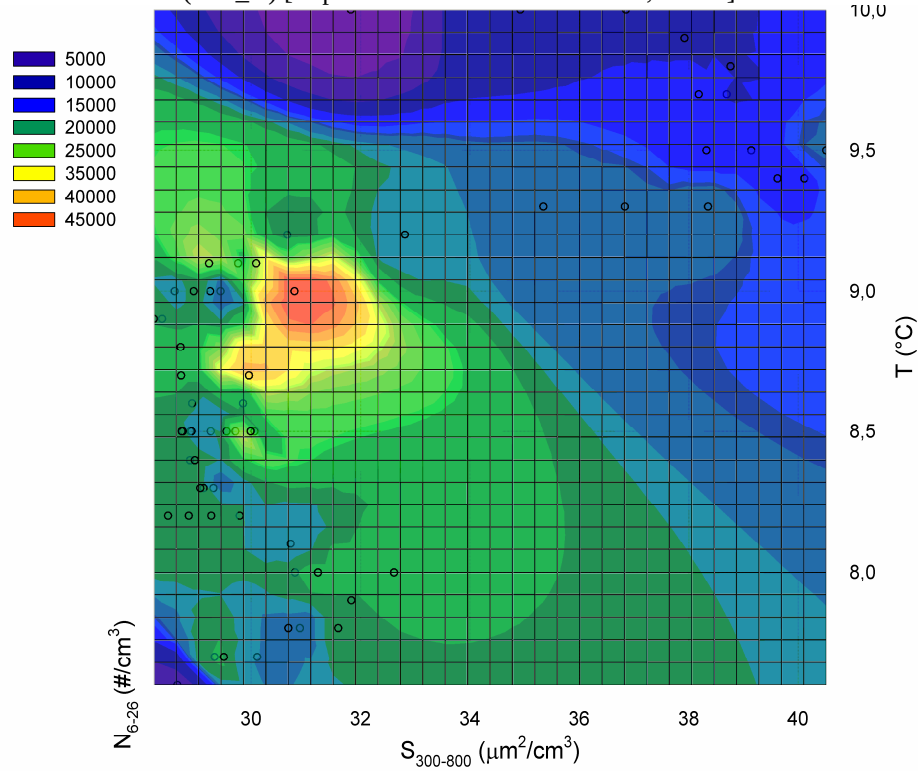

Figure 40. The measured relationship between the $S_{300-800}$ (x-axis), T (y-axis) and N_{6-26} (z-axis, colours). Triplets of raw data (circles) are smoothed by a tricube weigh function to weight the data, and a polynomial regression of degree 3 is used as smoother [Costabile, Allegrini, 2007a]. Each point along the smooth curve is obtained from a regression of data points close to the curve point with the closest points more heavily weighted. All data points were used for each regression. [Reproduced from Costabile et al., 2008b]

Vehicle counts from the near upwind road showed a eigenvalue < 0.5, and therefore were excluded from the further analysis. Little variations of $S_{300\text{-}800}$ appear to correspond to large variations of $N_{6\text{-}26}$ (Figure 40), so that two branches can be recognised in the (raw) data (black circles) for $S_{300\text{-}800}$ greater/lower than 32 $\mu m^2/cm^3$ (it should be again pointed out that these results are limited by the unavailability of aerosol surface area for particles smaller than 300 nm due to the OPC lowest cut-off size). $N_{6\text{-}26}$>30.000 #/cm^3 (N>40.000 #/cm^3, Figure 36) occurred only for the lowest $S_{300\text{-}800}$ values (vertical branch, bottom-left Figure 40). This likely suggests that lower $S_{300\text{-}800}$ could have not been sufficient for low volatile gases to condense and, thus, could allow the gases emitted from the passing vehicles to nucleate and grow (increasing $N_{6\text{-}26}$) [e.g., Holmes, 2007]. Conversely, higher $S_{300\text{-}800}$ values (horizontal branch, top-right, Figure 40) could have likely promoted the condensation of these gases (competing with the nucleation), so reducing particle formation (lower $N_{6\text{-}26}$) [e.g., Scheer et al., 2005]. In an attempt to clarify the connections between soot and nucleation mode particles (NMP), Imhof et al. (2006) observed a threshold value of the S of soot whose increase/decrease led to a correspondent decrease/increase of NMP. They suggested this value to be dependent on the ambient T. In our work, the relationship between N, S and T likely indicates higher $N_{6\text{-}26}$ for lower T [e.g.,Hussein et al., 2006; Virtanen et al., 2006; Voigtländer et al., 2006] only down to a threshold value of T (≈9°C, Figure 40). Below this value, $N_{6\text{-}26}$ decreases. Giechaskiel et al. (2005) also noticed a similar effect, with NMP appearing only when T of the exhaust gases (measured just before sampling) reached ≈165°. In our case, in absence of additional data, a tentative explanation could consider the balance between the twofold effect of T on particle nucleation. On one hand, for lower T the value of the saturation ratio, SR, provided by (5)

$$SR = \frac{p_A}{p_A^S(T)} = \frac{N_A}{N_A^S(T)} \quad (5)$$

can be sufficiently large to let sufficiently large clusters to be formed [Seinfield and Pandis, 2006; Kulmala et al., 2000; Kulmala et al., 2007]. On the other hand, however, the critical size that these clusters must exceed to grow and form a new phase (nucleate) is inversely proportional to T [Seinfield and Pandis, 2006]: a minimum T value could likely be required. In this meaning, the vehicle-emitted gases

could either nucleate (N_{6-26} increased considerably) or condensate over the available $S_{300-800}$ (N preserved, particles < 0.6-0.8 μm grew appreciably) according to both $S_{300-800}$ and ambient T. The highest values of N_{6-26} in Figure 40 could likely reflect the balance between the availability of pre-existing $S_{300-800}$ for condensation of vapours emitted on the near upwind road and the T-controlled availability of stable clusters for nucleation of the same emitted gases.

CHAPTER 9.
CONCLUSIONS AND OUTLOOK

The spatial variation of traffic related air pollution from tailpipe-to-road-to ambient was studied especially focussing on UFPs. The process was analysed using a two stage structure (tailpipe-to-road and road-to-ambient) due to the different spatial and temporal scales of the related processes. The methodological approach based on the analysis of frequency distributions of space-series was developed at both the stages firstly for major traffic-related air pollutants, and then applied to UFPs. Initially, a new methodology for assessing the spatial distributions of traffic air pollutants at urban (road-to-ambient) scale was developed. Concurrently, a new approach to link air quality and traffic air pollution at urban scale (stage road-to-ambient) was studied. Therefore, the two above mentioned approaches were applied to analyse a real case of UFP variation in an urban area (stage road-to-ambient). Then, the spatial distribution of reactive traffic-related air pollutants into a street-canyon (namely including chemistry and fluid-dynamics effects) was analyzed (stage tailpipe-to-road). Finally, the major findings of this work guided the assessment of ultrafine particles near-road, at stage tailpipe-to-road.

The methodology to analyse the spatial variation of traffic air pollution was developed by considering air pollutants' concentration in terms of frequency distributions (FD) of its space series. The dilution processes (indicated by a LogNormal FD, as explained by the theory of successive random dilution) was shown to be not the dominant process to fit the spatial variations. Conversely, space-FDs of traffic air pollutants were found to be fitted by the Gaussian FD, that is the data matched the pattern expected if the data was drawn from a population with a Normal distribution. When traffic emissions in urban areas can be considered as sources spatially diffused (no highways, etc.), pollutants mainly emitted by vehicle emissions show a Normal space-FD being other factors less relevant. This result is very important in understanding the characteristic of the spatial trend of these pollutants. Every process where the pollutant particles show a Normal distribution of the spatial trend density, satisfies the diffusion equation and thus represent such a mechanism. The predominant factors influencing the spatial FD type of air pollutant

concentrations may, therefore, be associated to the diffusion mechanisms in atmosphere, rather than mixing and diluting of source emissions. These factors are meteorology, relevant emission sources, seasonality, photochemistry, and topography. Moreover, being the spatial data distribution Normal, mean and median values (quite same) can correctly be used to represent the concentration values of these pollutants all over the city for air quality management purposes and calculation of air pollution indexes.

The methodology to allow the communication at road-to-ambient scale between transport emissions and air quality in real-time was developed by considering integrated systems. The successful approach, currently under way as case-study in Beijing, considered the integration of the modeling to interpret the data measured with the measurements to validate the data modeled. The work was intended to better understand how the improvement of transport technology, both private and public, the reduction of vehicles pollution proportion by technological, political and scientific measures and the improvement of emission performances, could be integrated with "intelligent" transport management system. However, there remains a need to continue research to improve our understanding of the mechanisms leading to air pollution impacts from transport emissions, to reduce the uncertainty in our ability to quantify the relationships between all emissions and all impacts. For urban air pollutants from road traffic there remain some doubts concerning both the existence and the mechanisms of cause and effect, particularly for particles, which are currently one of the air pollutants causing most concern.

To this meaning, the number concentration of UFPs were analysed at stage 1, from road-to-ambient both near emission sources and at a background location. They were found to be a clear indication of vehicle exhaust sources in ambient air. At urban scale UFPs resulted from three prevailing contributions. Firstly, a very low urban background UFP concentration (lower than 1000 #/cm^3) particularly visible in summer. Secondly, a significant contribution due to local traffic sources, up to 100.000 #/cm^3 (traffic site in winter time). Finally, a significant contribution due to secondary transformation processes closely linked to meteorology, particularly solar radiation. Transport from sources nearby were also found to be significant, indicating significant UFP lifetime in atmosphere. The conditions near mobile emission sources were found to differ from typical background conditions in that particle number concentrations were much higher, and dilution processes were much faster and

stronger. The stronger variability induced more rapid concentration fluctuations, probably due to faster and more intense dilution processes, which can reduce the number concentration more rapidly, as well as trigger physical processes other than dilution, such as nucleation, coagulation, and condensation.

The analysis of the stage 2, from tailpipe-to road, revealed traffic pollutants emitted at road level to vary relevantly on the vertical coordinate even to less than 15 m. The analysis of the frequency distribution (FD) of the (spatial) differences between the two measured (time) concentrations (for each pollutant) gave insights into the pollutant diffusion mechanisms in atmosphere from tailpipe to road (Costabile et al., 2006b). The spatial distribution of a pollutant governed largely by local vehicle emissions (e.g. NO into a street-canyon) was largely determined by the vertical diffusion of emissions: difference of concentrations distributed statistically according to the Gaussian curve. The higher the chemical reactivity of the pollutant (e.g., O3), the lower the spatial distribution with a variability strongly influenced by local fluid-dynamics effects, and a FD influenced by systematic factors deviating it from the Normal FD.

Finally, the number distribution of aerosol particles spanning from 6 nm to more than 20 μm was analysed on the road (stage 2, from tailpipe-to-road). It was found to be governed by the interaction of four Principal Components at 92.28% of total variance explained. This indicated major sources (traffic emissions and long-range transport) and “aging” processes of particles after the emission (dilution, coagulation, nucleation and condensation, and gravitational settling), grouped over the four orders of magnitude of diameters. The analysis of variables governing the occurrence of these processes revealed the number concentration of particles in the 6-26 nm size range (N_{6-26}, including nucleation mode particles) to be largely influenced by the surface area of particles smaller than 800 nm ($S_{300-800}$, including accumulation mode particles) and ambient T. The highest values of N_{6-26} occurred for threshold values of both $S_{300-800}$ and T. In absence of additional data, it was argued that the balance between two prevailing processes probably triggered the increase of N_{6-26}: the availability of $S_{300-800}$ for condensation of the vapours emitted, and the T-controlled availability of stable clusters for nucleation of the same emitted gases. This finding was a further evidence that nucleation particles can be both directly emitted from the engine and formed in atmosphere soon after the emission according to some governing factors.

There appear at least two directions to proceed from the present study. First, the pursuing towards a stage 0 for UFPs number size distribution from engine to tailpipe. Its analysis could result in a comprehensive emission inventory of combustion generated UFPs emitted by motor engines. In order to control level of atmospheric pollution caused by vehicle engine emissions, the international legislation has indeed established over the years a series of tests to evaluate the potential capability to pollute of different types of engines in order to impose restrictions to the commercialization of high polluting engines. These tests have been designed with the purpose of simulating real engine operating conditions by the performance of both steady and transient test cycles. For several sources the non-steady-state emissions are suspected to be a significant portion of the total air pollution emitted, and hence, their quantification may be important towards determining average emission factors, pollutant exposure and mode-specific pollutant minimization [e.g., Gullet et al., 2006]. The Engine Exhaust Particle Sizer spectrometer (Figure 1-1) acquired by the Department of Mechanical Engineering of Tor Vergata university during this Ph.D. work (see Appendix) is an instrument designed specifically for measuring particles emitted from internal combustion engines and vehicles. The EEPS [e.g., Johnson et al., 2004; Kittelson et al., 2006] gives particle size distribution in the 5.6-560 nm size range resolved with the fastest time resolution available—10 times per second—. It means that it's possible to investigate particle size distribution emitted by motor engines not only in steady-state engine operation but also in transient engine operation. In this way, great emphasis can be put on measurements during transient test cycles, representing real-world driving behaviour.

The main findings of this further study could, then, drive a further direction of research closing the circle indicated by this work, that is the assessment of the spatial distribution of UFP number size distribution from engine-to-tailpipe-to-road-to-ambient. This has the potential to finally indicate to what extent number size concentrations of UFPs measured at the exhausts of a single engine could reflect the outdoor concentrations in ambient air in a whole urban area.

APPENDIX [6]: ENGINE EXHAUST PARTICLE SIZER

The Model 3090 Engine Exhaust Particle Sizer spectrometer (EEPS™, mod.3090, TSI Inc., MN, USA) (Figure 41) is a fast-response, high-resolution instrument that measures very low particle number concentrations in diluted exhausts.

[6] This Appendix is reproduced from the *Model 3090 EEPS™ Engine Exhaust Particle Sizer: Operation and service Manual* (P/N 1980494, Revision E, August 2006) TSI Incorporated (www.tsi.com).

Figure 41. Model 3090 Engine Exhaust Particle Sizer spectrometer [Reproduced from TSI, 2006]

Instrument operating specifications are as follows (Table 8):

Particle Size Range	5.6 to 560 nanometers
Particle Size Resolution	16 channels per decade (32 total)
Electrometer Channels	22
Charger Mode of Operation	Unipolar diffusion charger
Inlet Cyclone 50% Cutpoint	1 µm
Maximum Data Rate	10 size distributions per second
Flow Rates	
Aerosol Inlet	10 L/min
Sheath Air	40 L/min
Inlet Aerosol Temperature	10 to 52°C
Storage Temperature	-20 to 50°C
Atmospheric Pressure Correction Range	700 to 1034 mbar
User Interface	Rotary knob and display/EEPS software
Front Panel Display	6.4-in. color VGA LCD
Data Averaging	0.1 to 60 sec
Computer Requirements	Pentium® 4 processor or better
Computer Operating System	Windows XP or newer
Communications	9-pin RS-232
Analog Inputs	2 analog input ports, 0 to 10V, 12 bit Electrically isolated to 500V
Analog Outputs	4 analog output ports, 0-5V or 0-10V, 14 bit Electrically isolated to 500V
Trigger Inputs	Two trigger input channels, potential-free contact closure or 3.3 V pulled to GND Electrically isolated to 500V
Trigger Output	Potential-free contact closure Electrically isolated to 500V
Dimensions (LWH)	70.4 cm × 34.3 cm × 43.9 cm (27.7 in. × 13.5.0 in. × 17.3 in.)
Weight	32 kg (70 lb)
Aerosol Inlet	3/8-in. OD
Exhaust Outlet	3/8-in. OD
Cyclone Inlet	3/8-in. OD
Power Requirements	100 to 240 VAC, 50/60 Hz, 170 W maximum
Fuse (internal—not user replaceable)	~T 6.3A SB/250V

Table 8. EEPS (mod.3090, TSI) operating specifications [Reproduced from TSI, 2006]

It's ideal for analysis of a wide range of engine exhaust situations, including engine tailpipe measurements (Engine Dynamometer test cells, Chassis Dynamometer test cells, Old diesel engines with high emissions, New generation diesels with active controls, Measurements upstream and downstream of Diesel Particulate, Filters or Particle Traps, Spark Emission engine emissions—GDI Engines), and mobile Measurements.

The first electrical mobility instrument was the Whitby Aerosol Analyzer, developed in the late 1960's [Whitby and Clark, 1966]. This was followed a few years later by a similar but smaller version called the EAA (Electrical Aerosol Analyzer) [Lui and Pui, 1974]. These instruments both used a unipolar charger assembly to place a positive charge on the particles. The level of charge depends on particle size and is correlated by the instrument calibration so that the instruments can report number concentrations. An improvement over the EAA was the development of the Differential Mobility Analyzer (DMA) column (Figure 42).

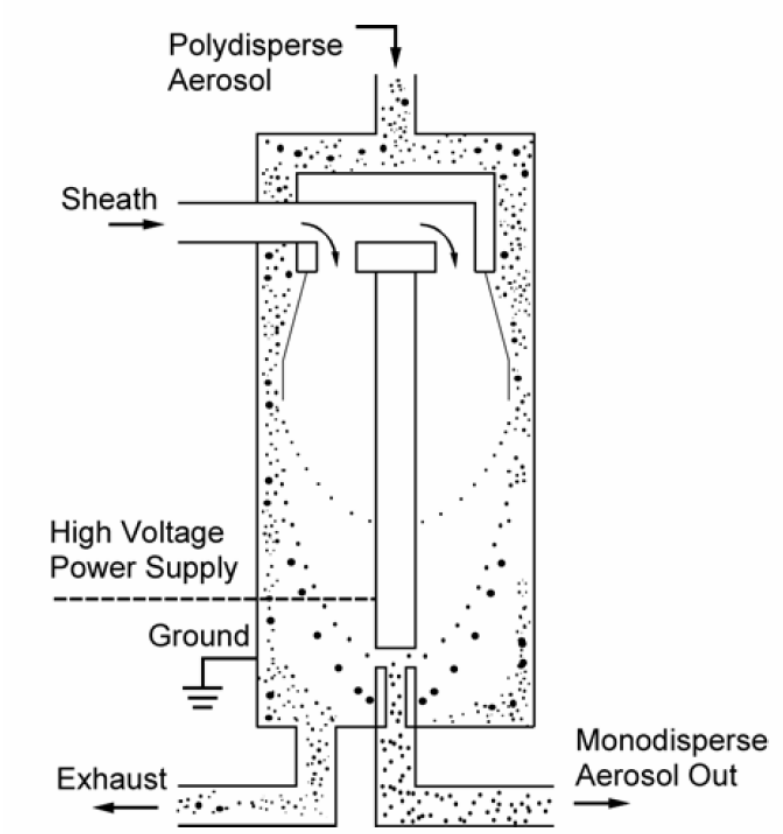

Figure 42. Schematic of a Differential Mobility Analyser [Reproduced from TSI, 2006]

Rather than using a unipolar charger, a very stable and predicable Krypton-85 radioactive bipolar charger was used [Fuchs, 1964; Wiedensohler, 1988]. When combined with a Condensation Particle Counter (CPC), the DMA can be stepped through various voltages, to detect different particle sizes [Fissan et al., 1983; Hoppel, 1978; Hussin et al., 1983; Kinney et al., 1991; Knutson and Whitby, 1975]. Using a computer, the voltages can be automatically stepped to generate a particle size distribution. This was the basis for the Differential Mobility Particle Sizing (DMPS) systems. An improvement in resolution is obtained by continuously scanning the rod

voltage with an exponential voltage ramp and counting to generate a size distribution [Wang and Flagan, 1990; Quant et al., 1993]. This is the basis for the current Scanning Mobility Particle Sizing (SMPS) system that is commonly used to obtain high resolution size distributions of engine exhaust particles. Unfortunately, the SMPS method has a drawback in that it takes a significant amount of time (30 seconds minimum with 60 or 120 seconds being more commonly used) to obtain a single size distribution. This makes it unsuitable for measuring engine transients on a second-by-second basis. This led to designs for an improved sizing instrument that could give complete size distributions in one second or less. The EEPS spectrometer is such an instrument.

The basic idea upon which the EEPS Model 3090 is based was developed at Tartu University in Estonia [Mirme and Tamm, 1991; Mirme and Tamm, 1993; Tammet et al., 1998]. The EEPS spectrometer is based on this fast-response instrument. Conceptually these instruments are similar to a DMA. But, rather than particles being drawn to the center, as in a DMA, the particles are repelled outward to electrodes. The EEPS spectrometer performs particle size classification based on differential electrical mobility classification (as with the SMPS). The charged aerosol enters the analyzer column near on-axis and above the central rod. The particles are deflected radially outward and collected on electrically isolated electrodes that are located at the outer wall (see Figure 43). The particle number concentration is determined by measurement of the electrical current collected on a series of electrodes.

The charging of the aerosol is accomplished through two unipolar diffusion chargers. First, a negative charger puts a negative net charge on the particles to reduce the number of highly positive charged particles and to prevent overcharging in the second charger. Then, a positive charger puts a predictable net positive charge on the particles.

The electrical analyzer consists of an inner cylinder composed of multiple electrical sections with different voltages and column diameters. By stepping the voltage and changing the central column diameter, the required height of the column is reduced and the particles are more evenly distributed across 22 electrodes. The electrode rings are made of a highly insulating plastic with metal rings molded into the inner diameter of the ring. Features in these parts provide a large electrical resistance between the electrometer rings while minimizing the gap between the rings. O-ring seals between

the electrode rings ensure a leak-tight column. Custom electrometers are used to obtain low noise, fast response and high resolution.

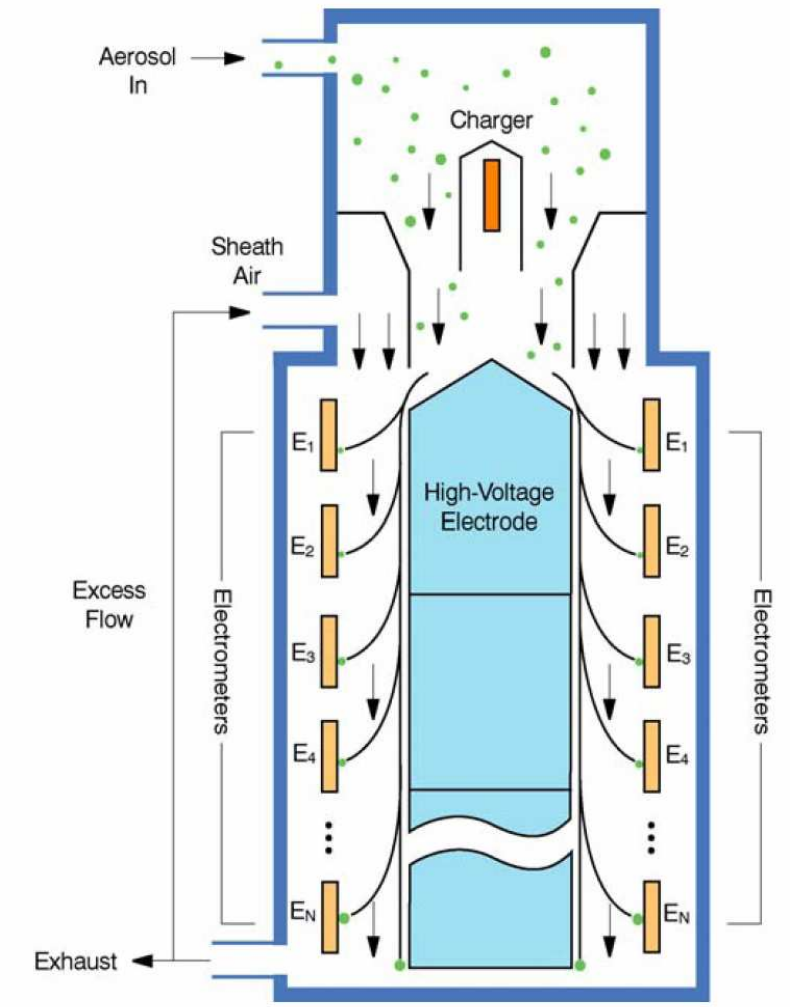

Figure 43. Schematic of EEPS measurement column [Reproduced from TSI, 2006]

After passing through a 1μm cut cyclone, the aerosol enters the charger at 10 L/min and close to atmospheric pressure (see Figure 44). It then passes through the charging region where it receives a predictable charge. In the charger, 0.6 L/min of clean air is added to the flow to keep the charger electrode clean. After the charger, 2 L/min is removed from the center of the charging region, where charging is less uniform, and the rest of the aerosol passes near the center electrode. A recirculating flow of particle-free, laminar sheath air at 39.4 L/min joins the particle flow at the top of the center electrode for a total of 48 L/min through the column. Particles are then separated by electrical mobility as flow moves from the top to the bottom of the column. Particles with high electrical mobility (small particles) are deflected to the

electrode rings near the top of the column, and those with low electrical mobility (large particles) are deflected further downstream. Air flow that is not filtered and recirculated is passed out of the exit of the instrument at 10 L/min.

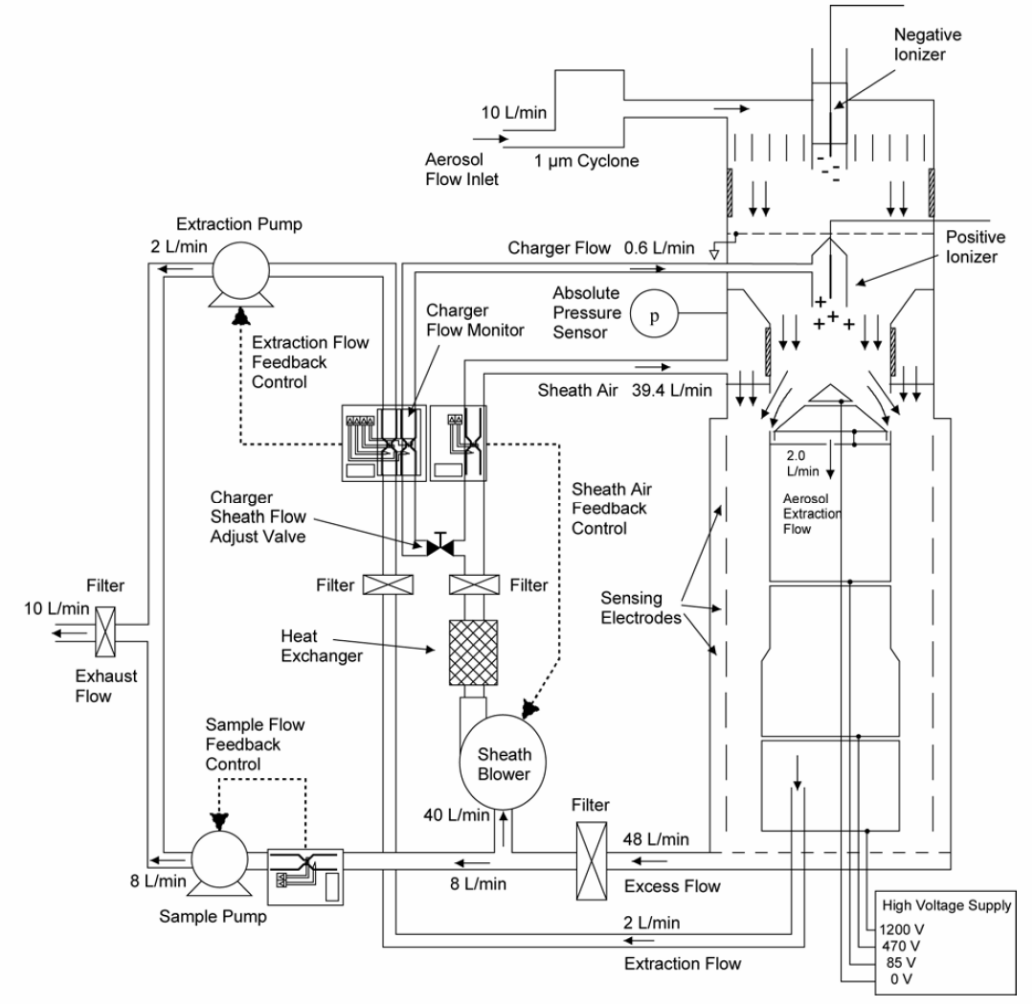

Figure 44. Flow schematic of EEPS spectrometer [Reproduced from TSI, 2006]

There are a number of parameters affecting the electrometer currents that need to be compensated if high time resolution is to be obtained. Particles that flow past the detection stages but don't contact the electrode rings can create image charges. In addition, there are time delays between when a small particle from an aerosol packet is detected on an upper stage of the column and when a large particle from the same aerosol packet is detected on a lower stage in the column. An inversion algorithm is used to deconvolute the data and make corrections for the image charges and the time delays in the column. The algorithm also converts currents from the 22 electrometers into 32 size channels of output. This allows the maximum resolution of the instrument

to be represented by output channels that are equally spaced on a log scale between 5.6 nm and 560 nm.

Unlike many instruments which have a single value as the lower detection limit, the EEPS has a range of values depending on particle size and averaging time. This is due to the inherent noise in each electrometer as well as the particle charging probability vs. particle size. Figure 45 gives a range of lower limits for several averaging intervals based on particle size.

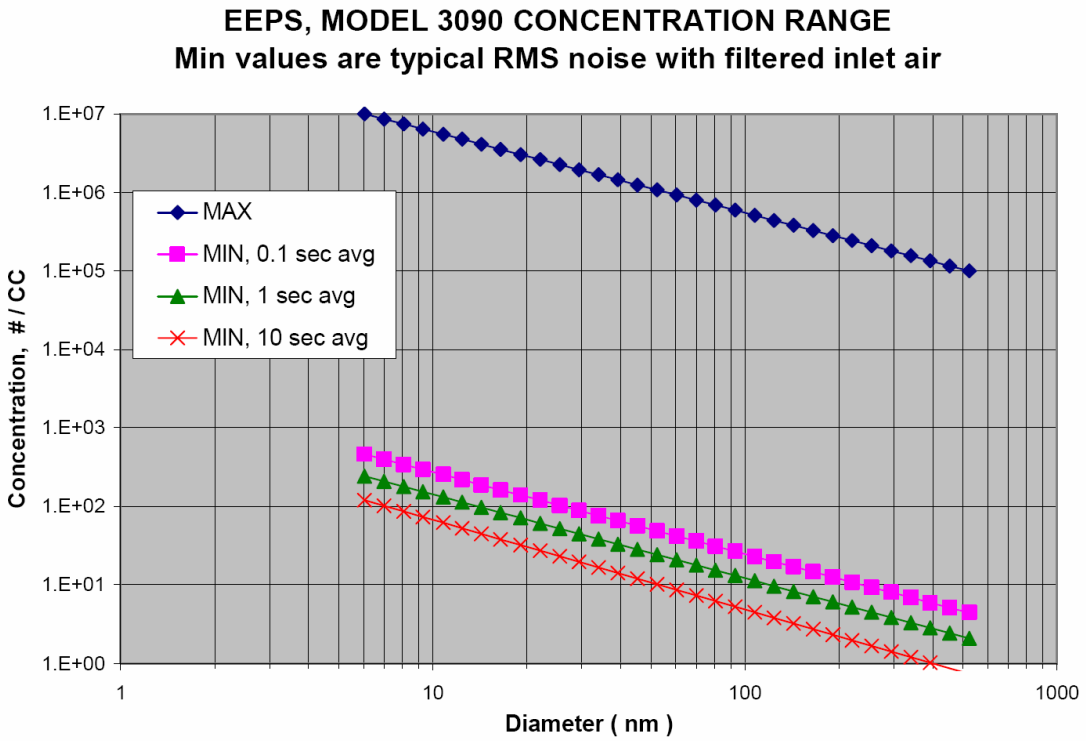

Figure 45. Graph of concentration limits [Reproduced from TSI, 2006]

The EEPS software calculates a different detection limit based on each of the possible averaging intervals that can be selected in the software. The upper limit of concentration is based on the fixed upper limit of current that can be detected by each electrometer channel. This limit is also plotted in Figure B-4. However, this limit does not change with averaging time. The EEPS software uses this limit to show maximum limit values (red boxes) at the top of any bar in the 2D histogram which has reached or exceeded this value. When a value is exceeded, the bar is clipped at the maximum value, affecting the shape of the distribution.

ACKNOWLEDGMENTS

This work has been part of a collaboration between the Department of Mechanical Engineering of the University of Tor Vergata and the Institute for Atmospheric Pollution of CNR. With this regard, the support of Dr. Ivo Allegrini is appreciatively acknowledged.

My truthful thanks are extended to Prof. Luca Andreassi, Prof. Montanari, Dr. Vincenzo Mulone, for their precious comments, and kindness.

A special gratitude is for Prof. Vittorio Rocco and Prof. Stefano Cordiner, whose help has been priceless.

Last but not least, I'd like to infinitely thank my parents, and my life- and PhD-mate, Antonio.

REFERENCES

Abdul-Khalek, I. S.; Kittelson, D. B.; Brear, F. , 1999. Influence of dilution conditions on diesel exhaust particle size distribution measurements. *SAE Technol. Pap. Ser.*, no. 1999-01-1142.

Abdul-Wahab, S.A., Al-Alawi, S.M., 2002. Assessment and prediction of tropospheric ozone concentration levels using artificial neural networks. Environmental Modelling and Software 17, 219-228.

Alam A., Shi Ping, J. and Harrison R. (2003), Observations of new particle formation in urban air. *J. Geophys. Res.* 108: D3, doi: 1029/2001/JD001417.

Alastuey, A., Querol, X. , Rodríguez, S., Plana, F., Lopez-Soler, A., Ruiz, C., Mantilla, E., 2004. Monitoring of atmospheric particulate matter around sources of secondary inorganic aerosol. Atmospheric Environment 38 (30), 4979-4992

Allegrini, I. , **Costabile, F.**, 2008. *Monitoring air quality and apportioning urban sources of air pollution. Experiences in China*. In: Sustainable development and environment protection, M.L. Gullino, I. Musu, C. Clini, Y. Xiaoling (ed.), Springer press, (English, Chinese) (in press)

Almeida, S.M. Pio, C.A., Freitas, M.C., Reis, M.A., Trancoso, M.A., 2005. Source apportionment of fine and coarse particulate matter in a sub-urban area at the Western European Coast. Atmospheric Environment 39 (2005) 3127–3138

APEG, UK Airborne Particles Expert Group, 1999. Source Apportionment of Airborne Particulate Matter in the United Kingdom. Report for Department of the Environment, Transport and the Regions in partnership with the Welsh Office, Scottish Office and Department of the Environment (Northern Ireland).

Atkins, D.H.F. and Lee, D.S., 1995. Spatial and temporal variation of rural nitrogen dioxide concentrations across the United Kingdom. Atmospheric Environment 29, 223-239.

Baker, C.J., 2001. Flow and dispersion in ground vehicle wakes. Journal of Fluids and Structures 15 (7), 1031–1060.

Baker, J., Walker, H. L., Cai, X., 2004. A study of the dispersion and transport of reactive pollutants in and above street canyons—a large eddy simulation. Atmospheric Environment 38, 6883–6892

Barletta, B., Meinardi, S., Sherwood Rowland, F., Chan, C, Wang, X., Zoud, S., Chan, L., Blake, D.R, 2005. Volatile organic compounds in 43 Chinese cities. Atmospheric Environment 39, 5979–5990.

Beijing Environmental Protection Bureau, 2003. Personal communication.

Bencala, K.E. and Seinfeld, J.H., 1976. On frequency distributions of air pollutant concentrations. Atmospheric environment 10, 941-950.

Berdowski, J.J.M., Mulder W., Veldt C., Visschedijk A.J.H., Zandveld, P.Y.J., 1997. Particulate matter emissions (PM10 – PM2.5 – PM0.1) in Europe in 1990 and 1993, TNO report, TNO_MEP – R 96/472.

Berkowicz, R., 1997. Modelling street canyon pollution: model requirements and expectations. International Journal of Environment and Pollution 8 (3–6), 609–619.

Birmili, W., Wiedensohler, A., Heintzenberg, J., and Lehmann, K., 2001. Atmospheric particle number size distribution in central Europe: statistical relations to air masses and meteorology, J. Geophys. Res., 106(D23), 32 005–32 018.

Biswas, S., Fine, P. M., Geller, M. D., Hering, S. V., and Sioutas, C., 2005. Performance Evaluation of a Recently DevelopedWater-Based Condensation Particle Counter. *Aerosol Sci. Technol.* 39, 419–427.

Boddy, J.W.D., Smalley, R.J., Dixon, N.S., Tate, J.E.; Tomlin, A.S., 2005. The spatial variability in concentrations of a traffic-related pollutant in two street canyons in York, UK—Part I: The influence of background winds. Atmospheric Environment 39(17), 3147-3161

Bosch H, Janssen R, 1987. Catalytic reduction of nitrogen oxides. Rev Fundamentals Technol Catal Today 2:369–521

Briggs DJ. 2000. Exposure assessment. In: Elliott P, Wakefield JC, Best NG, Briggs DJ, editors. Spatial epidemiology: methods and applications. Oxford: Oxford University Press; p. 335–59.

Brown, J.S., Zeman, K.L., Bennett, W.D., 2002. Ultrafine particle deposition and clearance in the healthy and obstructed lung. American Journal of Respiratory and Critical Care Medicine 166 (9), 1240–1247.

Brunekreef B, Dockery DW, Krzyzanowski M. Epidemiologic studies on short-term effects of low levels of major ambient air pollution components. Environ Health Perspect 1995;103:3–13.

Brunekreef, B., Holgate, S.T., 2002. Air pollution and health. The Lancet 360, 1233–1242.

Buccianti, A., Rosso, F., Vlacci, F., 2003. Metodi matematici e statistici nelle scienze della terra, ed. Liguori, Naples, pp. 204–206 (Italian).

Bukowiecki, N.; Dommen, J.; Prévôt, A. S. H.; Weingartner, E.; Baltensperger, U., **2003.** Fine and ultrafine particles in the Zürich (Switzerland) area measured with a mobile laboratory: An assessment of the seasonal and regional variation throughout a year. *Atmos. Chem. Phys., 3*, 1477-1494.

Burnett, R.T., Brook, J., Dann, T., Delocla, C., Philips, O.,Cakmak, S., Vincent, R., Goldberg, M.S., Krewski, D., 2000. Association between particulate- and gas-phase components of urban air pollution and daily mortality in eight Canadian cities. Inhalation Toxicology 12 (4), 15–39.

Charron, A., Harrison, R. M., 2003..Primary particle formation from vehicle emissions during exhaust dilution in the roadside atmosphere. Atmospheric Environment 37, 4109–4119

Chen, L., Mengersen, K., Tong, S., 2007. Spatiotemporal relationship between particle air pollution and respiratory emergency hospital admissions in Brisbane, Australia. Science of the total environment 373, 57–67

Chinese Academy of Science, 2006. Personal communication.

Clarke AD., 1992 Atmospheric nuclei in the remote free-troposphere. J Atmos Chem 14:479– 88.

Colvile, R.N., Hutchinson, E.J., Mindell, J.S., Warren, R.F., 2001. The transport sector as a source of air pollution. Atmospheric environment 35, pp.1537-1565.

CONCAWE (1998). A study of the number, size & mass of exhaust particles emitted from European diesel and gasoline vehicles under steady-state and European driving cycle conditions, prepared for the CONCAWE automotive emissions management group by its special task force AE/STF-10 (Brussels, Belgium) (56pp.). CONCAWE Report No. 98/51.

Costabile, F. , Desantis, F. , Wang, F., Hong, W., Liu, F. and Allegrini, I., 2006b. Representativeness of Urban Highest Polluted Zones for Sitting Traffic-Oriented Air Monitoring Stations in a Chinese City. JSME International journal-B 49 (1), 35-41.

Costabile, F. , Wang, F., Hong, W., Liu, F. and Allegrini, I., 2006c. Spatial Distribution of Traffic Air Pollution and Evaluation of Transport Vehicle Emission Dispersion in Ambient Air in Urban Areas. JSME International journal B 49 (1) 27-34.

Costabile, F., Allegrini, I., 2008b . Increase of particle number concentration at sunset time close to traffic emissions. Submitted to Science of the Total Environment (November 2007, Ms. Ref. No.: STOTEN-D-07-01887)

Costabile, F., Allegrini, I,., 2007b. Measurement and analysis in space and time of ultrafine particle number concentration in ambient air. The case of Parma. Proceeding of the International Conference UFIPOLNET, Dresden (Germany), 23-24 October 2007, pp.56-57.

Costabile, F., Allegrini, I., 2007a Measurements and analysis of nitrogen oxides and ozone in the yard and on the roof of a street-canyon in Suzhou. Atmospheric Environment 41(31), 6637- 6647

Costabile, F., Allegrini, I., 2008a. A new approach to link transport emissions and air quality: an intelligent transport system based on the control of traffic air pollution. Environmental Modelling & Software, 23 (3), 258-267, DOI 10.1016/J.envsoft.2007.03.001.

Costabile, F., Bertoni, G., Desantis, F., Wang, F., Hong, W., Liu, F., Allegrini, I., 2006a. A preliminary assessment of major air pollutants in the city of Suzhou, China. Atmospheric Environment 40 (33), 6380-6395.

Costabile,F., Wang,Q.,Bertoni, Ciuchini, Wang,F., Allegrini,I. 2006d. *A preliminary assessment of BTX pollution in urban air in the city of Lanzhou*. In: "Air Pollution XIV", pp.241-250, J.Longhurst & C.A. Brebbia (ed.), WIT press, UK

Cox, R.M., 2003. The use of passive sampling to monitor forest exposure to O_3, NO_2 and SO_2: a review and some case studies. Environmental pollution 126, 301-311.

Cox,W. M. and Chu, S. H., 1993. Meteorologically adjusted ozone trends in urban areas: A probabilistic approach. Atmospheric Environment, 27B(4):425–434.

Cyrys J., Pitz M., Bischof W., Wichmann H.-Erich & Heinrich J. (2004) J. Expo. Anal. Environ. Epidemiol. 14, 275-283.

Daigle CC, Chalupa DC, Gibb FR, Morrow PE, Oberdorster G, Utell MJ, Frampton MW., (2003). Ultrafine particle deposition in humans during rest and exercise. Inhal Toxicol. 2003 May;15(6):539-52.

de Hartog, J.J., Hoek, G., Peters, A., Timonen, K.L., Ibald-Mulli, A., Brunekreef, B., Heinrich, J., Tiittanen, P., van Wijnen, J.H., Kreyling, W., Kulmala, M., Pekkanen,J., 2003. Effects of fine and ultrafine particles on cardiorespiratorysymptoms in elderly subjects with coronary heartdisease—The ULTRA study. American Journal of Epidemiology157 (7), 613–623.

Dennis, R.L., Byon, W.D., Novak, J.H., Galuppi, K.J., Coats, C.J., 1996. The next generation of integrated air quality modelling: EPA's model-3. Atmospheric Environment 30, 1925-1938.

Dockery, D.W., 2001. Epidemiologic evidence of cardiovascular effects of particulate air pollution. Environmental Health Perspectives 109, 483–486.

Dockery, D.W., Pope III, A., Xu, X., Spengler, J.D., Ware, J.H., Fay, M.E., Ferris Jr., B.G., Speizer, F.E., 1993. An association between air pollution and mortality in six US cities. New England Journal of Medicine 329 (24), 1753–1759.

Donaldson, K., Li, X.Y., MacNee, W., 1998. Ultrafine (nanometre) particle mediated lung injury. Journal of Aerosol Science 29, 553–560.

Eder, B.K., 1989. A principal component analysis of SO_4 precipitation concentrations over the eastern United States. Atmospheric Environment 23, 2739–2750.

El-Fadel, M., Massoud, M., 2000. Particulate matter in urban areas: health-based economic assessment. The Science of the Total Environment 257,.133-146

Emmerson, K.M., Carslaw, N., Pilling, M.J., 2005. Urban atmospheric chemistry during the PUMA Campaign 2: radical budgets for OH, HO_2 and RO_2. Journal of atmospheric chemistry 52, 165-183

Englert, N., 2004. Fine particles and human health—a review of epidemiological studies. Toxicology Letter, 149, 235-242.

Fagundez, L. A., Fernández, v. L., Marino, T. H., Martín, I., Persano, D. A. , Rivarola, y Benítez, M, Sadañiowski, I. V., Codnia, J., Zalts, A., 2001. Preliminary air pollution monitoring in San Miguel, Buenos aires. Environmental Monitoring and Assessment 71, 61–70.

Feldpausch, P, Fiebig, M., Fritzsche, L., and Petzold, A., 2006 Measurement of ultrafine aerosol size distributions by a combination of diffusion screen separators and condensation particle counters, J. Aerosol Sci., 37, 577–597, doi:10.1016/j.jaerosci.2005.04.009.

Fell, T.P., Phipps, A.W., Kendall, G.M., Stradling, G.N., 1997. Recent developments in biokinetic models and the calculation of internal dose coefficients. Journal of radioanalytical and nuclear chemistry 226, 109-115]

Fenger, J., 1999. Urban air quality. Atmospheric Environment 33, 4877-4900.

Fissan, H.J., C. Helsper, and H.J. Thielen, 1983. Determination of Particle Size Distribution by Means of an Electrostatic Classifier. Journal of Aerosol Science, 14:354.

Fuchs, N. A., 1964. Mechanics of Aerosols. Pergamon Press, Oxford.

Gaydos, M., Stainer, C.O. and Pandis, S.N., 2005. Modeling of in-situ ultrafine atmospheric particle formation in the eastern United State, Journal of Geophysical Research 110, D07S12

Gelbard, F. and Seinfeld, J.H., 1979. The general dynamics equation for aerosols, Journal of Colloid and Interface Science 68 (2), 363–382.

Giechaskiel, B.; Ntziachristos, L.; Samaras, Z.; Scheer, V.; Casati, R.; Vogt, R.; Van Grieken, 2005. Formation potential of vehicle exhaust nucleation mode particles on-road and in the laboratory. Atmospheric Environment 39, 3191-3198

Graskow, B. R., Kittelson, D. B., Abdul-Khalek, I. S., Ahmadi, M. R., & Morris, J. E., 1998. Characterization of exhaust particulate emissions from a spark ignition engine. SAE Paper No. 980528 and SP-1326 also in 1998 Transactions of the Society of Automotive Engineering, Engine, Fuels and Lubricants, 3.

Greenwood, S., Coxon, J. E., Biddulph, T., & Bennett, J., 1996. An investigation to determine the exhaust particulate size distributions for diesel, petrol, and compressed natural gas fuelled vehicles. Society of Automotive Engineers Technical Paper Series 961085, Warrendale, PA.

Gullett, B.K. , Touati, A., Oudejans, L., Ryan, S. P.. 2006. Real-time emission characterization of organic air toxic pollutants during steady state and transient operation of a medium duty diesel engine. Atmospheric Environment 40, 4037–4047].

Hall, D. E., Goodfellow, C. L., Heinze, P., Rickeard, D. J., Nancekievill, G., Martini, G., et al. , 1998. A study of the size, number and mass distribution of the automotive particulate emissions from European light duty vehicles. Society of Automotive Engineers Technical Paper Series 982600, Warrendale, PA.

Harrison, R.M., Grenfell, J.L., Savage, N., Allen, A., Clemitshaw, K.C., Penkett, S., Hewitt, C.N., Davison, B., 2000. Observations of new particle production in the atmosphere of a moderately polluted site in Eastern England. Journal of Geophysical Research 105 (14), 17819-17832.

Harrison, R.M., Jones, M., Collins, G., 1999. Measurements of the physical properties of particles in the urban atmosphere. Atmospheric Environment 33, 309- 321.

Hausberger, S., Rodler, J., Sturm, P., Rexeis, M., 2003. Emission factors for heavy-duty vehicles and validation by tunnel measurements. Atmospheric Environment 37, 5237–5245.

Henry, R.C., Hidy, G.M., 1979. Multivariate analysis of particulate sulfate and other air quality variables by principal components—part 1. Annual data from Los Angeles and New York. Atmospheric Environment 13, 1581– 1596.

Hering, S. V., and Stolzenburg, M. R. (2005). A Method for Particle Size Amplification by Water Condensation in a Laminar, Thermally Diffusive Flow. *Aerosol Sci. Technol.* 39:428–436.

Hering, S. V., Stolzenburg, M. R., Quant, F. R., Oberreit, D. R., and Keady, P. B., 2005. A Laminar-Flow, Water-Based Condensation Particle Counter (WCPC). Aerosol Sci. Technol. 39:659–672.

Heywood, J.B., 1988. Internal combustion engine fundamentals. International edition, Mc-Graw-Hill publisher, pp.598.

Hinds, W. C. Aerosol Technology: Properties, Behavior, and Measurement of Airborne Particles; John Wiley and Sons: New York, 1982.

Hoffmann, T., O'Dowd, C.D., Seinfeld, J.H., 2001. Iodine oxide homogeneous nucleation: an explanation for coastal new particle production. Geophysical Research Letters 28, 1949–1952.

Holmes, N.S., 2007. A review of particle formation events and growth in the atmosphere in the various environments and discussion of mechanistic implications. Atmospheric Environment 41, 2183–2201

Hoppel, W.A., 1978. Determination of the Aerosol Size Distribution from the Mobility Distribution of Charged Fraction of Aerosols. Journal of Aerosol Sci. 9:41-54.

Hughes, L.S., Cass, G.R., Gone, J., Ames, M., Olmez, I., 1998. Physical and chemical characterization of atmospheric ultrafine particles in the Los Angeles area. Environmental Science and Technology 32 (9), 1153–1161.

Hunter, L.J., Johnson, G.T., Watson, I.D., 1992. An investigation of three-dimensional characteristics of flow regimes within the urban canyon. Atmospheric Environment 26B (4), 425–432.

Hussein, T., Karppinen, A., Kukkonen, J., Härkonen, J., Aalto, P. P., Hämeri, K., Kerminen, V.-M., and Kulmala, M., 2006 Meteorological dependence of size-fractional number concentrations of urban aerosol particles, Atmos. Environ., 40, 1427–1440.

Hussin, A., H.G. Scheibel, K.H. Becker, and J. Porstendörfer, 1983. Bipolar Diffusion Charging of Aerosol Particles I: Experimental Results Within the Diameter Range of 4–30 nm. Journal of Aerosol Science, 14:671.

ICRP, 1994. Human respiratory tract model for radiological protection: A report of a task group of the international commission on radiological protection. ICRP Publication, Annals ICRP, vol. 24(1–3), 267–272

Imhof, D., Weingartner, E. Vogt, U., Dreiseidler, A., Rosenbohm, E., Scheer, V., Vogt, R., Nielsen, O.J., Kurtenbach, R., Corsmeier, U., Kohler, M., Baltensperger, U., 2005. Vertical distribution of aerosol particles and NOx close to a motorway. Atmospheric Environment 39 (2005) 5710–5721

Imhof, D., Weingartner, E., Prévˆot, A. S. H. , Ord´o˜nez, C., Kurtenbach, R. , Wiesen, P., Rodler, J., Sturm, P., McCrae, I. , Ekstr¨om, M. , Baltensperger, U.., 2006. Aerosol and NOx emission factors and submicron particle number size distributions in two road tunnels with different traffic regimes. Atmos. Chem. Phys., 6, 2215–2230

Ito K, Xue N, Thurston G., 2004. Spatial variation of PM2.5 chemical species and source-apportioned mass concentrations in New York City. Atmos Environ 38:5269–82.

Jacobson, M. Z., and Seinfeld, J. H., 2004. Evolution of nanoparticle size and mixing state near the point of emission, *Atmos. Environ*., 38, 1839-1850.

Jain, A.K., Dubes, R.C., 1998. Algorithms for Clustering Data. Prentice-Hall, Englewood Cliffs, NJ, p. 320.

Jang, M., Kamens, R.M., 2001. Atmospheric Secondary Aerosol Formation by Heterogeneous Reactions of Aldehydes in the Presence of a Sulfuric Acid Aerosol Catalyst. Environ. Sci. Technol., 35 (24), 4758 -4766.

Janssen, N.A.H., van Vliet, P.H.N., Aarts, F., Harssema, H., Brunekreef, B., 2001. Assessment of exposure to traffic related air pollution of children attending schools near motorways. Atmospheric Environment 35, 3875–3884.

Jaques, P.A., Kim, C.S., 2000. Measurement of total lung deposition of inhaled ultrafine particles in healthy men and women. Inhalation Toxicology 12 (8), 715–731.

Jerrett M, Arain A, Kanaroglou P, Beckerman B, Potoglou D, Sahsuvaroglu T, et al., 2005 A review and evaluation of intraurban air pollution exposure models. J Expo Anal Environ Epidemiol. 15:185–204.

Johnson, T., Caldow, R., Pöcher, A., Mirme, A., & Kittelson, D. (2004). A new electrical mobility particle sizer spectrometer for engine exhaust particle measurements. Society of Automotive Engineers Technical Paper Series, No. 2004-01-1341, Warrendale, PA

Jung, JG., Adams, P. J., Pandis, S.N.,2006. Simulating the size distribution and chemical composition of ultrafine particles during nucleation events. Atmospheric Environment 40, 2248–2259

Kao, A.S., Friedlander, S.K., 1995. Frequency distributions of PM_{10} chemical componenets and their sources. Environmental science and technology 16, 401A-416A.

Kerminen V.-M., 1999. Roles of SO2 and secondary organics in the growth of nanometer particles in the lower troposphere. J. Aerosol Sci. 30, 1069-1078

Kerminen V.-M., Virkkula A., Hillamo R., Wexler A. S. and Kulmala M. , 2000. Secondary organics and atmospheric CCN production. J. Geophys. Res. 105, 9255-9264

Kerminen, V.-M., Pirjola, L., Kulmala, M., 2001. How significantly does coagulational scavenging limit atmospheric particle production? Journal of Geophysical Research 106, 24119–24125.

Kerminen, V.M., Wexler, A.S., 1995. The interdependence of aerosol processes and mixing in point-source plumes. Atmospheric Environment 29 (3), 361–375.

Ketzel, M, Berkowicz, R., 2004. Modelling the fate of ultrafine particles from exhaust pipe to rural background: an analysis of time scales for dilution, coagulation and deposition. Atmospheric Environment 38, 2639–2652

Khalek, I.A., Spears, M., Charmley, W., 2003. Particle size distribution from heavy-duty diesel engine: Steady-state and transient emission measurement using two dilution systems and two fuels. SAE Technical Paper, Series 2003-01-0285.

Kim E, Hopke PK, Pinto JP,Wilson WE, 2005. Spatial variability of fine particle mass, components, and source contributions during the Regional Air Pollution Study in St. Louis. Environ Sci Technol; 39:4172–9.

Kim, C.S., Jaques, P.A., 2000. Respiratory dose of inhaled ultrafine particles in healthy adults. Philosophical Transactions of the Royal Society of London Series A—Mathematical Physical and Engineering Sciences 358, 2693–2705.

Kim, D.H., Gautam, M., Gera, D., 2001. On the prediction of concentration variations in a dispersing heavy-duty truck exhaust plume using k-epsilon turbulent closure. Atmospheric Environment 35 (31), 5267–5275.

Kimmel, V. and Kaasik, M., 2003. Assessment of urban air quality in South Estonia by simple measures. Environmental modelling and assessment 8, 47-53.

Kinney, P.D., D.Y.H. Pui, G.W. Mulholland, and N.P. Breyer , 1991. Use of the Electrostatic Classification Method to Size 0.1 μm SRM Particles—A Feasibility Study. Journal of Research of the National Institute of Standards and Technology, 96:147.

Kittelson, D. B., 1998. Engines and nanoparticles: A review. J. Aerosol Sci., 29, 575-588.

Kittelson, D.B., W.F. Watts, J. Johnson, 2002. "Diesel Aerosol Sampling Methodology - CRC E-43: Final Report", University of Minnesota, Report for the Coordinating Research Council, 19 August 2002, http://www.crcao.com/reports/recentstudies00-02/UMN%20Final%20E-43%20Report.pdf].

Kittelson, D.B., Watts, W.F., Johnson, J.P., 2004. Nanoparticle emissions on Minnesota highways. Atmospheric Environment 38 (1), 9–19.

Kittelson, D.B., Watts, W.F., Johnson, J.P., 2006a. On-road and laboratory evaluation of combustion aerosols—Part1: Summary of diesel engine results. Aerosol Science 37, 913–930

Kittelson, D.B., Watts, W.F., Johnson, J.P., Rowntree, C., Payne, M., Goodier, S., Warrens, C., Preston, H., Zink, U., Ortiz, M., Goersmann, C., Twigg, M.V., Walker, A.P., Caldow, R., 2006. On-road evaluation of two Diesel exhaust aftertreatment devices. Aerosol Science 37, 1140 – 1151

Kittelson, D.B., Watts, W.F., Johnson, J.P., Schauer, J.J., Lawson, D.R., 2006b. On road and laboratory evaluation of combustion aerosol-Part 2: summary of spark-ignition engine results. Aerosol science 37, 931-949.

Kleeman, M.J., Schauer, J.J., Cass, G.R., 2000. Size and composition distribution of fine particulate matter emitted from motor vehicles. Environmental Science and Technology 34, 1132–1140.

Knutson E.O., and K.T. Whitby, 1975. Aerosol Classification by Electric Mobility: Apparatus Theory and Applications. Journal of Aerosol Science, 6:443.

Kourtidis, K., Ziomas, I., Zerefos, C., Kosmidis, E., Symeonidis, P., Christophilopoulos, E., Karathanassis, S., Mploutsos, A., 2002. Benzene, toluene, ozone, NO2 and SO2 measurements in an urban street canyon in Thessaloniki, Greece. Atmospheric Environment 36, 5355–5364

Krochmal, D. and Kalina, A., 1997. Measurements of nitrogen dioxide and sulphur dioxide concentrations in urban and rural areas of Poland using a passive sampling method. Environmental Pollution 96,3, 401-407.

Kulmala, M. and 16 others, 2007. Toward Direct Measurement of Atmospheric Nucleation. Science, 318 (89), 89-92.

Kulmala, M., 2003. How Particles Nucleate and Grow. Science 302, 1000-1001

Kulmala, M., Pirjola, L., Maèkela, J.M., 2000. Stable sulphate clusters as a source of new atmospheric particles. NATURE 404, 66-69

Laakso, L., Mäkelä , J.M., Pirjola, L., Kulmala, M., 2002. Model studies on ion-induced nucleation in the atmosphere. Journal of Geophysical Research 107 (D20), 4427.

Lanzhou EPB, 2005. Personal communication.

Lebret, E., Briggs, D., van Reeuwijk, H., Fischer, P., Smallbone, K., Harssema, H., Kriz, B., Gorynski, P., Elliott, P., 2000. Small area variations in ambient NO2 concentrations in four european areas. Atmospheric Environment 34, 177–185.

Lee, C.K., 2002. Multifractal characteristics in air pollutant concentration time series. Water, Air, and Soil pollution 135, 389-409.

Lehmann, U. , Mohr, M., Schweitzer, T. Rütter, J, 2003. Number size distribution of particulate emissions of heavy-duty engines in real world test cycles, Atmospheric Environment 37, pp. 5247–5259.

Lehtinen, K. and Kulmala, M., 2003. A model for particle formation and growth in the atmosphere with molecular resolution in size, Atmos. Chem. Phys. 3, pp. 251–258

Lim, L.L., Hughes, S.J., Hellawell, E.E., 2005. Integrated decision support system for urban air quality assessment. Environmental Modelling & Software 20, 947-303.

Liu, Z. G.; Skemp, M. D.; Lincoln, J. C., 2003. Diesel Particulate Filters: Trends and Implications of Particle Size Distribution Measurement; SAE Paper No. 2003-01-0046.

Liu, Z. G.; Thurow, E. M.; Caldow, R.; Johnson, T. R., 2005. Transient Performance of Diesel Particulate Filters as Measured by an Engine Exhaust Particle Size Spectrometer; SAE Paper No. 2005- 01-0185.

Liu, Z.G., Ford, D.C., Vasys, V.N. Chen, D.-R. and Johnson, T.R., 2007. Influence of Engine Operating Conditions on Diesel Particulate Matter Emissions in Relation to Transient and Steady-State Conditions. Environ. Sci. Technol., 41, 4593-4599

Lloyd AC, Darnall KR, Winer AM and Pitts Jr JN, 1976. Relative rate constants for reaction of the hydroxyl radical with a series of alkanes, alkenes and aromatic hydrocarbons. Journal of Physical Chemistry 80 (8):789-794

Lowenthal DH, Borys RD, Wetzel M, 2002. Aerosol distributions and cloud interactions at a mountaintop laboratory. J Geophys Res ;107(D18):4345. doi:10.1029/2001JD002046.

Lu, H.C., 2002. The statistical characters of PM10 concentration in Taiwan area. Atmospheric Environment 36, 491–502.

Lu, H.C., Fang, G.C., 2002. Estimating the frequency distributions of PM_{10} and $PM_{2.5}$ by the statistics of wind speed at Sha-Lu, Taiwan. The Science of the Total Environment 298 119–130

Lui, B. Y. H. and Pui, D. Y. H., 1974. On the performance of the Electrical Aerosol Analyzer. J. Aerosol Sci., 6, 249-264.

Mage, D.T., 1984. Pseudo-lognormal distributions. Journal of Air Pollutants and Control Assessments 31, 374–376.

Mage, D.T., Ott, W.R., 1984. An evaluation of the method of fractiles, moments and maximum likelihood for estimating parameters when sampling air quality data from a stationary lognormal distribution. Atmospheric environment 18, 163-171.

Mansurov, Z. A., 2005. Soot Formation in Combustion Processes (Review). Combustion, Explosion, and Shock Waves 41(6) 727–744

Maricq, M. M., Podsiadlik, D. H., & Chase, R. E., 1999b. Gasoline vehicle particle size distributions: comparison of steady state, FTP, and USO6 measurements. Environmental Science and Technology, 33, 2007–2015.

Maricq, M.M., Chase, R.E., Xu, N., Podsiadlik, D.H., 2002. The effects of the catalytic converter and fuel sulfur level on motor vehicle particulate matter emissions: light duty diesel vehicles. Environment Science and Technology 36, 283–289.

Maricq, M.M., Podsiadlik, D.H., Chase, R.E., 1999a. Examination of the size-resolved and transient nature of motor vehicle particle emissions. Environmental Science and Technology 33, 1618–1626.

Marti, J.J., et al., 1997. New particle formation at a remote continental site: assessing the contributions of SO2 and organic precursors. Journal of Geophysical Research 102, 6331–6339.

Mathis, U., Kaegi, R., Mohr, M., Zenobi, R., 2004a. TEM analysis of volatile nanoparticles from particle trap equipped diesel and direct-injection spark-ignition vehicles. Atmospheric Environment 38, 4347–4355.

Mathis, U., Ristima¨ ki, J., Mohr, M., Keskinen, J., Ntziachristos, L., Samaras, Z., Mikkanen, P., 2004b. Sampling conditions for the measurement of nucleation mode particles in theexhaust of a diesel vehicle. Aerosol Science and Technology 38, 1149–1160.

Meng, Z., Dabdub, D., Seinfeld, J.H., 1997. Chemical coupling between atmospheric ozone and particulate matter. Science 277, 116-119.

Mirme A. and Tamm E., 1991. Comparison of sequential and parallel measurement principles in aerosol spectrometry. J. Aerosol Sci., 22S1, pp. S331 - S334.

Mirme A. and Tamm E., 1993. Electric aerosol spectrometer— calibration and error account." J. Aerosol Sci., 24S1, pp. S211–S212.

Molina, L.T. and Molina, M.J., 2002. Air quality in the Mexico magacity. The Netherlands: Kluwer academic, p.139

Monn , C., 2001. Exposure assessment of air pollutants: a review on spatial heterogeneity and indoor/outdoor/personal exposure to suspended particulate matter, nitrogen dioxide and ozone. Atmospheric Environment 35, pp. 1–32.

Monod, A., Sive, B., C., Avino, P., Chen, T., Blake, D., Rowland, F., S., 2001. Monoaromatic compounds in ambient air of various cities: a focus on correlations between the xylenes and ethylbenzene. Atmospheric Environment 35, 135-149.

Morawska, L. Vishvakarman, D. Mengersen, K. Thomas, S. 2002. Spatial variation of airborne pollutant concentrations in Brisbane, Australia and its potential impact on population exposure assessment. Atmospheric Environment 36, 3545–3555

Morawska, L., He, C., Hitchins, J., Mengersen, K., & Gilbert, D. , 2003. Characteristics of particle number and mass concentrations in residential houses in Brisbane, Australia. *Atmospheric Environment, 37*, 4195–4203.

Morel, B., Yen, S., Cifuentes, L., 1999. Statistical distribution for air pollutant applied to the study of the particulate problem in Santiago. Atmospheric Environment 33, 2575–2585.

Namdeo, A., Mitchell, G., Dixon,R., 2002. TEMMS: an integrated package for modelling and mapping urban traffic emissions and air quality. Environmental Modelling & Software 17, 179-190.

Neeft, J.P.A., Makkee, M., Moulijn, J.A., 1996. Diesel particulate emission control. Fuel Processing Technology 47 (1996) 1-69

Nemmar, A., Hoet, P.H.M., Vanquickenborne, B., Dinsdale, D., Thomeer, M., Hoylaerts, M.F., Vanbilloen, H., Mortelmans, L., Nemery, B., 2002. Passage of inhaled particles into the blood circulation in humans. Circulation 105 (4), 411–414.

Nilsson, E.D., Kulmala, M., 1998. The potential for atmospheric mixing processes to enhance the binary nucleation rate. Journal of Geophysical Research 103 (D1), 1381–1389.

Nowak, D.J., Civerolo, K.L., Rao, S.T., Sistla, G., Luley, C.J., Crane, D.E., 2000. A modelling study of the impact of urban trees on ozone. Atmospheric environment 34, 1601-1613

Novakov, T., Penner, J.E., 1993. Large contribution of organic aerosols to cloud condensation nuclei concentrations. Nature 365, 323Ð365.

Ntziachristos, L., Giechaskiel, B., Pistikopoulos, P., Samaras, Z., Mathis, U., Mohr, M., Ristima¨ ki, J., Keskinen, J., Mikkanen, P., Casati, R., Scheer, V., Vogt, R., 2004. Performance evaluation of a novel sampling and measurement system for exhaust particle characterization. SAE Technical Paper Series 2004-01-1439.

Obersdorster, G., 2001. Pulmonary effects of inhaled ultrafine particles. International Archives of Occupational and Environmental Health 74 (1), 1–8.

Obersdorster, G., Finkelstein, J.N., Johnston, C., Gelein, R.,Cox, C., Baggs, R., Elder, A.C.P., 2000. Acute pulmonary effects of ultrafine particles in rats and mice. Health Effects Institute Report No. 96.

Orlinski, R., 2002. Multipoint moss passive samplers assessment of urban airborne polyciclic aromatic hydrocarbons: concentrations profile and distribution along Warsaw main streets. Chemosphere 48, 181-186.

Ott, W.R.A., 1990. Physical explanation of the lognormality of pollutant concentrations. Journal of Air and Waste Management Association 40, 1378–1383.

Palmgren, F., Berkowicz, R., Hertel, O., Vignati, E., 1996. Effects of reduction in NO_x on the NO_2 levels in urban streets. Science of the Total Environment 189/190, 409–415.

Pardo-Iguzquiza, E., Dowd, P. A., 2004. Normality tests for spatially correlated data. Mathematical Geology Vol. 36, No.6.

Pekkanen, J. and Kulmala, M., 2004. Exposure assessment of ultrafine particles in epidemiologic time-series studies, Scandinavian Journal Work Environment and Health 30 (Suppl. 2), pp. 9–18

Penttinen, P., Timonen, K.L., Tiittanen, P., Mirme, A., Ruuskanen, J., Pekkanen, J., 2001. Number concentration and size of particles in urban air: effects on spirometric lung function in adult asthmatic subjects. Environmental Health Perspectives 109 (4), 319–323.

Petäjä, T.; Mordas, G.; Manninen, H.; Aalto, P. P.; Hämeri, K.; Kulmala, M., 2006. Detection Efficiency of a Water-Based TSI Condensation Particle Counter 3785 Aerosol Science & Technology, 40(12):1090-1097

Pilidis, G.A., Karakitsios, S.P., Kassomenos, P.A., 2005. BTX measurements in a medium-sized European city. Atmospheric environment 39, 6051-6065.

Pinto JP, Lefohn AS, Shadwick DS., 2004. Spatial variability of PM2.5 in urban areas in the United States. J Air Waste Manage Assoc 54, 440–9.

Pirjola, L., Parviainen, T., Hussein, T., Valli, A., Ha¨ meri, K., Aaalto, P., Virtanen, A., Keskinen, J., Pakkanen, T.A., Ma¨ kela¨ , T., Hillamo, R.E., 2004. ‘‘Sniffer’’—a novel tool for chasing vehicles and measuring traffic pollutants. Atmospheric Environment 38, 3625–3635.

Pohjola, M., Pirjola, L., Kukkonen, J., Kulmala, M., 2003. Modelling of the influence of aerosol processes for the dispersion of vehicular exhaust plumes in street environment. Atmospheric Environment 37, 339–351.

Poissant, L., Bottenheim, J.W., Roussel, P., Reid, N.W., Niki, H., 1996. Multivariate analysis of a 1992 sontos data subset. Atmospheric Environment 30 (12), 2133-2144.

Pope III, C.A., Burnett, R.T., Thun, M.J., Calle, E.E., Krewski, D., Ito, K., Thurnston, G.D.,2002. Lung cancer, cardiopulmonary mortality, and long-term exposure to fine particulate air pollution, Journal of the American Medical Association 287 (9), 1132–1141

Pope III, C.A., Thun, M.J., Namboodiri, M.M., Dockery, K.S.,Evans, J.S., Speizer, F.E., Heath Jr., C.W., 1995. Particulate air pollution as a predictor of mortality in a prospective study of US adults. American Journal of Respiratory and Critical Cardiac Care Medicine 151, 669–674.

Qi, B., Wang, J.F., Wang, H., 2001. Characteristics of air pollution and its cause in Lanzhou city, Shaxi Meteorology (6), 18-20.

Qin, Y., Kot, S.C., 1993. Dispersion of vehicular emission in street canyons, Guangzhou city, South China (P.R.C.). Atmospheric Environment 27B, 283–291.

Quant, F. R., Flagan, R.C., Horton, K.D., 1993. Implementation of a Scanning Mobility Particle Sizer (SMPS). J. Aerosol Sci., 24, Supp. S83-S84.

Rao, K.S., Gunter, R.L., White, J.R., Hosker, R.P., 2002. Turbulence and dispersion modeling near highways. Atmospheric Environment 36 (27), 4337–4346.

Rencher, A. C., 1998, *Multivariate Statistical Inference and Applications*, John Wiley & Sons, Inc., 559 pp.

Rickeard, D. J., Bateman, J. R., Kwon, Y. K., McAughey, J. J., & Dickens, C. J., 1996. Exhaust particulate size distribution: vehicle and fuel influences in light duty vehicles. Society of Automotive Engineers Technical Paper Series 961980, Warrendale, PA.

Rivera-Carpio, C.A., Corrigan, C.E., Novakov, T., Penner, J.E., Rogers, C.F., Chow, J.C., 1996. Derivation of contributions of sulfate and carbonaceous aerosols to cloud condensation nuclei from mass size distributions. Journal of Geophysical Research 101, 19 483Ð19 493.

Ronkko T., Virtanen A, Vaaraslahti K., Keskinen J, Pirjola L, Lappic M., 2006. Effect of dilution conditions and driving parameters on nucleation mode particles in diesel exhaust: Laboratory and on-road study. Atmospheric Environment 40 (2006) 2893–2901

Saito, K., Shinozaki, O., Seto, T., Kim, C-S., Okuyama, K., Kwon, S-B., Lee, K. W., 2002. The origins of nanoparticle modes in the number distribution of diesel particulate matter. SAE Technical Paper, Series 2002-01-1008.

Samet, J.M., Dominici, F., Curriero, F.C., Coursac, I., Zeger, S.L., 2000. Fine particulate air pollution and mortality in 20 US Cities, 1987–1994. New England Journal of Medicine 343 (24), 1742–1749.

Sasaki, S., Nakajima, T., 2002. Study on the measuring method of vehicular PM size distribution to simulate the atmospheric dilution process. SAE Technology Paper 2002-01-2716.

Scheer, V., Kirchner, U., Casati , R., Vogt, R., Wehner, B., Philippin ,S., Wiedensohler, A., Hock, N., Schneider, J., Weimer , S., Borrmann, S., 2005. Composition of Semi-volatile Particles from Diesel Exhaust. SAE Paper 2005-01-0197

Schmidt, M., Schafer, R.-P., 1998. An integrated simulation system for traffic induced air pollution. Environmental Modelling & Software 13, 295-303.

Schwartz, J., Laden, F., Zanobetti, A., 2002. The concentration- response relation between PM2.5 and daily deaths. Environmental Health Perspectives 110 (10), 1025–1029.

Seaton, A., Dennekamp, M., 2003. Hypothesis: Ill health associated with low concentrations of nitrogen dioxide—an effect of ultrafine particles? Thorax 58 (12), 1012–1015.

Seinfeld JH, Pandis SN, 2006. Atmospheric chemistry and physics: from air pollution to climate change.New York: John Wiley & Sons, p. 1271.

Seinfeld, 1986. Atmospheric Chemistry and Physics of Air Pollution. , Wiley, New York.

Shi, J. P.; Harrison, R. M.; Brear, F. 1999. Particle size distribution from a modern heavy-duty diesel engine. Sci. Total Environ., 235, 305-317.

Shi, J.P., Evans, D.E., Khan, A.A., Harrison, R.M., 2001. Sources and concentration of nanoparticles (10nm diameter) in the urban atmosphere. Atmospheric Environment 35, 1193-1202

Shi, J.P., Harrison, R.M., Evans, D.E., Alam, A., Barnes, C., Carter, G., 2002. A method for measuring particle number emissions from vehicles driving on the road. Environmental Technology23 (1), 1–14.

Shi, J.P., Khan, A.A., Harrison, R.M., 1999. Measurements of ultrafine particle concentration and size distribution in the urban atmosphere. *The Science of Total Environment.* 235, 51-64.

Sigsby, J.E., Tejada, S.B., Ray, D.W., Lang, J.M., Duncan, J.W., 1987.Volatile organic compound emissions from 46 in-use passenger cars. Environmental Science and technology 21, 466-475.

Sillman, S., 1999. The relation between ozone, NO_x and hydrocarbons in urban and polluted rural environments. Atmospheric Environment 33 (2), 1821–1845.

Sioutas C, Delfino RJ, Singh M. Exposure assessment for atmospheric ultrafine particles (UFP) and implications in epidemiological research. Environ Health Perspect. 2005;113(8):947–955.

Smith, S. J. , Pitcher, H., Wigley, T.M.L., 2001b. Global and regional anthropogenic sulphur dioxide emissions. Global and planetary change 29, 99-199.

Smith, S., Cheng, U.S., Yeh, H.C., 2001a. Deposition of ultrafine particles in human tracheobronchial airways of adults and children. Aerosol Science and Technology 35 (3), 697–709.

Stanier, C, Khlystov, A.,Pandis, S., 2004. Nucleation Events During the Pittsburgh Air Quality Study: Description and Relation to Key Meteorological, Gas Phase, and Aerosol Parameters. Aerosol Science and Technology 38 (1), 253–264

Stohl, A., Forster, C., Huntrieser, H., Mannstein, H., McMillan, W. W. , Petzold, A., Schlager, H., Weinzierl, B., 2007.Aircraft measurements over Europe of an air pollution plume from Southeast Asia – aerosol and chemical characterization. Atmospheric Chemistry and Physics 7, 913–937.

Sturm, P.J., Baltensperger, U., Bacher, M., Lechner, B., Hausberger, S., Heiden, B., Imhof, D., Weingartner, E., Prevot, A.S.H., Kurtenbach, R., Wiesen, P., 2003. Roadside measurements of particulate matter size distribution. Atmospheric Environment 37, 5273–5281.

Ta,W., Wang, T., Xiao, H., Zhu, X., Xiao, Z., 2004. Gaseous and particulate air pollution in the Lanzhou Valley, China. Science of the Total Environment 320 (2004) 163–176

Taha, H., 1996. Modeling impacts of increased urban vegetation on ozone air quality in the south cost air basin. Atmospheric environment 30 (20), 3423-3430

Tammet H., Mirme A. and Tamm E, 1998. Electrical aerosol spectrometer of Tartu University." J. Aerosol Sci.29, Suppl. 1, S427–S428.

Theurer, W., 1999. Typical building arrangements for urban air pollution modelling. Atmospheric Environment 33, 4057–4066.

Trainer, M., Parrish, D.D., Goldan, P.D., Roberts, J., Fehsenfeld, F.C., 2000. Review of observation-based analysis of the regional factors influencing ozone concentrations. Atmospheric Environment 34 (12-14), 2045-2061

TSI, 2006. Model 3090 EEPS^{TM} Engine Exhaust Particle Sizer: Operation and service Manual (P/N 1980494, Revision E). TSI Incorporated (www.tsi.com).

Utell, M.J., Framptom, M.W., 2000. Acute health effects of ambient air pollution: the ultrafine particle hypothesis. Journal of Aerosol Medicine-Deposition Clearance and Effects in the Lung 13 (4), 355–359.

Vaaraslahti, K.; Virtanen, A.; Ristimaki, J.; Keskinen, J. Nucleation mode formation in heavy-duty exhaust with and without a particulate filter. Environ. Sci. Technol. 2004, 38, 4884-4890.

Vakeva, M., Hameri, K., Kulmala, M., Lahdes, R., Ruuskanen, J., Laitinen, T., 1999. Street level versus rooftop concentrations of submicron aerosol particles and gaseous pollutants in an urban street canyon. Atmospheric environment 33, 1385-1397.

Vallius, M., Lanki, T., Tiittanen,P., Koistinen, K., Ruuskanen, J., Pekkanen, J., 2003. Source apportionment of urban ambient $PM_{2.5}$ in two successive measurement campaigns in Helsinki, Finland. *Atmospheric Environment 37(5), 615-623*

Wang, S.C., and Flagan, R.C., 1990. Scanning Electrical Mobility Spectrometer, Aerosol Science and Technology. 13 p. 230-240.

Vardoulakis, S., Fisher, B., Pericleous, K., Gonzalez-Flesca, N, 2003. Modelling air quality in street canyons: a review. Atmospheric Environment 37 (2), 155–182

Vehkamäki, H., et al., 2002. An improved parameterization for sulfuric acid-water nucleation rates for tropospheric and stratospheric conditions. Journal of Geophysical Research 107, 4622–4632.

Wehner, B.; Birmili, W.; Gnauk, T.; Wiedensohler, A. Particle number size distribution in a street canyon and their transformation into the urban-air background: measurements and a simple model study. *Atmos. Environ.* **2002**, *36*, 2215-2223.

Weijers, E. P., Khlystov, A. Y., Kos, G. P. A., Erisman, J. W., 2004. Variability of particulate matter concentrations along roads and motorways determined by a moving measurement unit. Atmospheric Environment, 38 (19), 2993-3002

Verbeke, J.S., Hartog, J.C.D., Dekker, W.H., Coomans, D., Buydens, L., Massart, D.L., 1984. The use of principal components analysis for the investigation of an organic air pollutants data set. Atmospheric Environment 18 (11), 2471–2478.

Westerdahl, D., Fruin, S., Sax, T., Fine, P. M. Sioutas C., 2005. Mobile platform measurements of ultrafine particles and associated pollutant concentrations on freeways and residential streets in Los Angeles. Atmospheric Environment 39, 3597–3610

Wexler, A. S., Lurmann, F. W. and Seinfeld, J. H., 1994. Modeling urban and regional aerosols—I. Model Development. Atmospheric Environment 28A, pp. 531–546

Whitby, K. T., & Cantrell, B. K. (1976). Atmospheric aerosols: Characteristics and measurement. Proceedings of the International Conference on Environmental Sensing and Assessment (ICESA), Institute of Electrical and Electronic Engineers (IEEE). IEEE #75-CH 1004-1, ICESA paper 29-1 (6pp). Washington, DC: IEEE.

Whitby, K. T., Clark, W. E., 1966. Electrical Aerosol Particle Counting and Size Distributions Measuring System for the 0.015 to 1 μm Size Range. Tellus XVIII, 2

WHO, 2004. Health Aspects of Air Pollution.Results from the WHO Project "Systematic Review of Health Aspects of Air Pollution in Europe". WHO Regional Office for Europe, Copenhagen, Denmark.

WHO, 2006. Air Quality Guidelines. Global update 2005. WHO Regional Office for Europe, Copenhagen, Denmark (http://www.euro.who.int/Document/E90038.pdf)

WHO, 2007. Health relevance of particulate matter from various sources. WHO Regional Office for Europe, Copenhagen, Denmark. http://www.euro.who.int/Document/E90038.pdf

Wiedensohler ,A., 1988. An Approximation of the Bipolar Charge Distribution for Particles in the Submicron Size Range. Journal of Aerosol Science, Vol. 19, No. 3, pp. 387-389.

Wilson JG, Kingham S, Pearce J, Sturman AP. A review of intraurban variations in particulate air pollution: implications for epidemiological research. Atmos Environ 2005;39:6444–62.

Virtanen, A., Ronkko, T., Kannosto, J., Ristimaeki, J., Maekela, J., Keskinen, J., Pakkanen, T., Hillamo, R., Pirjola, L., and Haemeri, K., 2006. Winter and Summer time size distributions and densities of traffic-related aerosol particles at a busy highway in Helsinki, Atmos. Chem. Phys. 6, 2411–2421

Vogt, R., Scheer, V., Casati, R., Bender, T., 2003. On-road measurement of particle emission in the exhaust plume of a diesel passenger car. Environmental Science and Technology 37, 4070–4076.

Wåhlin, P., Berkowicz, R., Palmgren, F., 2006. Characterisation of traffic-generated particulate matter in Copenhagen Atmospheric Environment 40, 2151–2159

Xia, D.S. Chen, F.H. Bloemendal, J. Liu, X.M., Yu, Y. Yang, L.P., 2008. Magnetic properties of urban dustfall in Lanzhou, China, and its environmental implications. Atmospheric environment (in press), DOI: doi:10.1016/j.atmosenv.2007.11.040

Xu, H, Zha,i J, Liu, Z. Q., 2003. Study on current situation of atmospheric pollution of Lanzhou and the countermeasures, Environ Protect Science 29 (119), 4-6

Zhang, K. and Wexler, A., 2002a. A hypothesis for growth of fresh atmospheric nuclei. Journal of Geophysical Research 107(D21): 6.

Zhang, K. M , Wexler, A. S., 2002b. Modeling the number distributions of urban and regional aerosols: theoretical foundations. Atmospheric Environment 36, 1863–1874

Zhang, K. M., Wexler, A.S., 2004. Evolution of particle number distribution near roadways—Part I: analysis of aerosol dynamics and its implications for engine emission measurement. Atmospheric Environment 38 (2004) 6643–6653

Zhang, K. M., Wexler, A.S., Zhu, Y.F., Hinds, W. C., Sioutas, C., 2004a. Evolution of particle number distribution near roadways. Part II: the 'Road-to-Ambient' process. Atmospheric Environment 38, 6655–6665

Zhang, R., Suh, I., Zhao, J., Zhang, D., Fortner, E.C., Tie, X., Molina, L. T., Molina, M. J., 2004b. Atmospheric New Particle Formation Enhanced by Organic Acids, Science 304, 1487-1490

Zhu, Y., Hinds, W.C., Kim, S., Shen, S., Sioutas, C., 2002. Study of ultrafine particles near a major highway with heavy-duty diesel traffic. Atmospheric Environment 36 (27), 4323–4335.

Ziv, A., Berkowicz, R., Genikhovich, E., Palmgren, F., Yakovleva, E., 2002. Analysis of the St.Petersburg traffic data using the OSPM model. Water, air and soil pollution 2, 297-310.